Natural Resources Canada   Ressources naturelles Canada

GEOLOGICAL SURVEY OF CANADA
OPEN FILE 8405

Marine geology and landslides of the central Salish Sea, British Columbia: International Symposium on Submarine Mass Movements and their Consequences, field trip guidebook

D.H. Huntley, P.T. Bobrowsky, D.C. Mosher, J.J. Clague, N.J. Roberts, and D.G. Lintern

2018

Canada

GEOLOGICAL SURVEY OF CANADA
OPEN FILE 8405

Marine geology and landslides of the central Salish Sea, British Columbia: International Symposium on Submarine Mass Movements and their Consequences, field trip guidebook

D.H. Huntley[1], P.T. Bobrowsky[2], D.C. Mosher[3], J.J. Clague[4], N.J. Roberts[4], and D.G. Lintern[2]

[1] Geological Survey of Canada, 1500-605 Robson Street, Vancouver, British Columbia V6B 5J3 Canada
[2] Geological Survey of Canada, 9860 West Saanich Road, Sidney, British Columbia V8L 5T5 Canada
[3] Center for Coastal and Ocean Mapping, 24 Colovos Road, Durham, New Hampshire 03824 U.S.A.
[4] Department of Earth Sciences, 8888 University Drive, Burnaby, British Columbia V5A 1S6 Canada

2018

Permanent Link: https://doi.org/10.4095/313099
This publication is available for free download through GEOSCAN (http://geoscan.nrcan.gc.ca/).

Recommended citation
Huntley, D.H., Bobrowsky, P.T., Mosher, D.C., Clague, J.J., Roberts, N.J., and Lintern, D.G., 2018. Marine geology and landslides of the central Salish Sea, British Columbia: International Symposium on Submarine Mass Movements and their Consequences, field trip guidebook; Geological Survey of Canada, Open File 8405, 77 p. https://doi.org/10.4095/313099

Publications in this series have not been edited; they are released as submitted by the author.

Marine Geology and Landslides of the Central Salish Sea

FIELD TRIP LEADERS
Peter Bobrowsky[1], David Mosher[2], David Huntley[1] and Nicholas Roberts[3]

[1] Geological Survey of Canada; [2] University of New Hampshire; [3]Simon Fraser University

Preface

This field excursion guidebook was produced to compliment the 8th *International Symposium on Submarine Mass Movements and Their Consequences* (ISSMMTC 2018).

Future sustainable regional economic investment in exploration and development of energy and mineral resources and risk management in British Columbia and Canada re an understanding of the spatial distribution and range of earth materials and marine geohazards, and their potential response to climate change.

Eight field stops around the central Salish Sea on Vancouver Island and mainland British Columbia (**Figure P1-1**) have been selected where evidence of past submarine landslides, tsunamis, earthquakes, floods, wildfires and climate change is preserved in bedrock, surficial sediments, soils and vegetation.

Also highlighted are a number of innovative design solutions employed to overcome the complex geological engineering and construction challenges resulting from the mountainous terrain, liquefiable ground, congested utility corridors and restrictive property access in the region.

Figure P1-1 Field trip STOPS 1-7 and route indicate in solid red (road) and dotted red (ferry) lines. At each of these sites, group discussions will focus on consequences and impacts of these geohazards on society and the natural environment. From a geohazard perspective, geology, geomorphology, hydrology and climate combine to make this part of British Columbia some of the most challenging terrain in Canada. Historical earthquakes, landslides, tsunamis and floods at the sites visited have resulted in loss of life and significant and costly damage to infrastructure and property.

Itinerary

DAY 1 (MAY 5) Victoria to Squamish	DAY 2 (MAY 6) Squamish to Victoria
8 am depart Victoria	9 am depart Squamish
Quaternary Landscapes of southern Vancouver Island From Victoria, 5-hour drive north through Duncan and Nanaimo to Port Alberni	**Quaternary Landscapes of Howe Sound and Vancouver** From Squamish, 5 -hour drive south through Vancouver to Tsawwassen
STOP 1 *30 minutes* Malahat, Highway 1: Saanich inlet overview	**STOP 5** *30 minutes* Squamish: geohazards and emergency planning, policies and constraints
STOP 2 *30 minutes* Cathedral Grove: the ancient forests of Vancouver Island	**STOP 6** *30 minutes* Porteau Bluffs: mass movements and flood mitigation measures
STOP 3 *30 minutes* Port Alberni: plate boundary earthquakes and 1964, 1700 and older tsunami records	**STOP 7** *30 minutes* Cypress Mountain view point: bedrock, geological structures, earthquake hazards and mitigation
Group lunch *30 minutes* Picnic at STOP 3	**Group lunch** *30 minutes* Picnic at STOP 7
STOP 4 *30 minutes* Mapleguard Spit and Goose Spit, Comox: 1946 earthquake, tsunamis, coastal erosion and mitigation	**STOP 7** *30 minutes* Fraser River delta: geohazards and marine infrastructure
Ferry crossing *90 minutes* Nanaimo to Horseshoe Bay: dinner on ferry (Option A)	**Ferry crossing** *90 minutes* Tsawwassen to Swartz Bay: dinner on ferry
Drive 45 minutes north to Squamish: arrive early evening, with dinner at local restaurants (Option B); Overnight Squamish	Arrive before 9 pm Victoria, TRIP ENDS

DAY 1 Victoria to Squamish

STOP 1 Saanich Inlet: fjord geology and geomorphology (30 minutes)

Introduction

Sit back, read through the Field Excursion Guidebook, and enjoy the views from the bus window. Travelling north from Victoria on the Trans-Canada Highway (Highway 1 and Highway 4), our route on **DAY 1** takes you on a geological tour through the Vancouver Island Ranges and Nanaimo Lowland (**Figure S1-1**). The tour continues with a ferry crossing of the Salish Sea and a drive north on the scenic Sea to Sky Highway (Highway 99) to Squamish. We will visit sites along Highway 99 on **DAY 2** of the Field Trip, so take notes!

We begin at **STOP 1** on the Malahat Pass (Highway 1) overlooking Saanich Inlet and Saanich Peninsula, with views across to the Cascade Range and Mount Baker in Washington State, USA.

Figure S1-1 Location of STOPS 1-3 on southern Vancouver Island (DAY 1) and STOPS 5-7 on mainland British Columbia (DAY 2) in relation to major population centres around the Salish Sea. Google Earth image viewed looking south to Seattle, USA.

Bedrock and structural geology

The modern plate tectonic setting of British Columbia is depicted in **Figure S1-2**. Vancouver Island underlain by fault-bounded Paleozoic (ca. 450 Ma – 330 Ma) metamorphosed sedimentary and volcanic, plutonic bedrock comprising the Wrangellia terrane (**Figure S1-3**, **Figure S2-1b**). These rocks are intruded along regional-scale northwest-trending fault zones by middle to late Mesozoic plutonic rocks (ca. 165 Ma – 90 Ma). This composite of crustal fragments extends north into Alaska and southern Yukon (Massey et al. 2005).

Early Jurassic (ca. 190 Ma) basaltic, gneissic and granitic rocks of the Bonanza Formation, Island Intrusions and Westcoast Crystalline Complex are exposed in road cuts along the Vancouver Island Highway (Highway 1) north from Victoria. North of Duncan you will observe outcrops of the Upper Cretaceous Nanaimo Group (85-65 Ma).

Conglomerate, coal-bearing sandstone and mudstone units unconformably overlying some of the oldest rocks on Vancouver Island along this section of the highway (**Figure S1-3** b). Volcanic and carbonate rocks of the Sicker and Buttle Lake groups (ca. 370 Ma), are exposed as monadnocks rising 340 m to 780 m elevation above the coastal lowland around Duncan.

Northwest from Duncan to Port Alberni, tectonic slices of Triassic (ca. 220 Ma) Karmutsen Formation basalts and Quatsino Formation limestone are exposed in the folds and thrusts of the central sector of the Vancouver Island Ranges (*see* **STOP 2** and **STOP 3**).

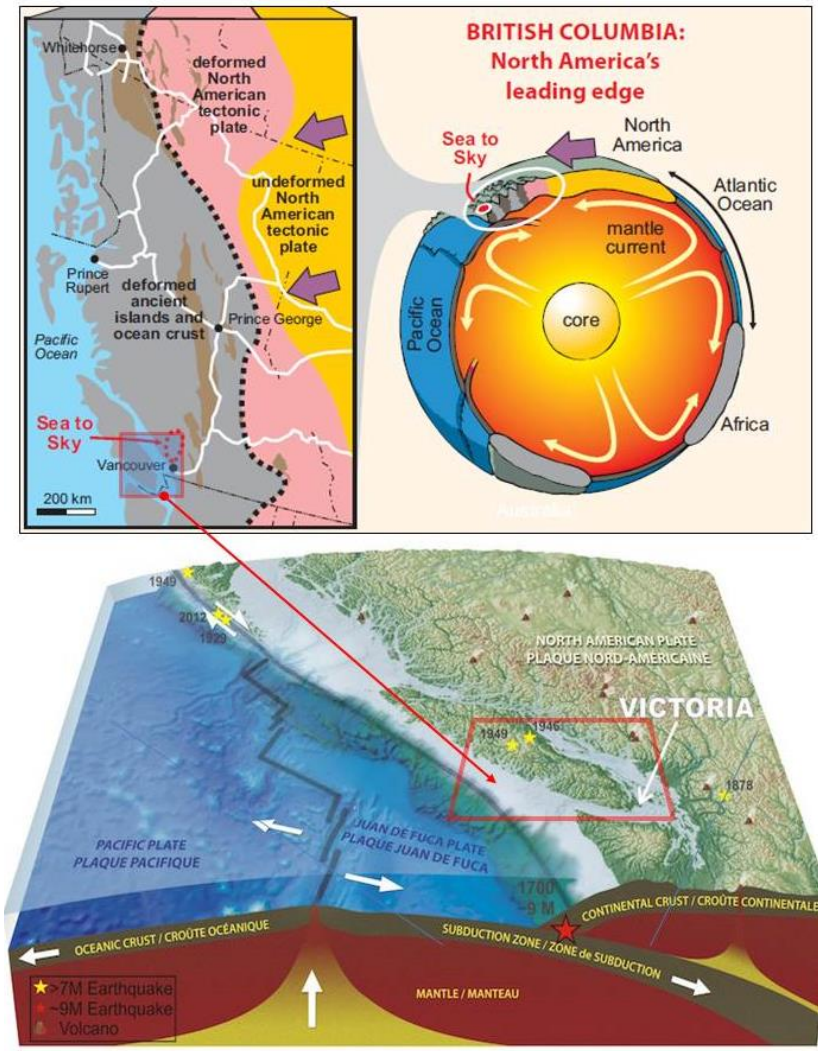

Figure S1-2 Plate tectonic setting of British Columbia and field trip area (red box), showing transition from a subduction to transform plate boundary, in relation to the hypothesized interior of the earth (modified from: Turner et al. 2010).

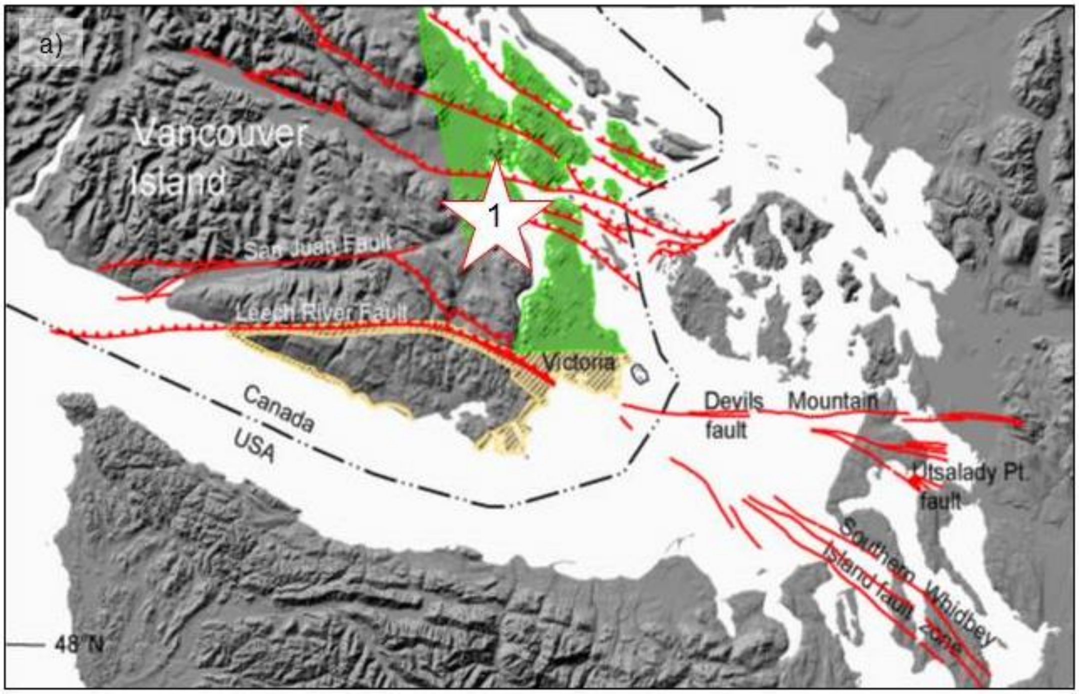

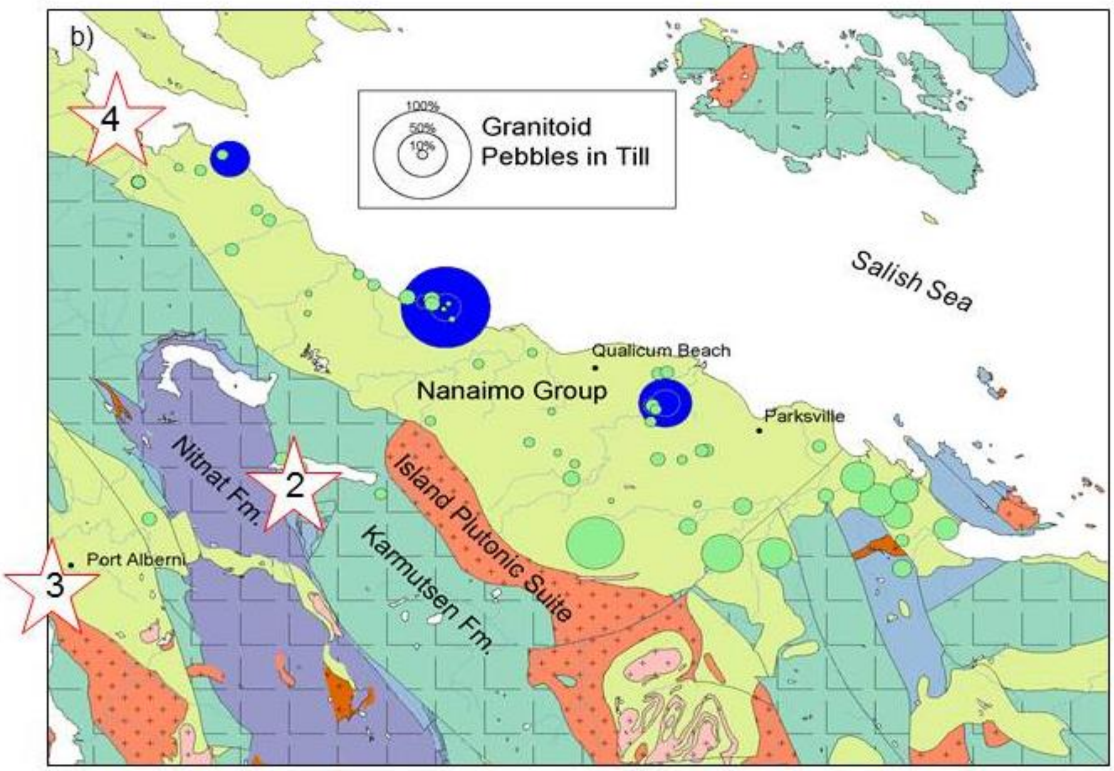

Figure S1-3 a) Regional morphology and tectonic elements near STOP 1 (green shaded area is part of the Nanaimo Lowland and Gulf Islands). Modified from GSC Open File 7681 Figure 4, Bednarski 2015). b) bedrock geology of central Vancouver Island with the distribution of granitic pebbles (erratic lithologies) in till in the Nanaimo Lowland. This pattern suggests a mixing of sources from Vancouver Island and the mainland of British Columbia. Modified from GSC Open File 7229 Figure 2 (Bednarski and Rogers 2012).

Nanaimo Group rocks are exposed again from Nanaimo north to Port Alberni and Comox (**Figure S1-4**). The broadly deformed conglomerates, coal-bearing sandstones and mudstone you will observe were deposited in a proto-Salish Sea sedimentary basin formed between Mesozoic Vancouver Island and mainland British Columbia (Cui et al. 2017).

Figure S1-4 Outcrop of sandstone of the Cretaceous Nanaimo Group at Nanaimo.

Quaternary landscape of south and east-central Vancouver Island

The present landscape is a product of several cycles of glacial and non-glacial erosion and deposition during the Quaternary Period, approximately the last 2 million years (Ma).

The dominant landforms and deposits are inferred to date to the Late Wisconsinan Fraser Glaciation (ca. 29 ka to 10 ka, thousands of years) and Holocene non-glacial interval (ca. 10 ka to present). Surficial earth material units on this field trip are defined on the basis of texture, sorting, fissility, colour, sedimentary structures, consolidation, contact relationships, material origin, in addition to surface expression and landform associations. Ice dispersal patterns are inferred from striae, flutes, drumlins, roches moutonnées, and long axes orientations of clasts in till. Meltwater flow directions are inferred from foreset-, cross- and ripple-bedding, clast imbrication and channel orientations.

Pre-Late Wisconsinan landscape

The present mountainous landscape is in part a product of pre-Quaternary uplift and dissection of Cenozoic erosion surfaces. In the field trip area, northeast- and northwest-trending structural lineaments control fluvial and glacial drainage patterns. The Cowichan, Chemainus, Nanaimo, Englishman, Little and Big Qualicum, Tsable and Comox rivers occupy broad, U-shaped troughs that dissect uplands and the Vancouver Island Ranges. Late Quaternary units are well exposed in these valleys (Fyles 1963).

For example, along Cowichan River, the oldest sediments are locally exposed in cut-banks, and include oxidized fluvial sand and gravels and organic-rich estuarine silt and clay (Huntley et al. 2001). These deposits are older than 23 ka and overlie a glacial erosion surface of greater antiquity: they are assigned to the Middle Wisconsinan Cowichan Head Formation, and older glacial or non-glacial intervals (Halstead 1968).

Late Wisconsinan Fraser Glaciation landscapes

<u>Glacial Advance</u>

Fraser Glaciation advance-phase sediments, termed Quadra Sand, were deposited after 23 ka (Halstead 1968; **Figure S1-5** a; *see* **STOP 4**). Advance phase deposits in the Cowichan (**Figure S1-6**, log 1) and other major valleys include: ice-distal fluvial sand and gravel, and lacustrine silt and clay; ice-proximal outwash gravels; and debris flow deposits (Clague et al. 1980).

Valleys draining the Vancouver Island Ranges and Nanaimo Lowland were glaciated before 19 ka. During the glacial maximum phase, the Vancouver Island Ice Sheet was confluent with Coast Mountain ice occupying the Gulf Islands and glacial Salish Sea, to form the Cordilleran Ice Sheet (Clague et al. 1980; **Figure S1-5** b).

Below 1100 m elevation, bedrock and older sediments are overlain by drumlinized morainal deposits consisting of lodgement and melt-out till, and subglacial fluvial sediments (**Figure S1-7** a-c). These tills are assigned to the Vashon Drift (Hicock and Armstrong 1983), and are best preserved in glacially-scoured bedrock depressions in uplands, in valleys and coastal bluffs (**Figure S1-6**, log 1; *see* **STOP 4**). Bedrock surfaces have been striated and streamlined by ice and subglacial meltwater flow. The distribution and orientation of roches moutonnées, drumlins, till fabrics and erratics (**Figure S1-3** b) indicate that between 19 and 15 ka, southeast-flowing glaciers from the Vancouver Island Ranges were confluent with south-flowing ice in the Salish Sea basin (**Figure S1-7** a-f). Subglacial meltwater flow was in the direction of iceflow (i.e., southward).

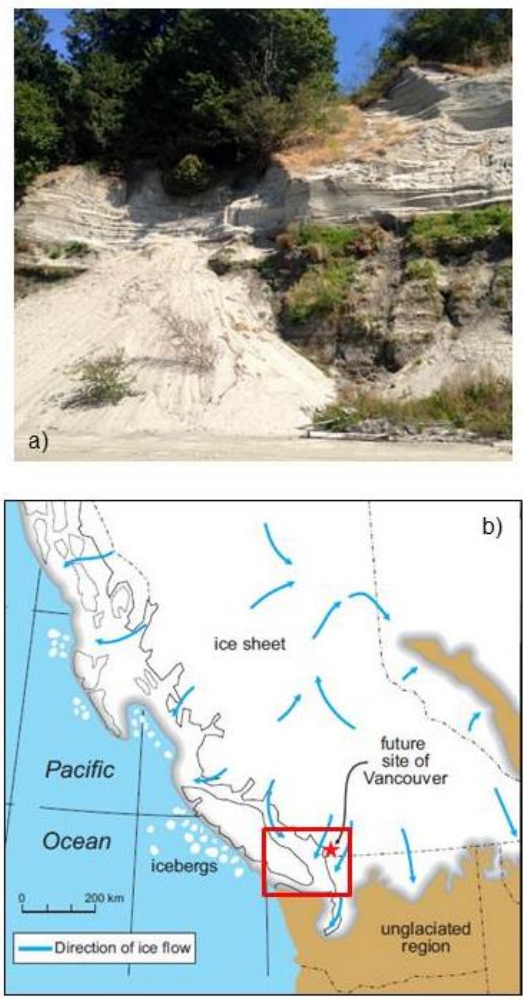

Figure S1-5 a) Quadra Sand exposed at Island View Beach on Saanich Peninsula, southern Vancouver Island (photo credit David Mosher). b) Maximum extent of the Cordilleran Ice Sheet during the last glaciation (adapted from: Turner et al. 2010).

Relict periglacial terrain occurs on mountain peaks above 1100 m elevation (**Figure S1-7** a). This elevation is interpreted to represent a minimum limit to glaciation prior to onset of deglaciation around 18 ka (Huntley et al. 2001). Almost a kilometre of ice from the Vancouver Island Ranges covered the lowlands around Victoria, Duncan, Nanaimo, Port Alberni and Comox at the last glacial maximum. The Comox Glacier is a remnant of the Vancouver Island Ice sheet.

<u>Glacial Retreat</u>

Retreat of the southern and western ice sheet margins began shortly after 14 ka (Clague et al. 1980). Mountains and uplands were deglaciated early as the regional equilibrium line altitude rose above the elevation of local cirques.

Between 14 and 12 ka, the Salish Sea was deglaciated as marine waters inundated glacio-isostatically-depressed coastal areas (Clague et al. 1982; **Figure S1-7** h-j). Recessional glacier trimlines at 900, 600, 400, 300 and 100 m elevation are inferred from the distribution and elevation range of glacially eroded bedrock scarps, proglacial colluvium and glaciofluvial outwash. Cowichan, Nanaimo Somass and Comox river valleys were ice-free before 10 ka (**Figure S1-7** k).

Retreat-phase deposits, termed Capilano Sediments (Hicock and Armstrong 1983), include ice-contact and proglacial colluvium, glaciofluvial, glaciolacustrine and glaciomarine deposits (*see* **STOP 3**).

In proglacial settings, exposed bedrock surfaces, subglacial sediments and supraglacial debris were extensively reworked by meltwater and submarine mass-movement. Ice-contact kame deposits at 900 and 400 m elevation indicate that early during deglaciation, sub-aerial meltwater flow was directed southwest and southeast (**Figure S1-7** b, c). Hydrologic continuity between ice-free areas was likely maintained by eskers, subglacial sheet flow and supraglacial channels. Valley floors from 300 to 100 m elevation are blanketed by kettled moraine, ice-contact debris flows and ice-marginal alluvial fans (**Figure S1-6**, log 1). These deposits are extensively winnowed, channelized and mantled by glaciofluvial outwash and glaciolacustrine deposits.

Ice-marginal meltwater channels, outwash plains and kame terraces in the Chemainus and Cowichan valleys have average surface gradients of 10.4 m/km and 4.4 m/km, respectively. Lakes impounded by stagnant ice and outwash were short-lived and probably drained rapidly. West of Duncan, a series of southeast-trending ice-contact deltas onlap morainal and glaciofluvial deposits.

These features are graded to elevations between 100 and 80 m elevation and delimit stable grounding line positions for retreating glaciers in Sansum Narrows, Stuart Channel, Cowichan Bay, Quamichan lake basin, and the Cowichan and Koksilah river valleys (**Figure S1-5**, log 2). Foreset-facing directions, clast imbrication trends and channel orientations indicate meltwater drainage and sediment transport to an interlobate embayment formed near Victoria, Duncan and Somenos Lake basin (**Figure S1-7** d-i). Similar deposits are observed in valleys draining the Vancouver Island Ranges north of Nanaimo to Cumberland, Courtney and Comox (**Figure S1-8**).

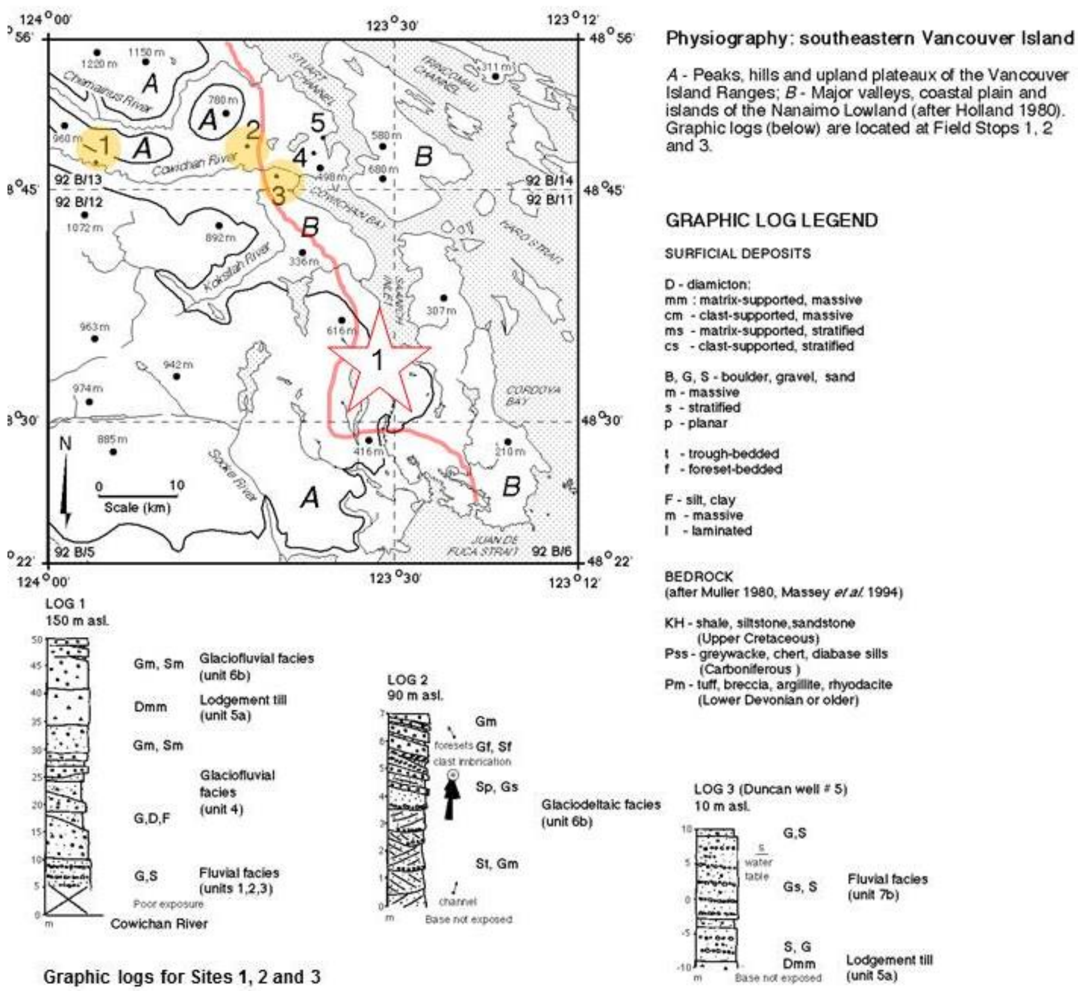

Figure S1-6 Surficial geology and physiography of the Victoria and Duncan areas; bold line marks physiographic boundary (modified from Huntley et al. 2001). STOP 1 (red star).

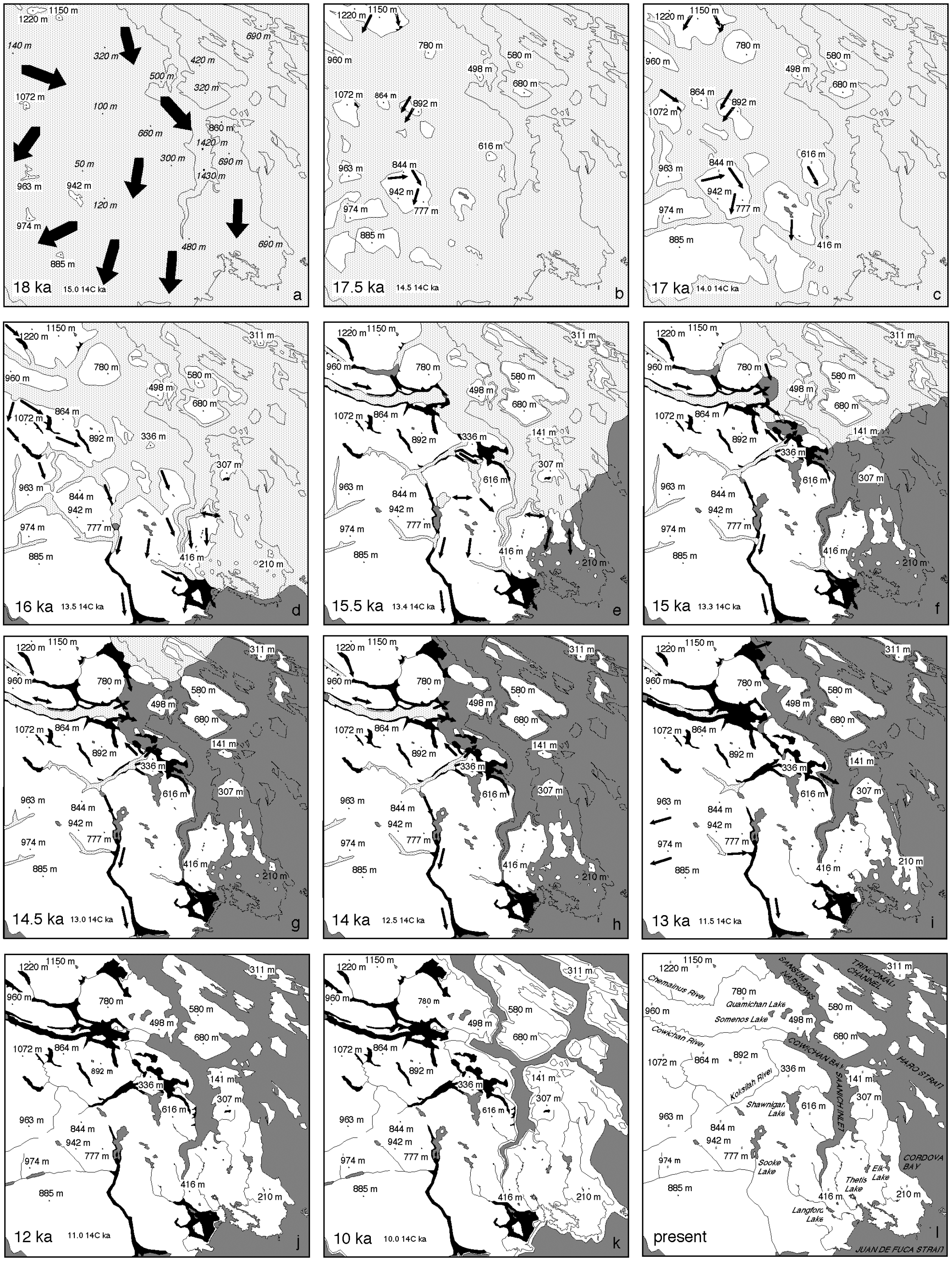

Figure S1-7 Deglaciation model for southwestern Vancouver Island spanning the last 18 ka, showing the consequences of changing relative sea level on the paleography of Saanich Inlet and lower Cowichan River valley; black areas are glaciofluvial outwash deposited graded to former marine high stands (modified from Huntley et al. 2001).

Ice-proximal glaciomarine debris-flows, sand and gravel outwash, and silt deposits drape winnowed till and bedrock below 80 m elevation (**Figure S1-6**, log 2). Southwest of Chemainus, ice-proximal glaciodeltaic sediments are graded to a lower marine stand of 40 m elevation (**Figure S1-7** i-j). The orientation of foreset beds and palaeochannels indicate that Chemainus River was deflected southward into Cowichan Bay by ice grounded in Stuart Channel late during deglaciation.

Figure S1-8 Late Wisconsinan ice-retreat phase glaciofluvial outwash in the upper Qualicum River valley. Gravel and sand aggregate is an important natural resource in British Columbia.

The elevation range of glaciodeltaic deposits delimits the extent of marine transgression in response to glacio-isostatic depression and eustatic sea-level rise during deglaciation (Mathews et al. 1970). Extensional faults and folds in glaciodeltaic and marine sediments are attributed to loss of support and relaxation of sediments as buried ice masses melted, ice margins retreated and relative base-level fell (Huntley et al. 2001).

Depositional high-stands range from 150 m elevation in Comox to 80 m elevation at Duncan and Victoria, indicating greater amounts of glacio-isostatic depression at the north end of the Salish basin. Lower still-stands below 40 m elevation indicate that sea-level fell relative to land as ice retreated, and likely represent periods when glacio-isostatic rebound and eustatic sea-level rise were approximately equal.

Saanich Inlet

Saanich Inlet is a glacial fjord that varies from 0.4 km to 7.6 km over its 26 km length. It has a maximum water depth of 238 m and averages water depth of about 120 m. The inlet consists of a single basin separated by a bedrock sill at the north end of the fjord from open ocean waters in Haro Strait (**Figure S1-6**, **Figure S1-9**). This sill rises to within 70 m of the surface, thereby restricting deep-water circulation. As a result, the lower part of the water column is anoxic (Bornhold et al. 1998).

A small amount of sediment enters from the south at the head of the inlet through Goldstream River. Most of the 9 x 10^4 tons of terrigenous sediment deposited annually in the fjord comes from the sediment plume of Cowichan River, which enters Cowichan Bay to the northwest of the head of the inlet (**Figure S1-6**, **Figure S1-9)**. A minor amount comes from the Fraser River plume which, on rare occasions, penetrates into the inlet. The sill also prevents any axial input of coarse sediments into the fjord as turbidity currents from the north. The abundance of freshwater in Haro Strait beyond the sill, principally from Fraser River, plus the high primary productivity in the inlet in spring and summer, and the sluggish estuarine circulation and anoxia, promote deposition and preservation of varves in the depths of the basin.

As a result of this rhythmic sedimentation pattern dating back through most of the Holocene (Bobrowsky and Clague 1990), the inlet was seen as a primary target for resolving paleoclimate and paleo-seismological records (Clague 1996). The inlet was drilled by ODP in 1996 (ODP Leg 169S, Blais-Stevens et al. 2001). Blais-Stevens et al. (2011) analyzed the stratigraphy of Saanich Inlet from these drill results and piston cores, using massive layers of coarser sediments deposited by submarine debris flows as proxies for an earthquake record.

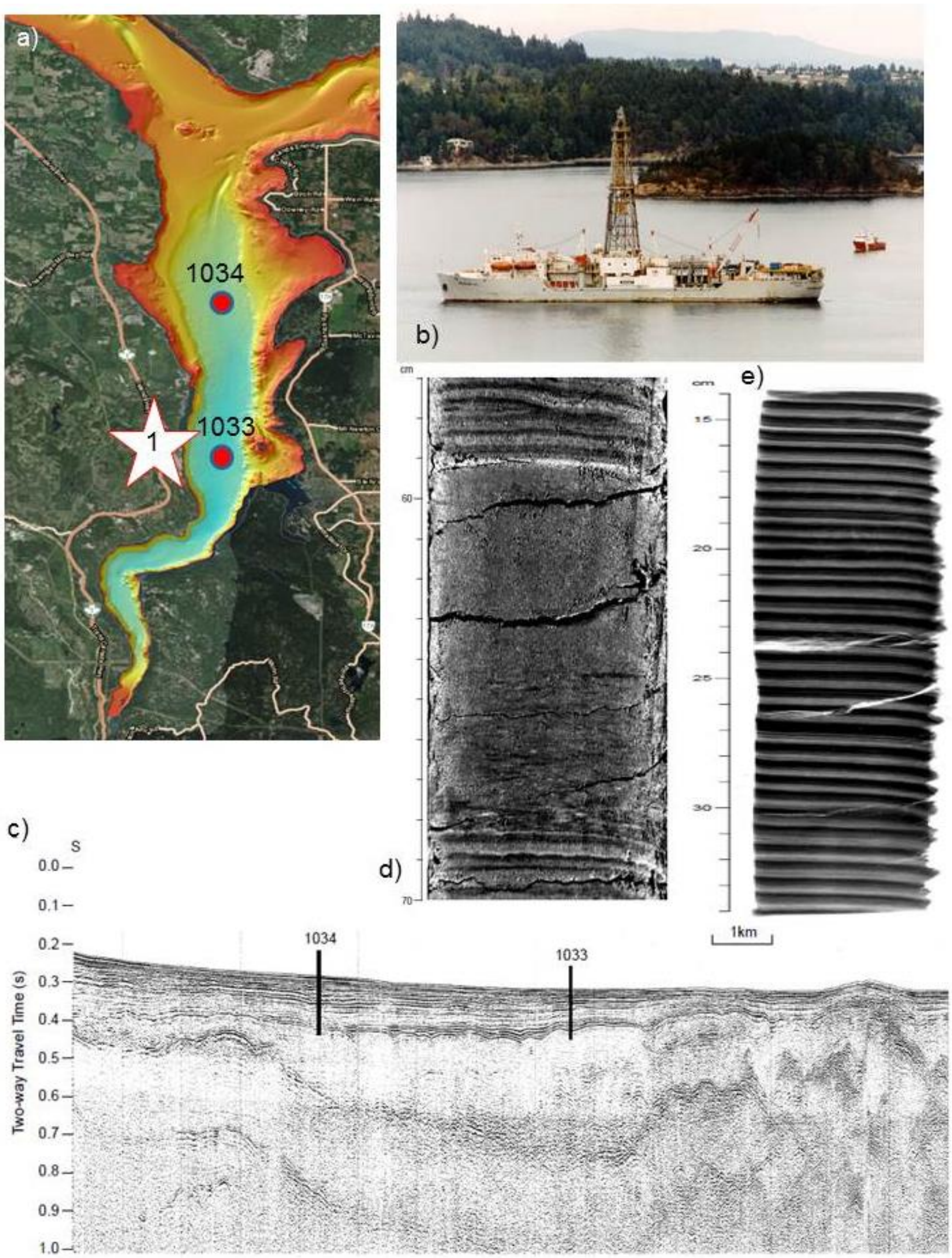

Figure S1-9 a) Saanich Inlet with drill site locations marked with red dots; b) JOIDES Resolution drilling in Saanich Inlet, 1996 (photo: D. Mosher); c) Seismic reflection profile down the axis of Saanich Inlet showing the location of the two drill sites (from Mosher and Moran 2001); d) core photograph of a massive layer bounded top and bottom by varves - these deposits are believed to represent a record of seismicity (from Bornhold et al. 1998); e) X-ray image of varves from ODP core (from Bornhold et al. 1998).

Two of the debris flow deposits correspond to known earthquakes: A.D. 1946 Vancouver Island (magnitude (M) 7.3) and the A.D. 1700 Cascadia plate-boundary subduction earthquake (M >9). Based on varve counts, 18 debris flows correlate among two or more cores during this time period, suggesting an average return period of strong shaking from earthquakes of about year 220. Nine of the debris flow deposits overlap with the age ranges for great plate-boundary earthquakes that have been determined by other paleoseismic studies (e.g., Clague and Bobrowsky 1994). The remaining nine events give an average return period of about 470 yr for strong shaking from local earthquakes.

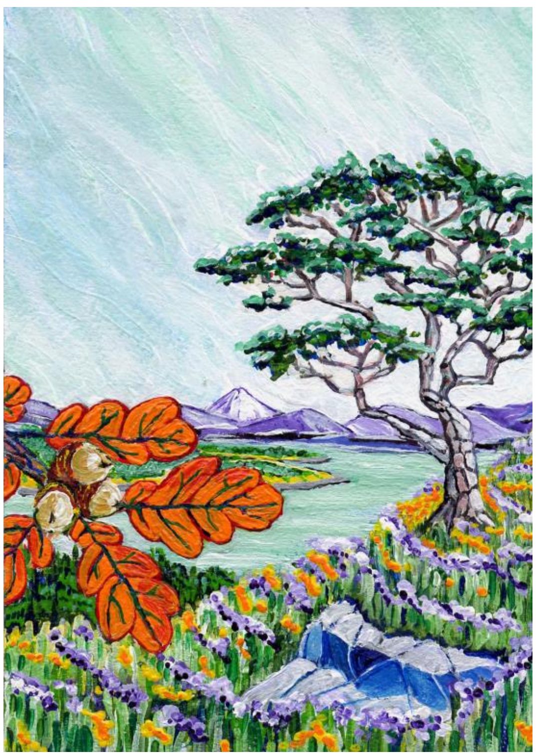

Figure S1-10 Garry oak and Camas are a part of the distinctive vegetation of the low-lying coastal plains around Victoria, Nanaimo and Vancouver comprising the Coastal Douglas-fir Biogeoclimatic Zone (painting: Orange Oak, D. Huntley 2001).

Forest ecosystems

Victoria, Nanaimo, Courtney and Comox all lie in the dry Coastal Douglas-fir Biogeoclimatic Zone (**Figure S1-10**). A unique ecosystem to this part of the Pacific Northwest is an open grassy woodland populated with Garry oak (*Quercus garryana*), Douglas-fir (*Pseudotsuga menzieseii*), Arbutus (*Arbutus menzieseii*), Camas (*Camas quamash*), invasive Broom (*Cytisus scoparius*) and numerous other shrubs, grasses, herbs, ferns, mosses and lichens (Pojar and MacKinnon 1994). You will learn more about BC forests and their ecological and historical importance at **STOP 2**.

Brief history of the Salish Sea area

Prior to first contact with Europeans, the Coast Salish nations built permanent winter villages and had fishing camps and other resource sites along shorelines and river mouths, whereas nearby mountains were used for hunting and spirit questing. Travelling by canoe, they accessed a network of sites on Vancouver Island, the Gulf Islands, Howe Sound, Burrard Inlet, Indian Arm, and the major rivers draining into the Salish Sea.

Oral traditions in the Pacific Northwest hold that long ago, but not remotely so, a struggle between Thunderbird (**Figure S1-11** a), who often perched on Black Tusk near Whistler, and Orca, the Whale, triggered an earthquake, tsunami and flooding in Pacific Northwest coastal regions (Thom 2003). Landslides, floods and other geological hazards leading to loss of life and property damage of villages do not feature explicitly in local stories and myths of villages on Vancouver Island, in Burrard Inlet or the Howe Sound area (Ludwin et al. 2005).

With the arrival of the first European explorers, fur traders, miners and loggers in the 19th Century, trails were cut across the mountains to access the resource-rich interiors of Vancouver Island and mainland British Columbia. Victoria, Duncan, Nanaimo, Port Alberni, Comox, Squamish and Vancouver were all established population centres by the late 1800s, supporting growing port facilities, ship building, fishing, mining and logging industries (**Figure S1-11** b).

By the early 1900s rail lines extended across Vancouver Island and connected Squamish with Lillooet on Fraser River in British Columbia's interior. Squamish remained the major shipping port for resources from the Interior until the 1950s. Through much of the 20th Century, coal mining on Vancouver Island, copper mining in Howe Sound, and clear-cut logging of old growth coastal rain forests have resulted in widespread disturbance of steep slopes.

In the 21st Century, transportation corridors on Vancouver Island and coastal mainland British Columbia include highways, railway tracks, oil and gas pipelines, hydroelectric power transmission lines, forestry operations, mines, quarries, borrow pits, public recreational facilities, and vibrant communities. The region is prone to significant earthquakes, high precipitation events, glacial melting, snow and debris avalanches, flooding and tidal surges, debris torrents, debris flows, rock and debris slides, and rockfalls.

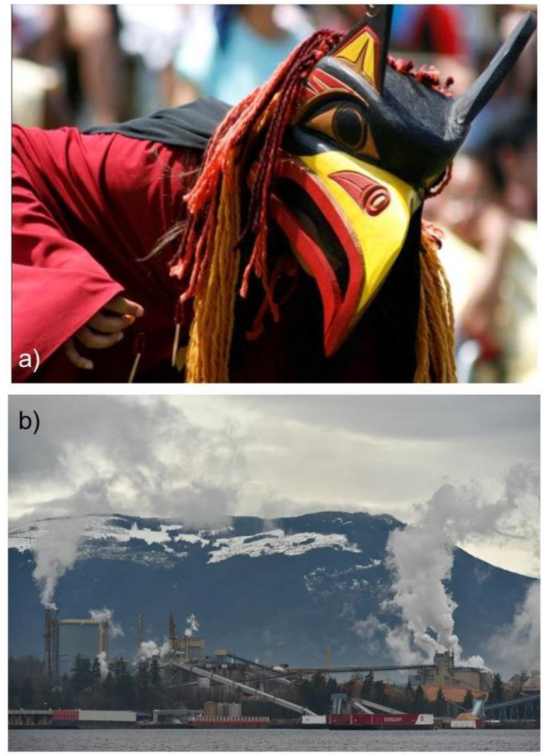

Figure S1-11 Changing cultural landscapes of the Salish Sea basin: a) Coast Salish First Nations were strongly dependent on the natural marine and terrestrial resources for food, clothing and ritual regalia (Thunderbird ceremonial mask, source: Tourism Vancouver); b) Pulp mills, like the facility at Crofton south of Nanaimo, processes timber (predominantly Western redcedar and Amabilis fir) harvested in the valleys draining the leeward Vancouver Island Ranges. Similar mills are located around the Salish Sea, Alberni Inlet (*see* DAY 1) and in the Howe Sound (*see* DAY 2).

STOP 2 Cathedral Grove: the ancient forests of Vancouver Island (30 minutes)

Introduction

STOP 2 is at Cameron Lake in the heart of the central Vancouver Island Ranges (**Figure S2-1** a). Here, you will take a short walk through an ancient "cathedral" forest grove dominated by Western redcedar (*Thuja plicata*) and Douglas-fir (*Pseudotsuga menzieseii*) developed in a riparian area in the transition zone between the Windward Island Mountain and Leeward Island Mountains ecosections (Pojar and Mackinnon 1994). McMillan Provincial Park, containing Cathedral Grove and Mt. Arrowsmith, was designated as a Biosphere Reserve by UNESCO in 2000 (**Figure S2-2**).

Geological setting

Cathedral Grove sits just west of Upper Cretaceous Nanaimo Group sedimentary rocks and within Devonian Nitinat Formation and Triassic Karmutsen formation volcanic rocks and Quatsino limestones of the Wrangellian Terrane (**Figure S1-2**). Wrangellia collided and accreted with North America about 100 Ma. The park lies along a major NW-SE trending thrust fault/fold belt created by this collision (**Figure P1-1**, **Figure S2-1** b).

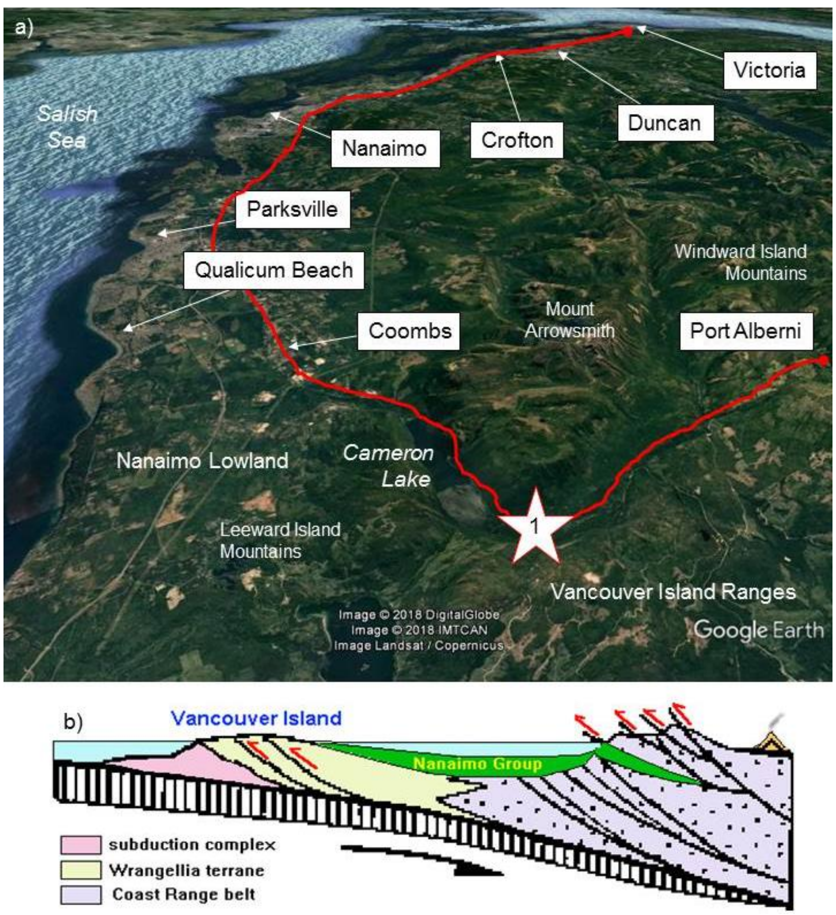

Figure S2-1 a) Location of STOP 2 in Cathedral Grove on southern Vancouver Island; also showing communities mentioned in the text. Google Earth image viewed looking south to Victoria; b) geological and plate tectonic setting of Vancouver Island in relation to mainland British Columbia (source: S. Earle, Vancouver Island University).

Figure S2-2 STOP 2, Cathedral Grove in McMillan Provincial Park**:** a) Cameron Lake; b) Western redcedar (*Thuja plicata*) and c) Douglas-fir (*Pseudotsuga menzieseii*).

But this is not a geology stop; it is an example of a British Columbia coastal old growth forest. Cathedral Grove is the only highway-accessible protected old growth forest in the Province.

Some of the trees are more than 800 years old and 9 m in circumference (**Figure S2-3**).

Figure S2-3 This old growth Douglas-fir is almost 3 m in diameter (photo source: B. Mosher).

Biogeoclimatic zones

The climate of southern and central Vancouver Island is characterized by relatively mild, wet winters and cool, partly overcast summers. Precipitation values range greater than 5000 mm on the west coast to less than 1000 mm on the east side of Vancouver Island. Coastal lowlands remain ice-free for most of the year. Snow fall is more persistent in mountainous valleys.

The forest at **STOP 2** is transitional between the drier Coastal Douglas-fir Biogeoclimatic Zone, which characterizes the east coast of Vancouver Island, and the wetter Coastal Western Hemlock Biogeoclimatic Zone, found along the island's west coast (Pojar and Mackinnon 1994).

Coniferous trees acclimatized to growing in low temperatures and with the summer-dry and winter-wet conditions dominate the forest landscape of southern Vancouver Island. On the wet, western maritime fringe and the Windward Island Mountain Ecosection, wind storms play a dominant role in the history of forest development. Drier forests in the Leeward Island Mountain Ecosection have disturbance histories in which fires have been frequent (Pojar and Mackinnon 1994).

Vegetation

The flora of the park is typical of the region. The dense, productive Pacific coastal temperate (seasonal) rain forest is populated by Western hemlock (*Tsuga heterophylla*), Western redcedar (*Thuja plicata*), Yellow-cedar (*Chamaecyparis nootkatensis*), Douglas-fir (*Pseudotsuga menzieseii*) and Amabilis fir (*Abies amabilis*). Sitka spruce (*Picea sitchensis*), Lodgepole (Shore) pine (*Pinus contorta* vr. *contorta*), Western yew (*Taxus brevifolia*), Bigleaf maple (*Acer macrophyllum*) and Red alder (*Alnus rubra*) are less common forest components.

The understory includes Sword fern (*Polystichum munitum*, **Figure S2-4**), Red huckleberry (*Vaccinium parvifolium*), White-flowered rhododendron (*Rhododendron albiflorum*), Salal (*Gaultheria shallon*) and Devil's club (*Oplopanax horridus*).

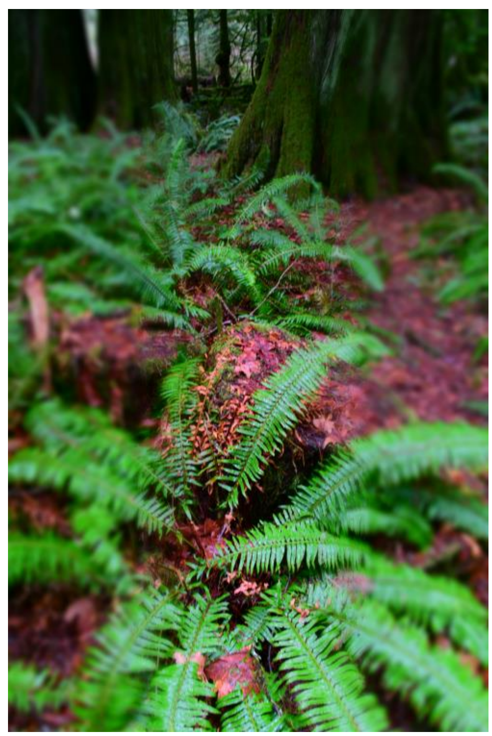

Figure S2-4 Sword fern (*Polystichum munitum*) is an indicator plant of productive vegetative growth on the hill slopes and riparian zones of Vancouver Island and coastal mainland British Columbia.

As you walk around the grove, take the time to identify the following trees:

Douglas-fir

A large tree, reaching heights of 85 m. Old trees have a long, branch-free trunk and a short cylindrical crown with a flattened top. Needles are flat with a pointed tip. The upper surface is bright yellowish-green with a single groove down the centre; the lower surface is paler. The needles appear to stand out around the twig (**Figure S2-5** a). Cones are 5 to 11 cm long, turning from green to grey as they mature. Between each scale, long three-pronged bracts are easily seen (**Figure S2-5** b. Seeds are winged at the tip. The bark is smooth and pale grey with blisters of pitch. It becomes scaly with age (**Figure S2-2** c; **Figure S2-3**).

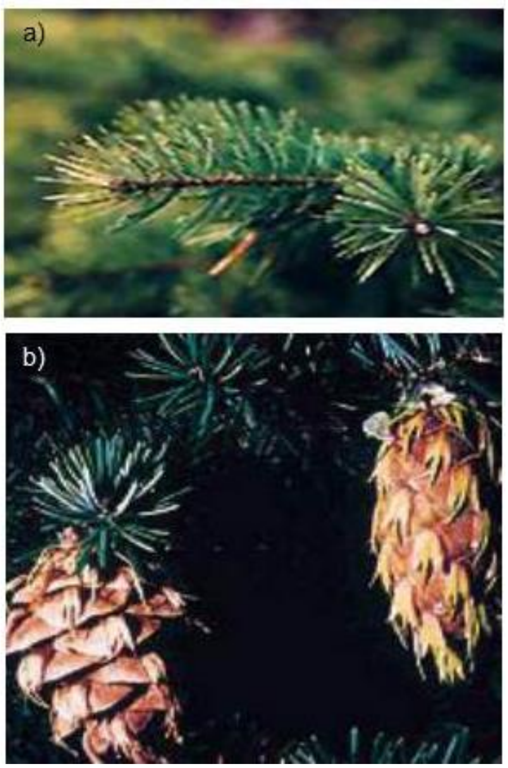

Figure S2-5 Douglas-fir: a) needle form; b) cone form (photo source: Parish et al. 1994).

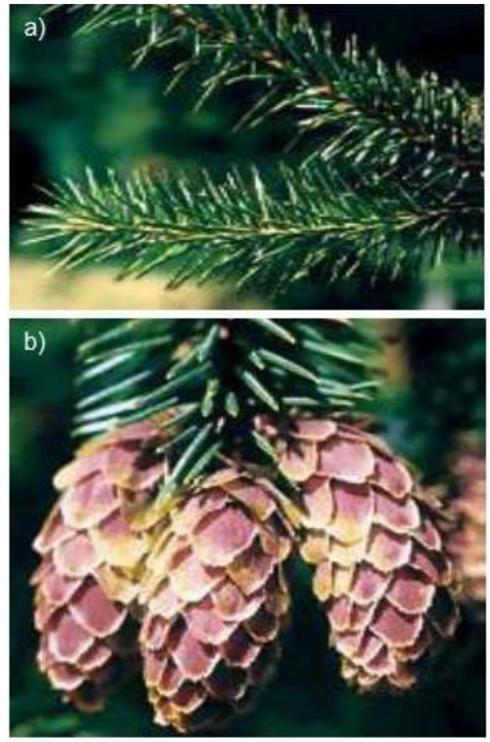

Figure S2-6 Sitka spruce: a) needle form; b) cone form (photo source: Parish et al. 1994).

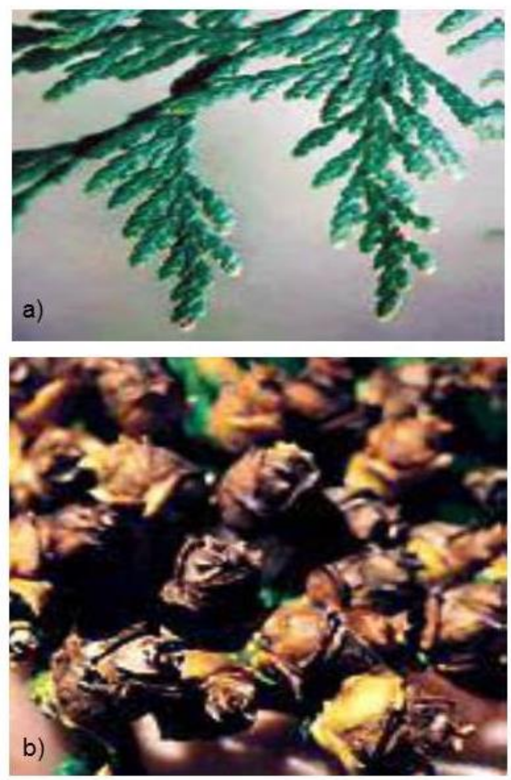

Figure S2-7 Western redcedar: a) needle form; b) cone form (photo source: Parish et al. 1994).

Sitka spruce

This tree commonly grows up to 70 m tall and 2 m across when mature. The largest known Sitka spruce is 93 m tall and 5 metres across! Needles are light green to bluish-green, stiff, and sharp. They are four-sided but slightly flattened with two white bands running along the upper surface and two narrower bands along the lower surface (**Figure S2-6** a). The needles are arranged spirally along the twig and are attached by small pegs which remain on the twig after the needles fall. Seed cones are reddish to yellowish-brown and hang from the crown (**Figure S2-6** b). Their seed scales are thin, wavy, and irregularly toothed. Pollen cones are red. The bark is very thin, brown or purplish grey, and breaks up into small scales.

Western Redcedar

This is a large tree, up to 60 m tall when mature, with drooping branches; trunk often spreading out widely at the base. Leaves are scale-like, in opposite pairs, in four rows, folded in one pair but not in the other and overlapping like shingles (**Figure S2-7** a). They are arranged on the twigs in flat, fan-like sprays. Leaves have a very strong aroma. Seed cones are egg-shaped, 1 cm long, with several pairs of scales (**Figure S2-7** b). Pollen cones are small and reddish. The bark is grey, stringy, tearing off in long strips on mature trees.

Wildlife

The park is home to several species of birds, including eagles, owls and woodpeckers; as well as such mammals as black bear, elk and cougar. The Cameron River and Cameron Lake are stocked with rainbow, brown, and cutthroat trout.

Vancouver Island Marmot

The Vancouver Island Marmot is one of 14 marmot species worldwide and one of the most critically endangered mammals in the world (**Figure S2-8**). Found only on Vancouver Island, they are easily identified by their unique appearance and differ from other marmot species in behaviour, genetics and ecology. Due to the efforts of a recovery program, the marmot count in the wild increased from less than 30 wild marmots in 2003, to an estimated 250-300 in 2015 (E-Fauna BC 2018).

Figure S2-8 Vancouver Island Marmot (photo source: A. Bryant).

Roosevelt Elk

This is the largest of the four surviving subspecies of elk in North America (**Figure S2-9**). They live in the rain forests of the Pacific Northwest and Cathedral Grove is a critical habitat for the elk. Adults grow to around 1.8–3 m in length and stand 0.75–1.5 m tall at the shoulder. Elk bulls generally weigh between 300 and 500 kg, while cows weigh 260 to 285 kg.

Figure S2-9 Roosevelt Elk (image source: http://www.geog.uvic.ca/viwilds/iw-elk.html).

Cougars

Mountain lions, or pumas, range up and down the western part of North America. A fully grown male weighs around 70 kg (**Figure S2-10** a). About 600-800 of the big cats reside on Vancouver Island, representing the highest density of the animal in North America. **Figure S2-10** (b) is a map of Cougar attacks in North

America. Guess where we are? Because we are on an island that is becoming increasing populated by humans, coupled with the fact that there is no hunting of the big cats permitted, there are significantly more human/cat encounters than elsewhere in North America (E-Fauna BC 2018).

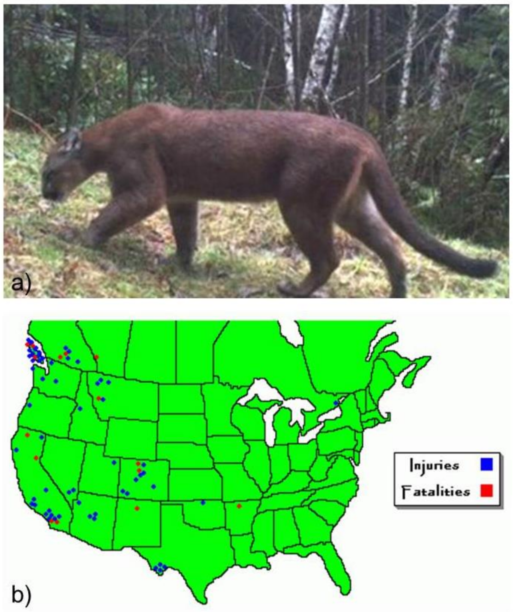

Figure S2-10 a) Cougar or Mountain Lion; b) Cougar attacks in the US and Canada since 1970 (photo source: J. Mosher).

Black Bears

The Black Bear is one of the most common large mammals on Vancouver Island (**Figure S2-11**). Contact with humans is frequent (E-Fauna BC 2018). Island bears are a larger and blacker than their mainland cousins, with females growing up to 180 kg, and the males reaching 275 kg. This is likely as a result of Vancouver Island being a genetically "older" variation of the bear, having remained relatively isolated from the mainland breeding pool. Skeletons found in caves near Port Hardy indicate that the bear has been a resident of the island for the last 10 ka.

Wolves

Wolves of Vancouver Island are one of its shyest and most elusive creatures (**Figure S2-12**). A subspecies of the mainland grey wolf, this animal is endemic to Vancouver Island, and is considered an endangered species (E-Fauna BC 2018). Living in packs from five to 20, the wolves usually stay far from human activity. They are most common on the northern portions of the island, and as well within Barkley and Clayoquot Sounds, where most of their human contact takes place. The Vancouver Island wolf weighs between 20 and 60 kg (male, females smaller), and is generally lighter in colour than the mainland species, with some animals appearing almost completely white. These animals prey mainly on black-tailed deer and Roosevelt elk, only taking smaller game, such as squirrels, rodents, and beaver, when larger prey are scarce. Another hallmark of the Vancouver Island subspecies is their higher living density, up to 14 animals per km^2.

Figure S2-11 Black Bear (image source: http://www.geog.uvic.ca/viwilds/iw-bear.html).

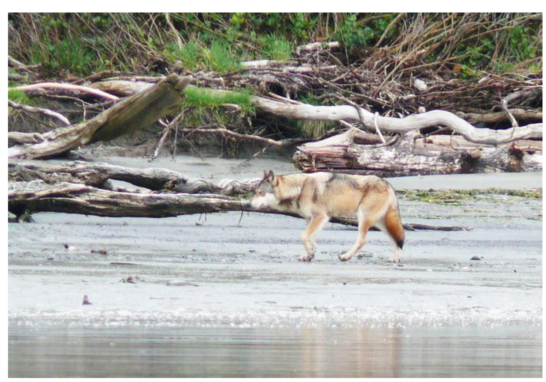

Figure S2-12 Wolf (image source: Source: http://www.geog.uvic.ca/viwilds/iw-wolf.html).

Land use changes and impacts

Pre-contact aboriginal land management practices, together with modern urban and rural development have profoundly impacted the forest structure of southern Vancouver Island and the Gulf Islands.

Nuu-Chah-Nulth (Nootka) people, specifically the Tseshaht and Hupacasath First Nations, are believed to have used the area for ceremonial purposes prior to the arrival of European settlers in the mid-19th Century. Evidence of *culturally modified* trees (**Figure S2-13** a) have been dated as far back as AD 1137. This suggests First Nations have used Cathedral Grove for 1000s of years as a source for medicinal plants and cedar bark for traditional regalia, hats and baskets (**Figure S1-11** a, **Figure 2-13** b).

Most gentle to moderately sloping hillsides you will observe on the field trip were clear-cut logged between the late-1800s and late 20th century. Many forests now are second- or third-growth stands that are of harvestable age. A significant change in forest management practices occurred in the 1990s and early 21st century. Selective logging, stand retention, riparian protection and minimizing the impact on forest soils are now standard forest practices on Vancouver Island and mainland British Columbia.

Figure S2-13 a) Culturally-modified Western redcedar trunks (photo source: J. Lawrence); b) Nootka ceremonial mask (photo source: D. Mosher).

STOP 3 Port Alberni: plate boundary earthquakes and tsunami records (1 hour, including lunch)

Introduction

STOP 3 in Port Alberni is a site that been inundated by earthquake-generated tsunamis on multiple occasions during Holocene times. You will also have lunch at this spot.

Physiography of Port Alberni area

The Alberni Basin is an area of low relief extending from the head of Alberni Inlet northwest to the Vancouver Island Ranges. It is 40 km long by 10 to 15 km wide. Numerous rivers (e.g., Sproat and Somass rivers) and creeks drain into Alberni Canal and Alberni Inlet.

To the northeast it is sharply bounded by an abrupt fault scarp along the western front of the Beaufort Range. The 300 m elevation contour delimits the boundary with the Vancouver Island Ranges in the south and west. The basin is underlain by upper Cretaceous sedimentary rocks (Nanaimo Group) derived from surrounding older uplifted volcanic and intrusive rocks (e.g., Island Intrusions and Karmutsen Formation, **Figure S1-3** b).

Earthquakes and the consequences

Coastal British Columbia has a complex tectonic history (Parrish 1983). Pre-Upper Jurassic (ca. 200-160 Ma) to early-Upper Cretaceous (100-66 Ma) ductile sinistral shearing accompanying magmatic events was followed by Neogene (Miocene-Pliocene, ca. 20–2 Ma) brittle dextral faulting during the formation of the Queen Charlotte Basin underlying Hecate Strait and reorganization of plate boundaries along the western continental margin (Massey et al. 2005; **Figure S3-1** b).

The region is presently seismically active (Hyndman 1995). The plate boundary structure of the Pacific Northwest and low Arctic latitudes includes: 1) the Cascadia subduction zone; 2) the Fairweather-Queen Charlotte transform fault zone; and 3) the Aleutian subduction zone (**Figure S3-1** a, b). Large and great earthquakes in coastal British Columbia, including a M 7.3 event in 1946, a M 8.1 event in 1949, and a M 7.8 event in 2012 did not generate significant or damaging tsunamis, and geological records are not preserved.

Subduction triggered great and giant earthquakes in the Pacific Basin include Japan in 2011 (M 9.1); Alaska in 1964 (M 9.1); the Aleutian Islands in 1957 (M 9.1), 1946 (M 8.1), and 1788 (M >8.0); and Cascadia in 1700 (M 8.7-9.2). Geological evidence of such failures is preserved in offshore turbidites; submarine sediments in fjords; in lacustrine sequences of low elevation lakes; and terrestrial soils in inlets, embayments and coves along the Pacific coastline from northern California, Oregon and Washington to British Columbia and Alaska (**Figure S3-1** a).

Earthquake and geophysical modelling indicate that subduction boundaries can fail by breakage of short segments or by almost simultaneous rupture along most of their length, generating tsunami events with the potential to preserve evidence over a wide geographic extent. Although historical deposits of far-field tsunamis have been reported from the Pacific Northwest (e.g., Clague and Bobrowsky 1994), and as far north as the Aleutian-Alaska coast, knowledge gaps remain in understanding the frequency and magnitude of paleotsunami events for much of coastal British Columbia.

Paleo-tsunami research

The Geological Survey of Canada (GSC) and international partners are focusing their attention on salt marsh peat deposits as geological records of marine inundation and flood events in the Pacific Northwest. Pioneering research by Clague and Bobrowsky (1994) identified multiple thin sheets of sand and gravel in Holocene tidal mud and peat (**Figure S3-2**). These deposits were attributed to tsunamis generated by great earthquakes in the Pacific basin at Port Alberni and other locations on the west coast of Vancouver Island (e.g., Tofino and Ucluelet).

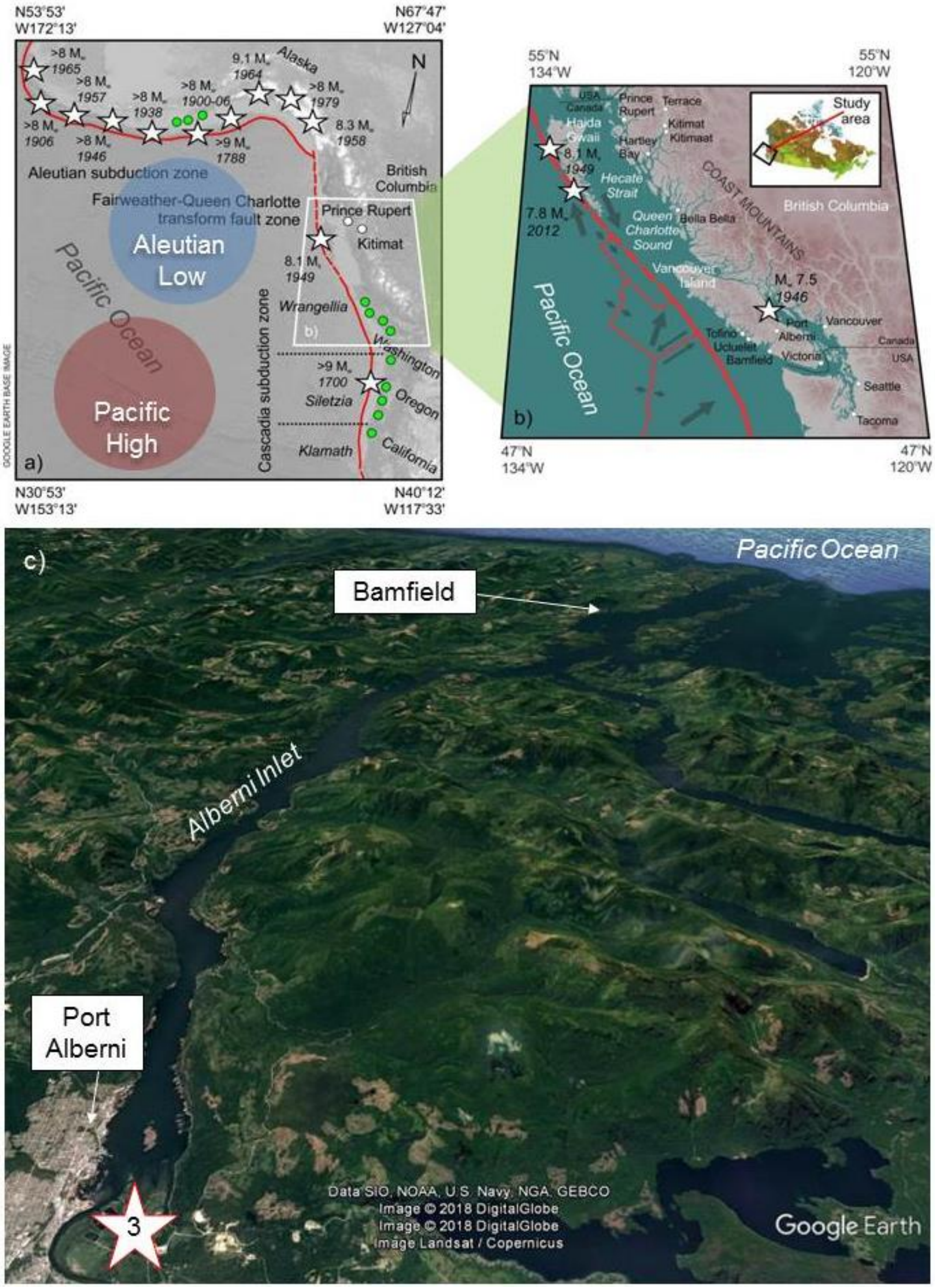

Figure S3-1 STOP 3, Port Alberni: a) location of > M 8 earthquakes in the Pacific Northwest (green dots are terrestrial tsunami deposits in coastal lowlands), and relative positions of the north Pacific pressure cells; b) tectonic plate margins off the coast of Vancouver Island; c) location of field stop at the head of Alberni Inlet (view to southwest).

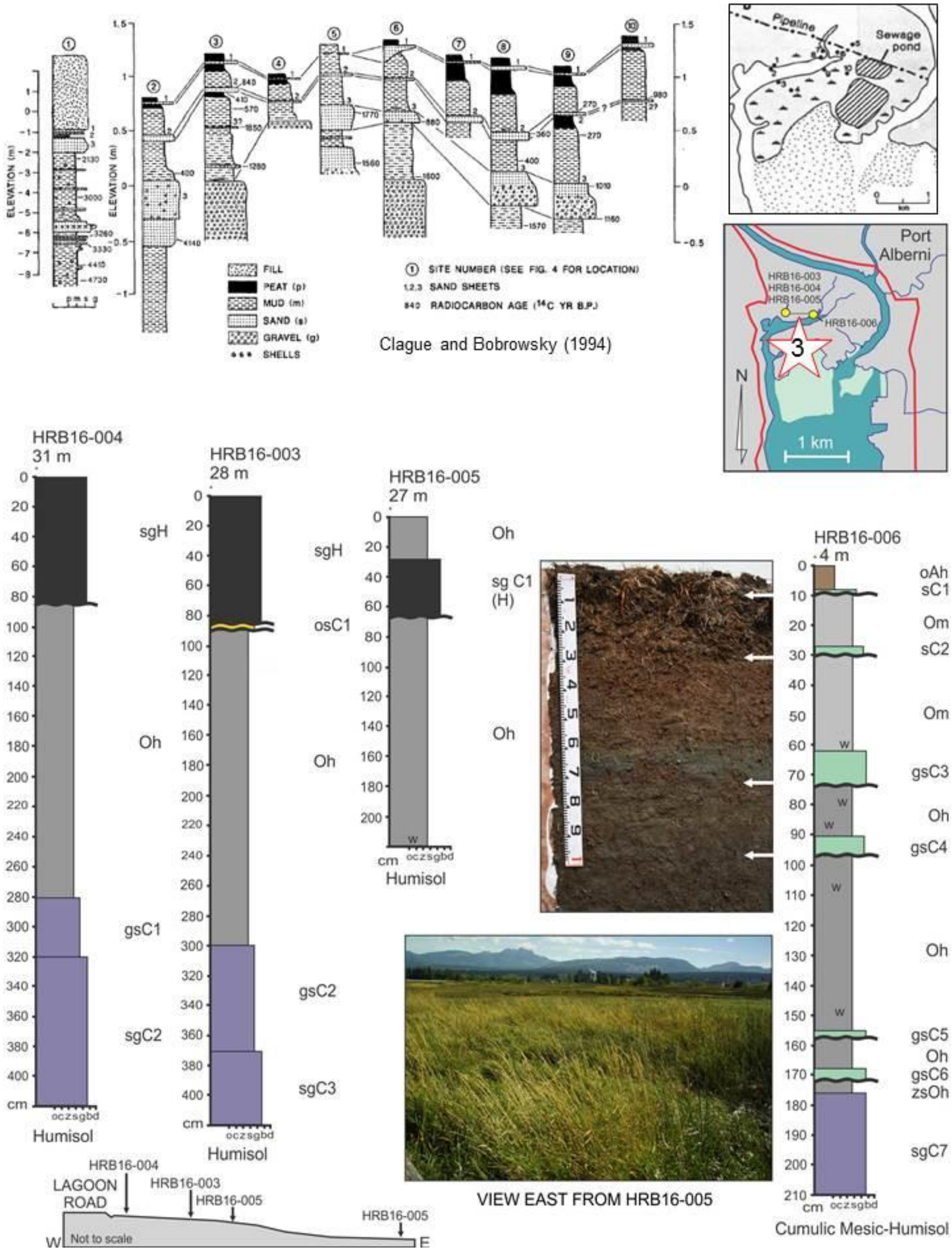

Figure S3-2 Tsunami deposits preserved in cumulic organic soils at the head of Alberni Inlet. Pioneering descriptions by Clague and Bobrowsky (1994) reveal multiple sand sheets interpreted as tsunami deposits. Site re-visited and sampled in 2015 and 2016. For HRB16-004, mineral horizon C1 is interpreted as the tsunami deposit from the 1964 Alaska earthquake; C2 is a possible storm or flood deposit; C3 is the tsunami deposit associated with the 1700 Cascadia event; C4 is a >1700 tsunami deposit; C5 and C6 are interpreted as storm or flood deposits of early postglacial Somass River; C7 is ice-proximal glaciomarine gravel and sand.

History of tsunamis

Most recently, the 1964 Alaska tsunami caused significant damage to coastal infrastructure on the west coast of Vancouver Island. At Port Alberni, three main waves struck the town over a 3 hour interval, with the most destructive wave being the second.

A municipal water pipe near **STOP 3** was broken (**Figure S3-3**) and around 260 homes were inundated. Damage costs were approximately equivalent to $80 million in 2018 dollars: considerable, given that Port Alberni was relatively undeveloped at that time.

At **STOP 3**, the 1964 tsunami reached a maximum height of 7 m and inundated the tidal marsh to a depth of 4 to 5 m. Sand and mud was deposited widely across the site and elsewhere in low-lying parts of the town. This deposit is now buried under 54 years of peat accumulation (**Figure S3-2**). Two lower tsunami layers are related to the 1700 Cascadia and earlier earthquakes (Tanigawa et al. 2017).

Field recognition of tsunami deposits

At **STOP 3** you will examine clastic deposits in intertidal peat marshes and supratidal forest soils collected from the Port Alberni sewage and water treatment site on the Somass River delta (**Figure S3-2**). Marine inundation deposits are attributed to great earthquake-generated tsunamis, displacement waves triggered by landslides on steep coastal slopes and storm surge waves in the Alberni Inlet, and flood events from glacierized Cordilleran watersheds.

Detailed analyses of sedimentology, radiocarbon dates, fossils, and geochemistry are helping to establish a postglacial record of tsunami, storm and flood events spanning much of the Holocene. This extended record will constrain modelling of future geohazard events, thereby reducing development risks in north coastal British Columbia where recurrent storm surges, floods, landslides, earthquakes and tsunamis challenge development of safe, secure infrastructure and communities (**Figure S3-4**).

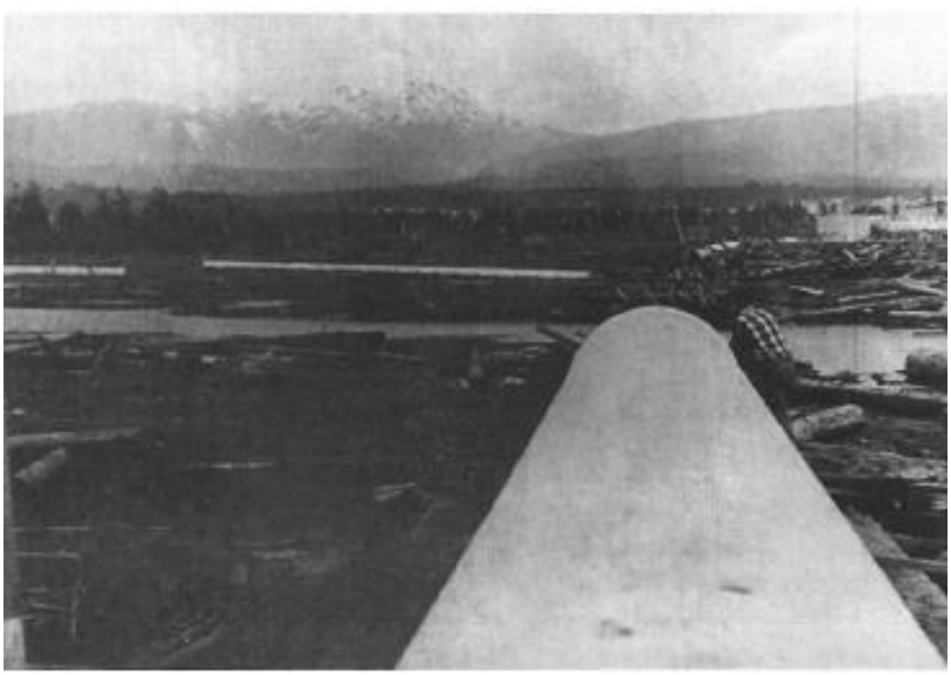

Figure S3-3 Breached water pipeline on the Somass River delta shortly after the 1964 tsunami. Source image: Port Alberni Museum photo 4383 (from Clague and Bobrowsky 1994).

Figure S3-4 STOP 3, Port Alberni highlights: a) harbour facilities, pulp mills and civic buildings in low-lying parts of the town are at risk during a tsunami; and, b) risk reduction measures include signage and early warning sirens.

STOP 4 Mapleguard and Goose Spits: Earthquakes, tsunamis, coastal erosion and mitigation (30 minutes)

Introduction

STOP 4 (A and B) is near the epicentre of the Comox 1946 M 7.3 (M_w 7.5) earthquake (Mathews 1979; **Figure S4-1** a, b). This strike-slip fault triggered soil disturbances sand boils, liquefaction and minor shoreline changes in low lying coastal areas around the central Salish Sea, and damaged buildings and infrastructure (Rogers 1980; **Figure S4-1** c, d).

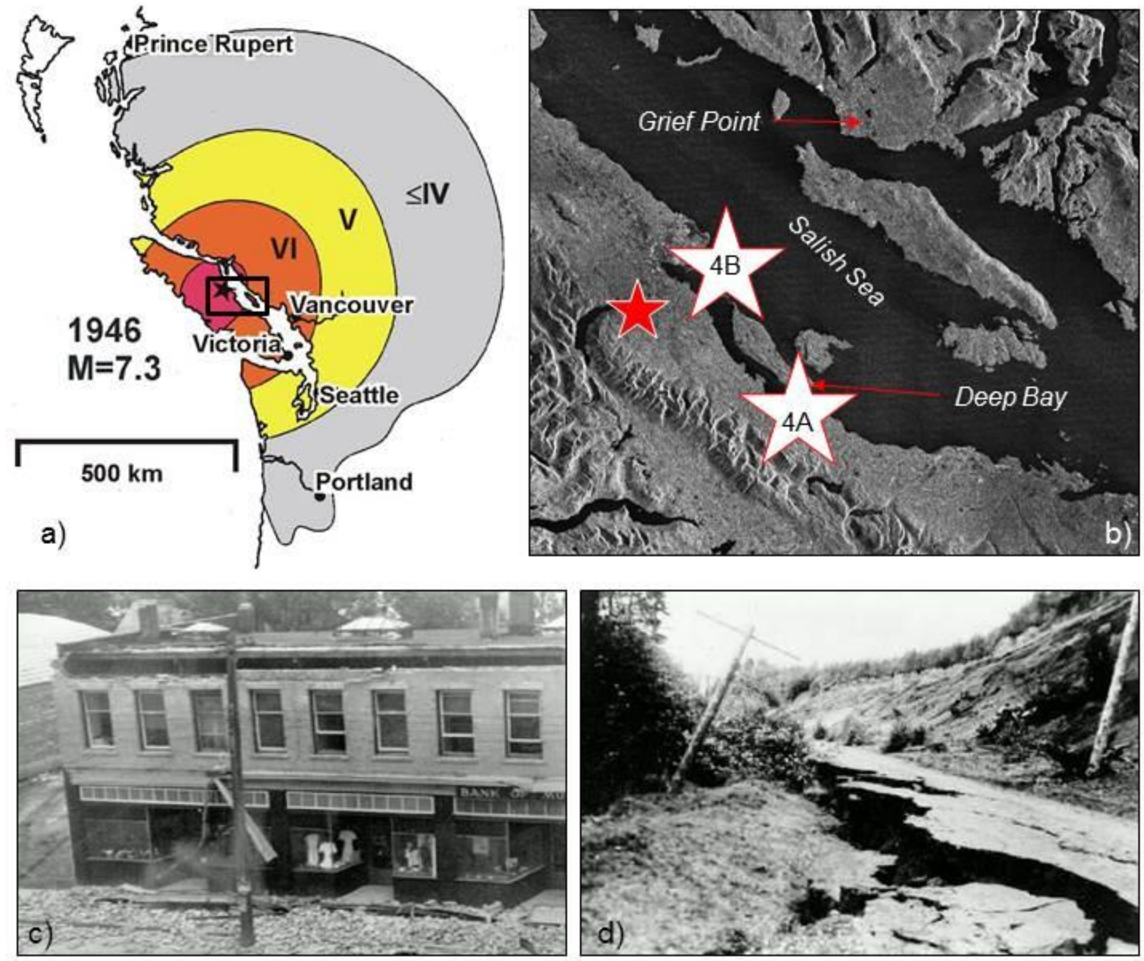

Figure S4-1 a) Location of 1946 Vancouver Island M 7.3 strike-slip earthquake (from Rogers 1980); b) location of submarine slides generated by earthquake shaking; c) consequences of 1946 Comox valley earthquake, damage to buildings and dock structures; d) damage to roads and railway tracks (from Mosher et al. 2009).

Marine surveys

Mapleguard Spit and Goose Spit (**Figure S4-1** b) were surveyed in November 1999 with a Kongsberg-Simrad EM-3000 multibeam sonar system. The EM-3000 is a 300 kHz sonar system. It has 127 beams per ping in an angular sector of up to 130 degrees, and can map a swath as wide as 4 times the water depth. The multibeam data were gridded at 1 m for analysis and display (Mosher et al. 2009).

Mapleguard Spit

This subaerially exposed gravel barrier spit faces Baynes Channel on one side and Deep Bay on its back-barrier side (**Figure S4-2**, **Figure S4-3** a, b). It is oriented east-west and is about 1 km long. A 1 km-wide intertidal sandy platform flanks the north side of the spit to within 250 m of the west end (**Figure S4-3** a). About 25 homes are built on the spit itself and Deep Bay contains marina and dock facilities (Blais et al. 2006).

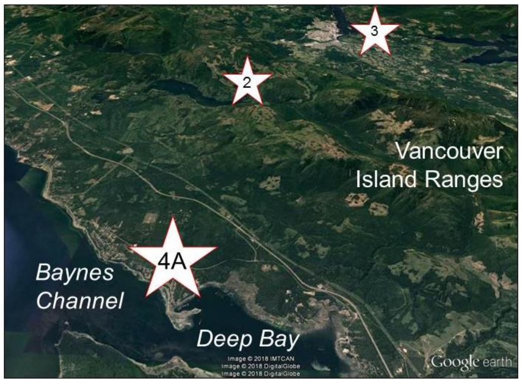

Figure S4-2 Location of Mapleguard Spit (STOP 4A); view to west; distance from STOP 3 to STOP 4 is approximately 50 km.

Mapleguard Spit is 55 km from the epicentre of the 1946 earthquake (**Figure S4-1** a). Sand boils and liquefaction trenches (lateral spreading) were observed on the spit following the earthquake. The western end of the spit failed during the earthquake, producing a steep embankment at the west tip and north side. The initial retreat was reported to be about 6 m, and the steep initial slopes continued to fail for 3 to 4 weeks afterwards. Water depths on this western portion of the spit increased from 0.6 m to over 30 m during this period. A large wave generated by this submarine failure capsized a boat and resulted in the only death directly related to the 1946 earthquake (Mosher et al. 2009).

The present-day morphology of Mapleguard spit shows slope angles up to 35° on the upper slope near the low tide water line (Mosher et al. 2009). The average slope angle of the spit is about 20°. The failure area, presumably resulting from the 1946 earthquake landslide, totals 362,000 m^2. The failure lobes have a blocky morphology, which is unexpected given that the material exposed at the beach is unlithified, well-sorted, well-rounded gravel. These blocks are up to 4 m in height and diameter and can reach 60 m^3 in volume. The failure lobes also show high backscatter intensity relative to the surrounding seafloor (**Figure S4-3** c-e).

From shallow sediment cores, the top of the landslide material is gravel or gravel in mud, overlying coarse sand to muddy sand, with possible intervals of gravel to gravelly-mud elsewhere in the core (**Figure S4-3** f). Cores Tul00A-16 and 17 are from the toe of the lobe deposit and have about 0.5 m of sandy gravel overlying sand at their tops. Core Tul00A-16 has several 0.5 m thick intervals of sandy gravel deeper in section, whereas Tul00A-17 becomes finer-grained (silty fine sand) down core. Core Tul00A-018 has about 0.75 m of gravel and gravelly mud overlying medium-sized sand, whereas Core Tul00A-21 has no gravel at all and consists entirely of fine sand with wood fragments. Cores Tul00A-19 and 20 are from the northern sediment lobe. Core 19 consists of 2 m of gravel and muddy gravel. Core 20 shows gravel at the surface with several intervals of sandy gravel within mostly sand down core (Mosher et al. 2009).

The stiff mud matrix of the failed material and the blocky nature of the deposit indicate that consolidated soil must have failed in the earthquake to maintain its competence during flow. This inference is supported by the fact that a large wave was generated at the time of the landslide; a fully liquefied flow would not displace water to generate a wave (Mosher et al. 2009).

Two more recent collapses of the spit with associated beach regression have taken place on April 28, 1998 and April 21, 1999 (**Figure S4-3** b). The beach retrogressed at its western tip during the first of these events by an estimated 100 m. During the 1999 event, the beach on the southern side of the western tip retrogressed an estimated 10 m. Long-time residents had not observed such events since the 1946 earthquake. The western Canada seismograph network showed no correlative ground accelerations and no significant tide or wave heights were noted (Mosher et al. 2009).

The first failure occurred during a spring tide with a predicted low-tide that day of 0.95 m. The second failure followed a 1.23-m low tide, two days after the spring tide. There is no obvious trigger mechanism for these failures. Relatively normal tidal drawdown causing excess pore pressure, acting on a beach profile that had surpassed its equilibrium slope is one explanation. These failures were presumably liquefied relative to the submarine landslide of 1946, as there is little evidence of deposits on the seafloor (Mosher et al. 2009).

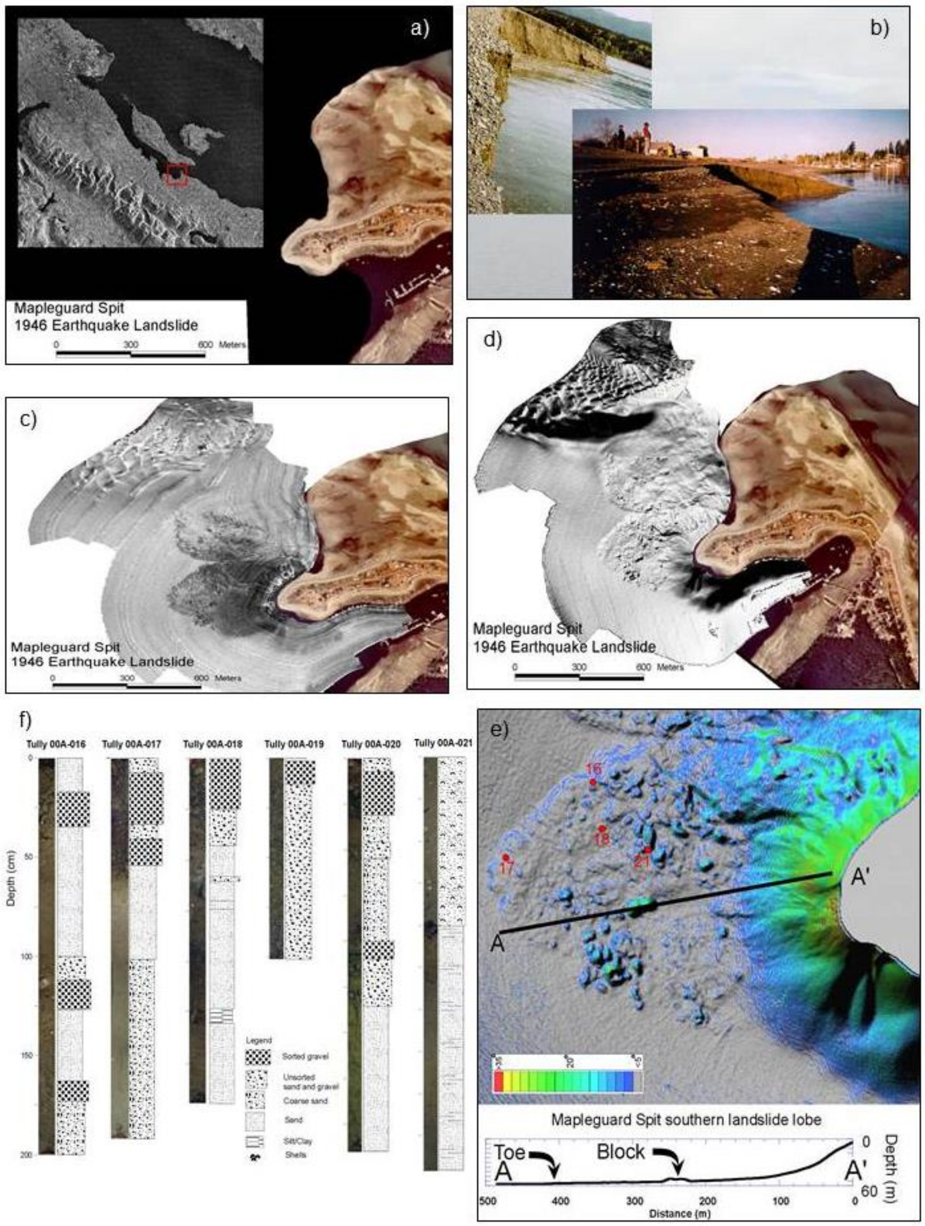

Figure S4-3 Surface renderings of the multibeam data revealed two submarine lobe-shaped deposits of sediment on the west-facing, exposed side of the spit: a) location of Mapleguard Spit; b) ground recent collapses of the spit on April 28, 1998 and April 21, 1999; c) backscatter intensity of slump lobes; d) sun-shaded surface render of the offshore and an air photo image of the subaerial and intertidal region; e) slope angle render, profile is at 1:1 scale, red points represent core sites; f) cores collected from sites on slump (modified from Mosher et al. 2009).

Goose Spit

West-facing submarine portions of Goose Spit (**Figure S4-4**) failed during the earthquake and retreated up to 6 m, generating damaging tsunamis in Comox Harbour. Similar to Mapleguard Spit, Goose Spit continued to retreat for a month following the earthquake, possibly related to smaller aftershocks (Mosher et al. 2009). These smaller submarine slumps did not generate tsunamis, implying that only earthquakes and submarine mass movement above threshold volume and impulse energy produce geomorphically significant inundation events. However, even small submarine landslides have tsunamigenic potential in the Salish Sea since they occur in shallow water.

Submarine slumps scars and debris that generated a tsunami in Comox Harbour during the 1946 earthquake was imaged by backscatter and multibeam (**Figure S4-5** c, d). Vibrocores (22, 23) were also recovered from the toe slope (**Figure S4-5** e, f).

Also at this stop, you will observe some of the common mass movement processes and other geomorphic activity taking place around the modern Salish Sea shoreline. The main longshore current direction is from the north. Storm waves and the longshore current contribute to the erosion of Quadra Sand exposed in the Willemar Bluffs, providing sediment that is moved alongshore to create Goose Spit (**Figure S4-5** a). The current extends into Comox Harbour where it slows, depositing much of its sediment load. A lagoon has formed behind the spit (**Figure S4-4**). You can gauge the effectiveness of engineering solutions aimed at reducing the rate of beach erosion and lowering the risk to the properties at the top of the bluff (**Figure S4-6**). Concrete blocks and riprap have been placed at the base of the bluff over a length of several hundred metres, with the objective of protecting the bluffs from wave erosion. Beyond, several groins have been placed to limit the effectiveness of the longshore current in eroding sediment from the beach.

Figure S4-4 Location of Goose Spit and Comox Harbour (STOP 4B); view to south.

Sea level is projected to rise between 0.2 m and 0.8 m by the end of this century and have significant implications for coastal communities and infrastructure around the Salish Sea coastline (cf. IPCC 2013). It is debateable whether or not the measures taken to reduce erosion will be effective in preserving the integrity and value of the properties at the top of the bluff. If they are effective, then they will reduce the sediment supply to the Goose Spit area. The spit could start to degrade, and the protected lagoon behind it could become exposed to the rough water of the Salish Sea. These areas are important marine habitats and much of this could be lost.

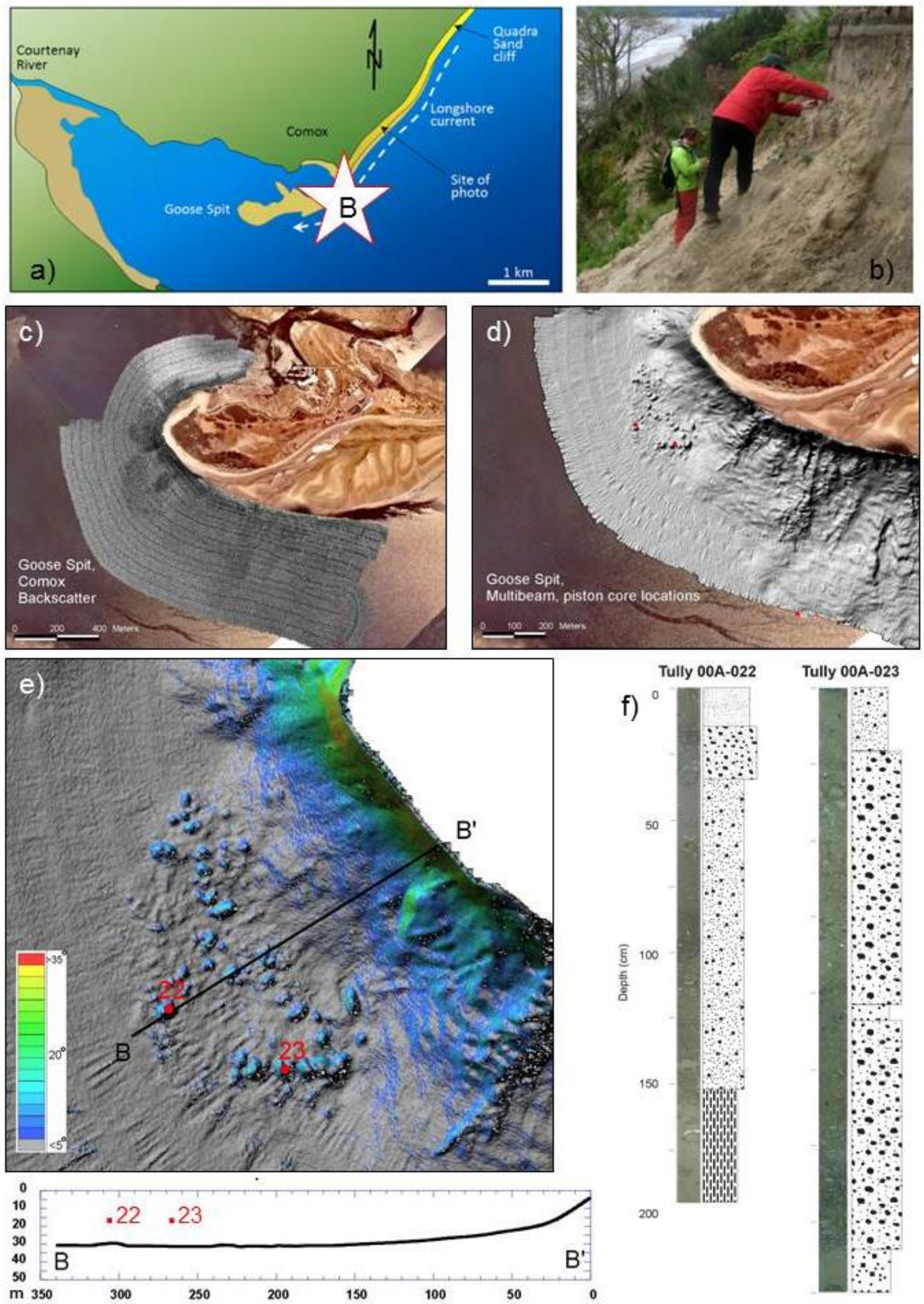

Figure S4-5 a) Location of STOP 4B on Goose Spit, Comox; b) exposure of Quadra Sand in Willemar Bluffs; c) backscatter image of submarine slump that generated a tsunami in Comox Harbour; d) multibeam image of submarine slump scars and debris related to the 1946 event; e) slope angles over the slope and location of vibrocores 22 and 23; f) vibracores (22, 23) recovered from the toe slope of the Goose Spit submarine slump (modified from Mosher et al 2009).

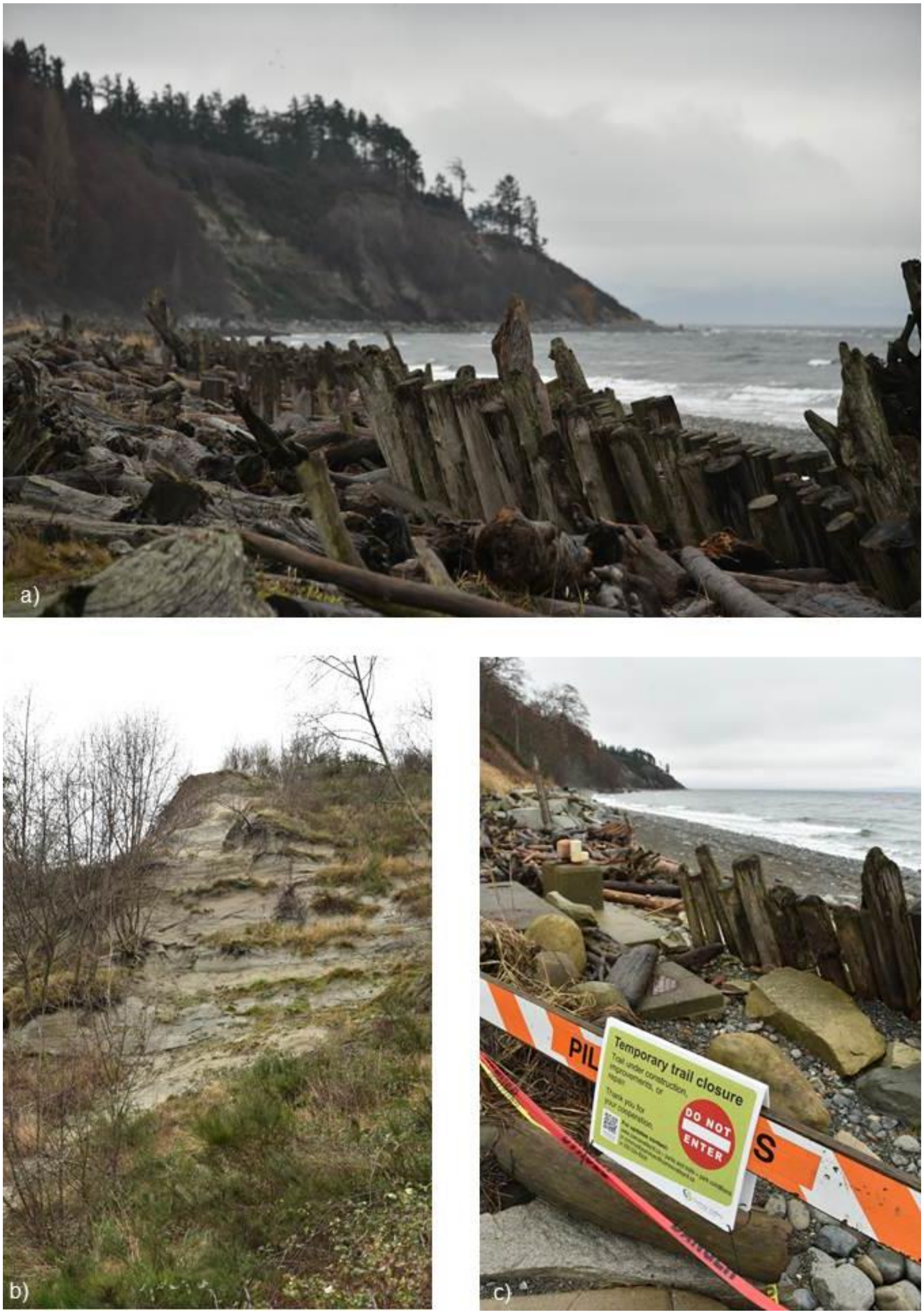

Figure S4-6 a) STOP 4, Goose Spit and Willemar Bluffs in 2018; b) exposure of Quadra Sand and Vashon till in coastal bluffs; c) with rising sea level and stronger storm surges, concrete blocks, riprap (broken rock) barriers and groins are proving to be ineffective at managing coastal erosion.

Anthropocene landscape: Nanaimo

The modern city of Nanaimo lies in the traditional Coast Salish territory of the Snuneymuxw First Nation (**Figure S4-7**).

Coal was discovered inland of the Wintuhuysen Inlet in 1849 and initially mined by the Hudson's Bay Company. At the same time, clear-cutting of old growth Douglas-fir, Western redcedar and other conifers began the deforestation of the Nanaimo Lowland and lower slopes of the Vancouver Island Ranges. A small forestry and coal mining community, Colville, became Nanaimo in 1860. Peak coal production was in 1922 with 1.4 million tons mined. The last mine closed in 1968.

Today, Nanaimo faces a number of environmental challenges related to past mining activities including localized subsidence and contamination of streams and lake basins. On a positive note, some old mine shafts have become flooded with geothermally heated groundwater, and are a potential energy targets for the city to exploit. Since the 1970s, the timber industry has dominated the city's economy, with a number of pulp mills in the surrounding are supplied by a rich hinterland of productive second and third growth forest.

Figure S4-7 a) Many Coast Salish petroglyphs at Nanaimo are greater than 300 years old and are representative of rock art at ceremonial sites from Oregon to Alaska; b) Modern infrastructure and urban environment: the port city of Nanaimo, Vancouver Island was established in the traditional Wintuhuysen Inlet.

DAY 2 Squamish to Victoria

STOP 5 Squamish: geohazards and emergency planning, policies and constraints (30 minutes)

Introduction

DAY 2 begins in Squamish and ends in Victoria, with stops along the Sea to Sky Highway (Highway 99) in Howe Sound and overlooking the Fraser River delta (**Figure P1-1**, **Figure S5-1** a). You return to Vancouver Island on the ferry from Tsawwassen to Swartz Bay, arriving back in Victoria around 9 pm.

STOP 5 is at Squamish (**Figure S5-1** b). At this stop, you will review the Quaternary history southwestern British Columbia and discuss the terrestrial and marine geohazards impacting critical infrastructure in the Sea-to-Sky corridor in Howe Sound.

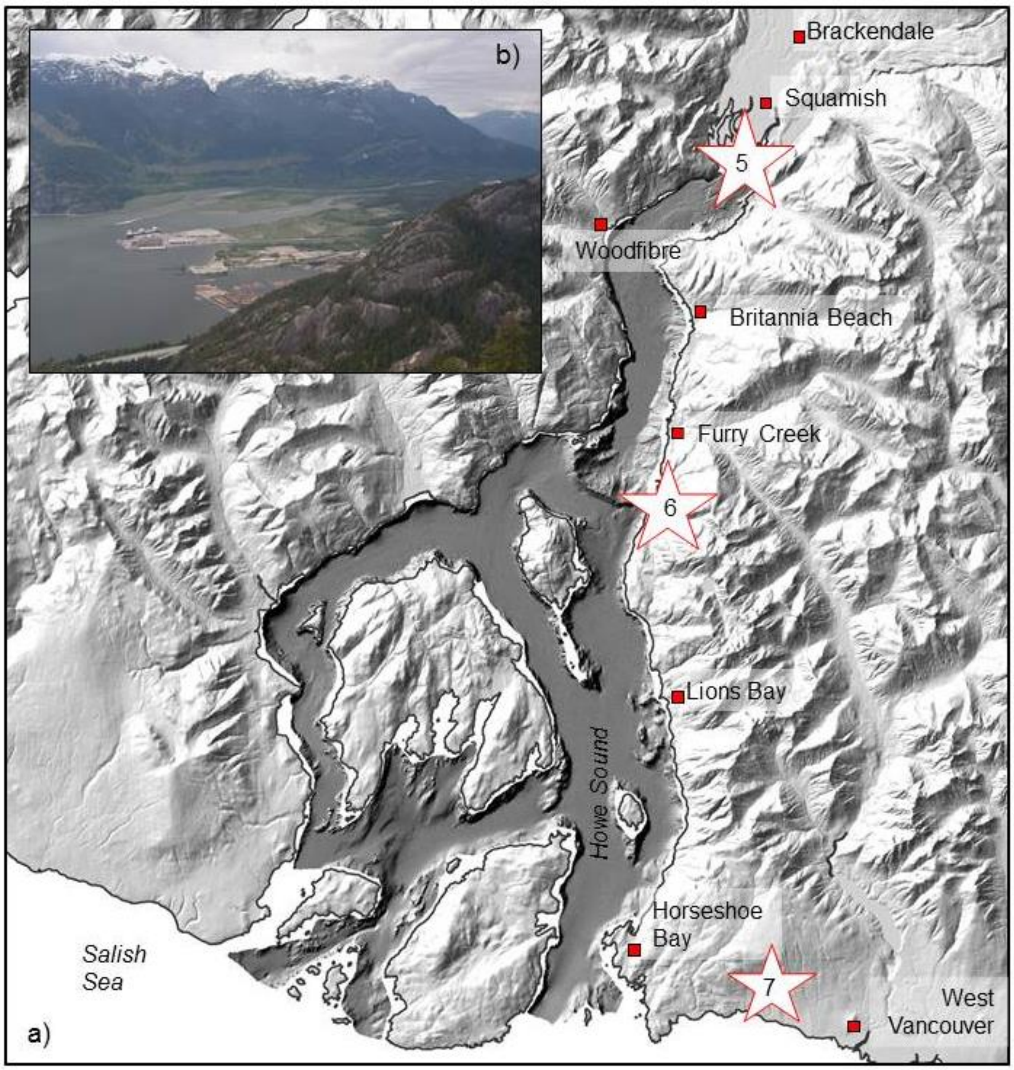

Figure S5-1 a) Field stops along the Sea-to-Sky Highway (Highway 99) and Howe Sound, with major communities and location of the Woodfibre pulp mill. b) Squamish River delta with deep-water port facilities and BC Hydro power transmission corridor on the far wall; in the foreground, Highway 99 and CN Rail run at the base of very steep and glacially streamlined granodiorite.

Quaternary landscape of Howe Sound, and lower Fraser River valley and delta

Howe Sound is western Canada's most populated and industrialized fjord (Blais-Stevens and Hungr 2008). Geophysical investigations indicate the maximum depth of water in Howe Sound to be 300 m, and the depth to bedrock to be a further 500 m. Thus, a 200 m thick Quaternary sedimentary record of multiple cycles and volcanism is preserved in the fjord (Prior and Bornhold 1984).

Quaternary volcanism

Quaternary volcanoes in southern British Columbia occur in the linear, north-trending Garibaldi belt in the southern Coast Mountains (Read 1990). This now dormant (or extinct) volcanic belt includes about 32 cones and domes of andesite, dacite, and minor basalt which probably formed in response to subduction of the Juan de Fuca plate and glacio-isostatic adjustment of the crust during repeated glacial and interglacial cycles through the Quaternary Period.

At **STOP 5**, Mt. Garibaldi overlooks Squamish and Brackendale (**Figure S5-2** a, b). During the last glaciation, the Squamish River valley was filled by glacier ice. Explosive eruptions led to the build-up of a volcanic edifice partly founded on bedrock to the east and supraglacially to the west. The western flank collapsed as ice retreated from the valley in a series of extremely large landslides. Erosion of this unstable landslide debris led to the formation of paraglacial fans that spread across the Squamish River valley. The most common geological hazards associated with volcanoes in the Squamish River valley are rockfalls and debris flows (Blais-Stevens and Septer2008; **Figure S5-2** c).

Late Wisconsinan Fraser Glaciation landscapes

Glacial deposits in the Howe Sound fjord are approximately correlative with similar sediments on southern Vancouver Island (*see* **DAY 1**). The unconsolidated (surficial) sediments that drape the slopes of Howe Sound and infill the valleys and north of Squamish were deposited during the last major glaciation (Late Wisconsinan Fraser Glaciation, *ca*. 30 ka to 10 ka) and preceding non-glacial period (Olympia Non-glacial Interval 65 ka to 30 ka). Southwest of the mountains, around Vancouver, West Vancouver and North Vancouver, and further afield in the Salish Sea, Gulf Islands and on southeastern Vancouver Island, thick accumulations of proglacial sand (Quadra Sand) were deposited between 29 ka and 19 ka years ago (**Figure S1-5** a).

<u>Glacial Advance</u>

Glacial advance phase deposits were subsequently covered by till and gravelly ice-contact sediments (Vashon Drift) between 19 ka and 13 ka (cf. **Figure S1-5**).

At its maximum extent, the Cordilleran Ice Sheet reached an elevation of 2 km in the southern Coast Mountains and the weight of the ice sheet glacioisostatically depressed the crust up to 300 m. In comparison, 1000 m of ice over Vancouver Island resulted in glacioisostatic depression and late glacial relative sea level stands of 80 m to 150 m elevation (Friele and Clague 2002).

Major south-flowing outlets of the Cordilleran Ice Sheet occupied the Cheakamus and Squamish valleys at this time. These and other valley ice streams coalesced in the Howe Sound fjord then drained into the Salish Sea to merge with glaciers from Vancouver Island. By the onset of deglaciation, the ice sheet extended more than 300 km south of the US-Canada border (**Figure S1-5** b).

<u>Glacial retreat</u>

Deglaciation of coastal British Columbia began approximately 13.5 ka with glaciers retreating to cirque basins and local ice caps in the Coast Mountains by 10 ka. Ice retreat was accompanied by resurgent volcanic activity, particularly in the Garibaldi Volcanic Belt. Volcanic cliffs that formed above and in the contact with glaciers became unstable escarpments as ice retreated. These cliffs remain unstable and continue to fail by sporadic large rock avalanches and debris flows: for example, The Barrier on the southern flank of the Black Tusk (**Figure S5-2** A).

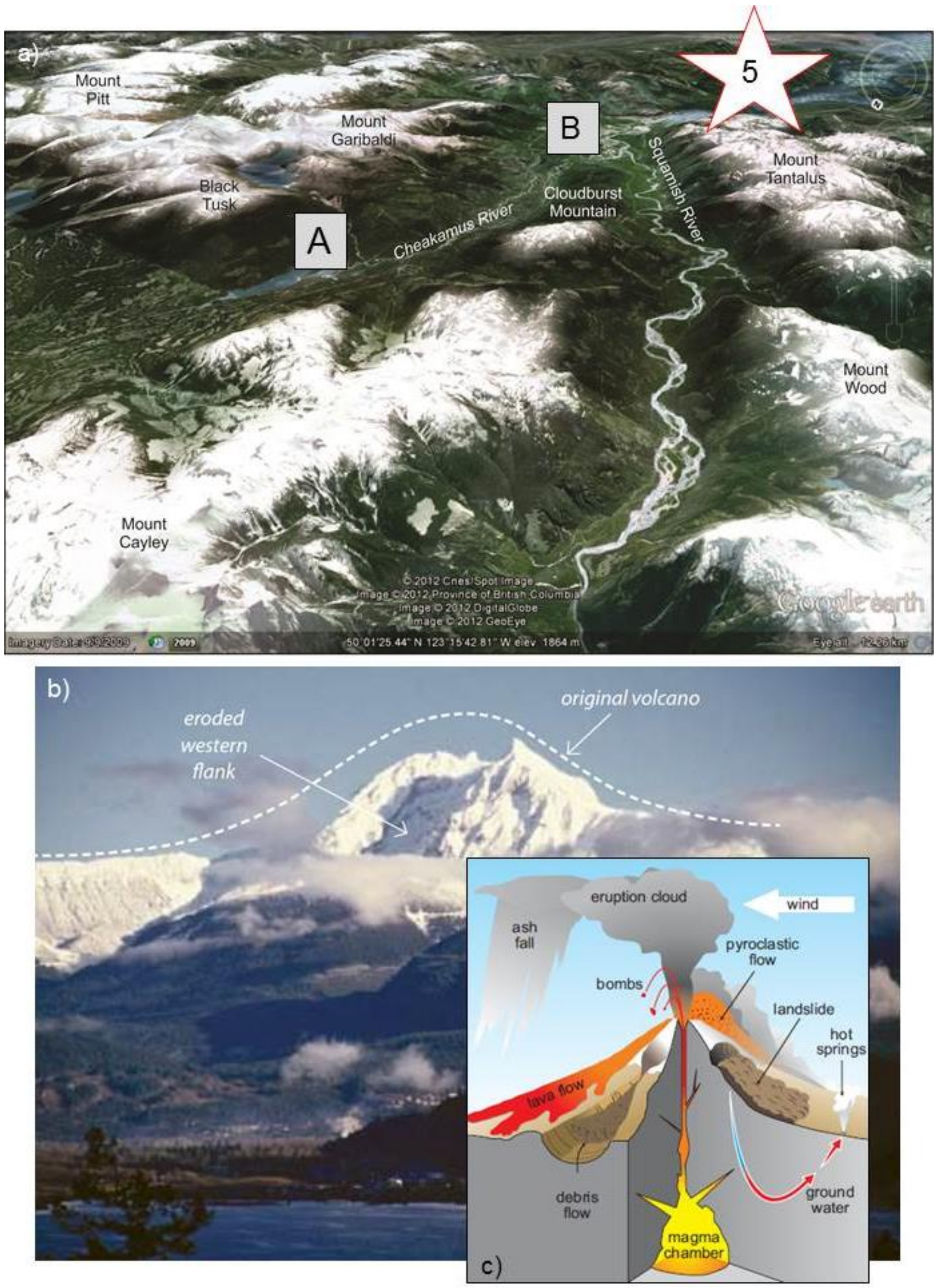

Figure S5-2 a) STOP 5: Lower Squamish Valley south of Mount Cayley, showing major rivers and creeks prone to debris avalanches and floods; The Barrier and Daisy Lake (A), Squamish-Brackendale (B) and Squamish River delta (red star 4). b) Mount Garibaldi viewed from Howe Sound showing projected cone developed during the waning stages of the last glaciation, 13 ka; c) Geological hazards accompanying volcanoes (active and dormant), landslides and debris flows are the most common in the Squamish River valley (modified from Turner et al. 2010).

Rising eustatic sea levels contributed to an initial rapid marine inundation of the Salish Sea and Howe Sound. Inundation along British Columbia's southern coast was determined by the magnitude of isostatic depression and the timing of local deglaciation. The marine limit at

Vancouver reached 200 m above modern sea level, reflecting the relatively early deglaciation of Fraser Lowland. Ice persisted later in Howe Sound blocking marine inundation until rebound was nearly complete. Consequently, the local marine limit in Howe Sound ranges from 100 m elevation (Blais-Stevens 2008) to between 45 m and 55 m above sea level, as recorded by numerous deltas along Highway 99 (Friele and Clague 2002).

Ice-free coastal slopes and valleys were draped with complex successions of unconsolidated, saturated and unstable glaciomarine, diamictons, subaqueous outwash sands and gravels, rhythmites with dropstones, fan delta deposits, and marine clays. Glacio-isostatic uplift, locally exceeding 300 m, was rapid and complete in the Vancouver area about 11 ka. With crustal rebound, stream delta and fan surfaces rose well above present sea level. Raised deltas and fans were deeply entrenched by mountain creeks which continued to build new deltas and fans into Howe Sound (Clague 1981).

Holocene and Anthropocene landscapes

Over the last 10 ka, the dominant geomorphic processes in the region have been: a) debris flows, debris torrents and floods along the creeks and in coastal zones (Hungr et al. 1984); b) rockfalls and rock slides on steep bedrock slopes (Evan and Savigny 1994; c) submarine slope failures in unconsolidated deposits (Prior and Bornhold 1986); d) debris avalanches in drainage basins with steep slopes exposing volcanic rock (Mathews 1958); and e) rock avalanches involving gravitational failure of over-steepened glaciated bedrock slopes (Thompson et al. 1997).

Coarse depositional debris fans, cones and deltas have formed where steep creeks drained into Howe Sound. Gravity-driven turbidity currents and debris flows, sliding and avalanching (rockfall) were the dominant processes in the underwater development of coarse-grained fan deltas in Howe Sound (Prior and Bornhold 1986).

Britannia Beach is an example of a coarse-grained fan delta undergoing gravitational sliding on the lower delta-slopes without extensive run-out of debris over the fjord bottom (Hizzett et al. 2017). Modern creeks draining into Howe Sound derive much of their sediment from eroding banks of relict delta and fan deposits, Pleistocene ice-contact debris and Holocene rockfall talus along the crests of steep catchment areas (Blais-Stevens and Kung 2009).

Under present climate conditions, landslide- and debris flow-triggering rainstorms most frequently occur when pronounced atmospheric depressions stall in the north Pacific Ocean causing strong south-westerly winds, warm air temperature and local storm cells (*see* **Figure S3-1** a). Orographic cooling of warm moist Pacific air as it rises up the western slopes of the Coast Mountains is responsible for periods of heavy precipitation on the North Shore Mountains, in Howe Sound, the Squamish River valley and Whistler areas.

Rainfall intensities are typically uneven, so that major runoff events in small drainage basins can occur at the same time moderate rainfalls are recorded at weather stations nearby. Most precipitation falls in autumn and winter, with mean annual precipitation ranges from approximately 1,500 mm in Vancouver to 3,500 mm in the high mountains (Evans and Savigny 1994).

During periods of unusually high annual precipitation, saturated soil veneers, unconsolidated earth materials and fractured bedrock along creeks and on the slopes are prone to failure and erosion by potentially destructive water floods, landslides, debris torrents and debris flows (Eisbacher 1983).

Temperature-sensitive slopes facing the Pacific Ocean also control the winter snow line. Winter snow packs of 300 to 400 cm can accumulate above 1,000 m elevation, whereas no snow remains on the lowlands. Sudden rises of the freezing level accompanied by heavy precipitation can enhance torrential runoff in winter and spring.

Depending on location, climate change may trigger positive or negative feedback in the groundwater recharge, flow and discharge, flooding and stream erosion, the extent and duration of wildfires, magnitude and frequency of landslides, and the distribution of wildlife and vegetation (IPCC 2013).

Over the next 50 years, measurable changes in spatial variations of temperature, precipitation and other climatic factors are expected to across Canada. For southwestern British Columbia, a number of geohazards are anticipated to negatively impact terrain, leaving communities, infrastructure, ecosystems and natural resources vulnerable to loss or damage.

For the Howe Sound, Fraser River delta and Salish Sea basin, future changes in maritime and polar storm system tracks, air pressure gradients, wind strength and duration, seasonal variations in temperatures, precipitation amounts, intensity and distribution of rainfall, and the snow line are expected result in an increase in the magnitude and frequency of: a) slides, slumps, debris flows and rockfalls; b) lightning strikes, wildfires, loss of vegetation on steep slopes and wind erosion of exposed sediment; and c) flooding, erosion and deposition in gullies, streams and rivers.

Community Geohazards

The traditional territory of the Skwxwú7mesh Úxwumixw (Squamish First Nation) in the lower Squamish River valley is now occupied by the communities of Squamish, Garibaldi Highlands and Brackendale (**Figure S5-1** a). Residential, commercial and industrial developments, along with transportation and power infrastructure in the lower Squamish River valley and Sea-to-Sky transportation corridor are at risk from seismic activity, flooding and damage by rivers, creeks, high tides, storm surges, tsunamis, debris flows and debris avalanches (**Figure S5-3**; Blais-Stevens and Septer 2008).

Geological hazards of the Squamish River valley

Flank collapses on Mount Garibaldi and Mount Cayley during deglaciation triggered a series of debris avalanches that deposited large volumes of volcanic material in the Squamish River and Cheakamus River valleys (**Figure S5-2** a). The collapse of Mount Garibaldi delivered some 2.5 billion m^3 of dacite blocks in a matrix of pulverized tuff and breccia in the lower Squamish River valley (Moore and Mathews 1978). Large debris avalanches continued to occur through the Holocene (Mathews 1958). Collapse of Mount Cayley started around 4800 years ago and ended in the 1500s, triggering at least three debris avalanches that have dammed the Squamish River and formed temporary lakes upstream that were then breached and rapidly drained (Clague and Souther 1982).

In the 1930s and 1958, debris flows in Cheekye River formed a temporary dam across the Cheakamus River with an estimated volume of 100,000 m^3. The western flank of Mount Cayley was the source of a 1963 debris avalanche with a volume of 5 million m^3 and an estimated velocity of 15 to 20 m/s.

In October of 1984, a debris avalanche triggered a debris flow in Turbid Creek that dammed Cheakamus River that subsequently flooded downstream (Clague and Souther 1982). A number of other catchments experienced flood conditions, debris flows and debris torrents during this storm. The Squamish River changed its channel, and the flood destroyed homes, logging roads and bridges. Protective dykes were also damaged on the Cheekye, Cheakamus and Squamish Rivers.

The Squamish River was diverted to the west by a training dyke in 1971 away from the current position of the Mamquam Channel (Hickin 1989) resulting in the abandonment of a meandering submarine channel that extends 2.5 km from the delta lip (**Figure S5-4** b, **Figure S5-5**). Three active channels extend from the current position of the Squamish River terminating in water depths between 100-160 m below sea level.

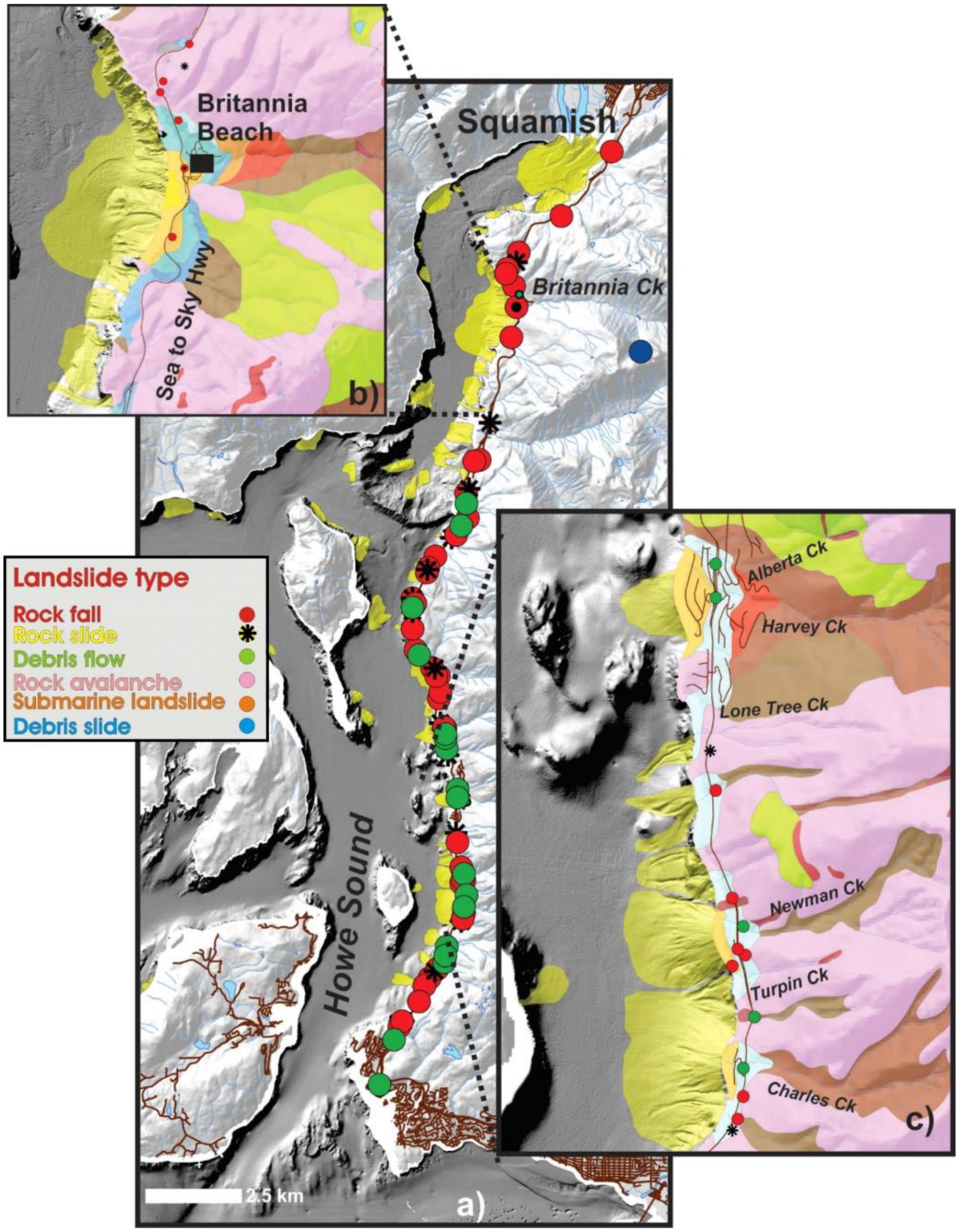

Figure S5-3 a) Distribution of landslides along the Sea-to-Sky Corridor. b) and c) Submarine fan deltas formed along the eastern flank of Howe Sound with surficial geology of catchment basins; bedrock – pink; Fraser Glaciation till – green; glaciomarine – light blue; glaciofluvial – orange; colluvial deposits – red, browns; submarine fan deposits - yellow (modified from Blais-Stevens 2008; Blais-Stevens and Kung 2009).

Rockfalls in the Sea-to-Sky Transportation Corridor

The Sea-to-Sky Highway and CN railway tracks pass through one of the most hazardous rockfall zones in British Columbia between Squamish and Horseshoe Bay (Clague and Turner 2003; **Figure S5-1**). High, steep, natural rock slopes dominate this area, and both the highway and rail line follow the base of these slopes near the shoreline. Construction of Highway 99, completed in 1958, necessitated the excavation of numerous steep rock cuts, some of which are more than 100 m high. Rockfalls from road cuts and natural rock slopes have caused frequent traffic interruptions. Rockfall impacts on vehicles have killed at least five people since 1969, and trains have derailed on at least two occasions.

Rockfalls from the Stawamus Chief and steep slopes of Howe Sound are a constant risk to highway and rail infrastructure south of Squamish to Britannia Beach. For the 2010 Winter Olympics, significant upgrades were made to the 20 km section of Highway 99 in the District of Squamish that included widening the highway to four lanes with a centre line divider, wide shoulders, pedestrian overpasses, plantings and landscaping (Blais-Stevens and Hungr 2008). Technically challenging sections required construction of two new bridges and large rock excavations.

Squamish River delta

Port facilities and low-lying residential and industrial land in Squamish (**Figure S5-1** b) are at risk from a range of geohazards, including: debris avalanches, debris flows, rockfalls, floods and tsunamis. Submarine failures and displacement waves (tsunamis) have occurred on the slopes of a number of fan deltas in Howe Sound during ice retreat from the fjord, through the Holocene (Hughes Clarke et al. 2012).

Squamish River delta is of strategic economic importance but also prone to similar submarine failures. Past marine slide events are indicated by heavily scarped and stepped submarine lobes, intensely disturbed delta front channels, dendritic gullies and debris splays mapped on floor of Howe Sound at the head of the fjord and Squamish River delta (**Figure S5-4**, **Figure S5-5**).

<u>Submarine slides and turbidity currents</u>

In a detailed time-lapse monitoring survey in 2011, Hughes Clarke et al. (2012) focused on the active Squamish River delta front and in particular the lobe of the northern active channel (**Figure S5-4**). Two types of events were observed including large-scale failures at the delta-lip and numerous bedform-moving events that were associated with sediment settling from the river plume (Hizzett et al. 2017).

More than 100 turbidity flows were observed in the channels but these flows dissipate rapidly upon reaching the un-channelized margin (Church et al. 2012). Less than six flows travel as far as the mid-slope each year. In the distal basin there is a bimodal distribution of event beds originating from the Squamish River delta; fine grained, millimetre-scale laminations that are deposited every year or two are interpreted as the distal expression of less powerful flows that deposit thin sand beds on the mid-slope, and thick (up to 1 m) sand beds that have occurred on average every 100 years over the past 500 years (**Figure S5-6**; Stacey et al. 2018).

Thick mass transport deposits (MTDs) in the distal ponded basin originate from the east fjord wall and the north side of the Porteau Cove sill (**Figure S5-5** a, **Figure S5-6**).

Woodfibre Creek

A 1955 submarine failure of the fan delta front at Woodfibre, 6 km northwest of Britannia Beach on the west shore of Howe Sound (**Figure S5-4** A) caused the collapse of a dock and warehouses (**Figure S5-7**) resulting in the loss of five forklifts and 1400 tons of pulp (Squamish Museum Archives). Its initiation only minutes after an extremely low tide on 22 April led to postulation that high pore-water pressure played a key role in the landslide.

No displacement wave was reported, despite the large volumes of mobilized subaqueous debris and of pulp falling into Howe Sound. The failure involved a ~10-m-thick wedge of coarse-grained, steeply dipping (27-28°) sediment extending to ~150 m water depth (Terzaghi 1956). The landslide thus appears to have arrested on the lower fan delta front, and not run-out onto the local fjord bottom at ~220 m water depth.

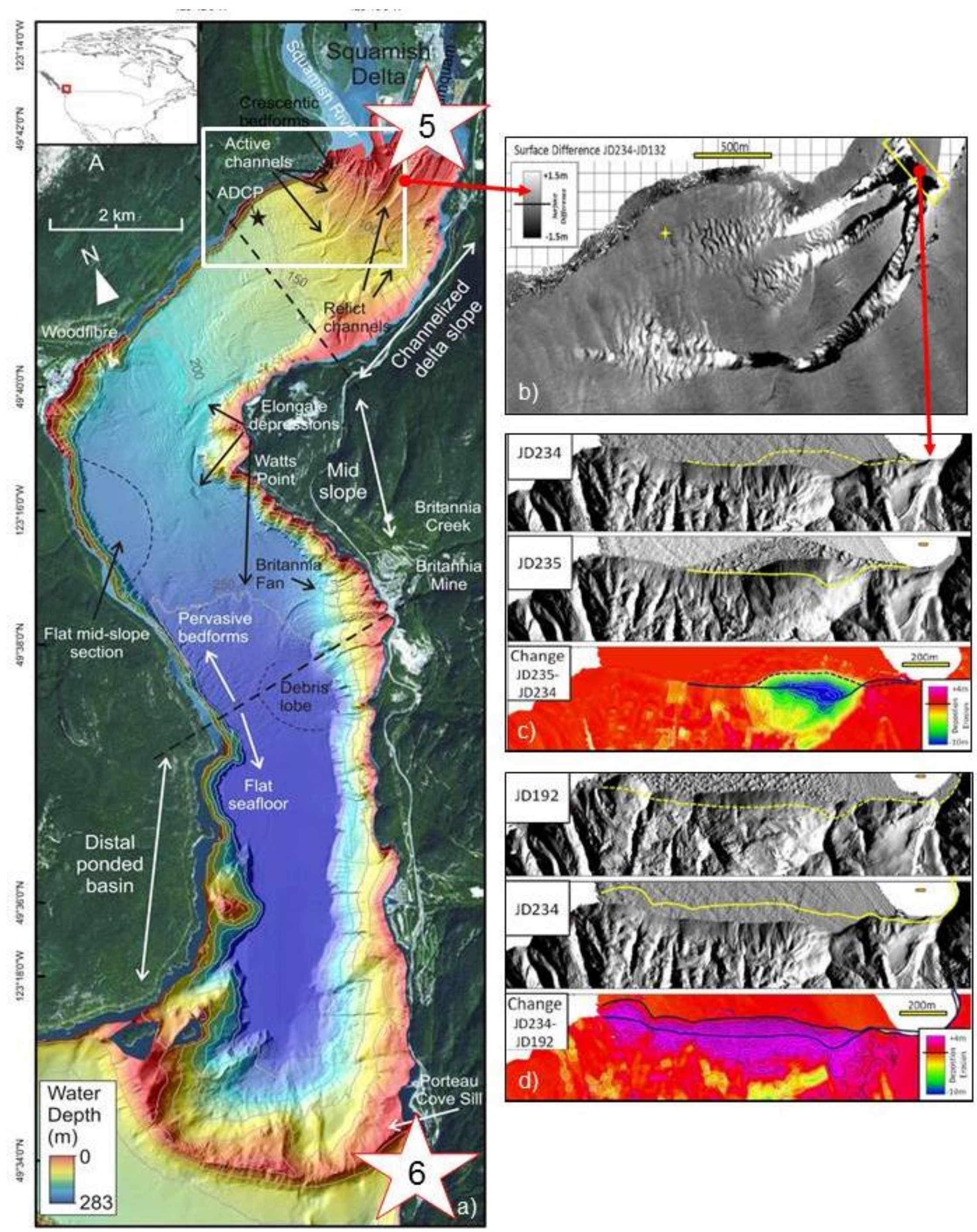

Figure S5-4 a) Multibeam bathymetry of upper Howe Sound showing the entire shore to sink turbidite system from the Squamish Delta to the Porteau Cove sill (source: Stacey et al. 2018); b) Cumulative differences over summer freshet from April to August 2011 (source: Hughes Clarke et al. 2012); c) single ~50,000m^3 collapse of the delta lip occurring within a 24 hour period, clearly associated with the last pronounced (~1000m^3) river surge of the summer period (source: Hughes Clarke et al. 2012); d) cumulative progradation of the delta lip over a 42 day period without significant collapse events (source: Hughes Clarke et al. 2012).

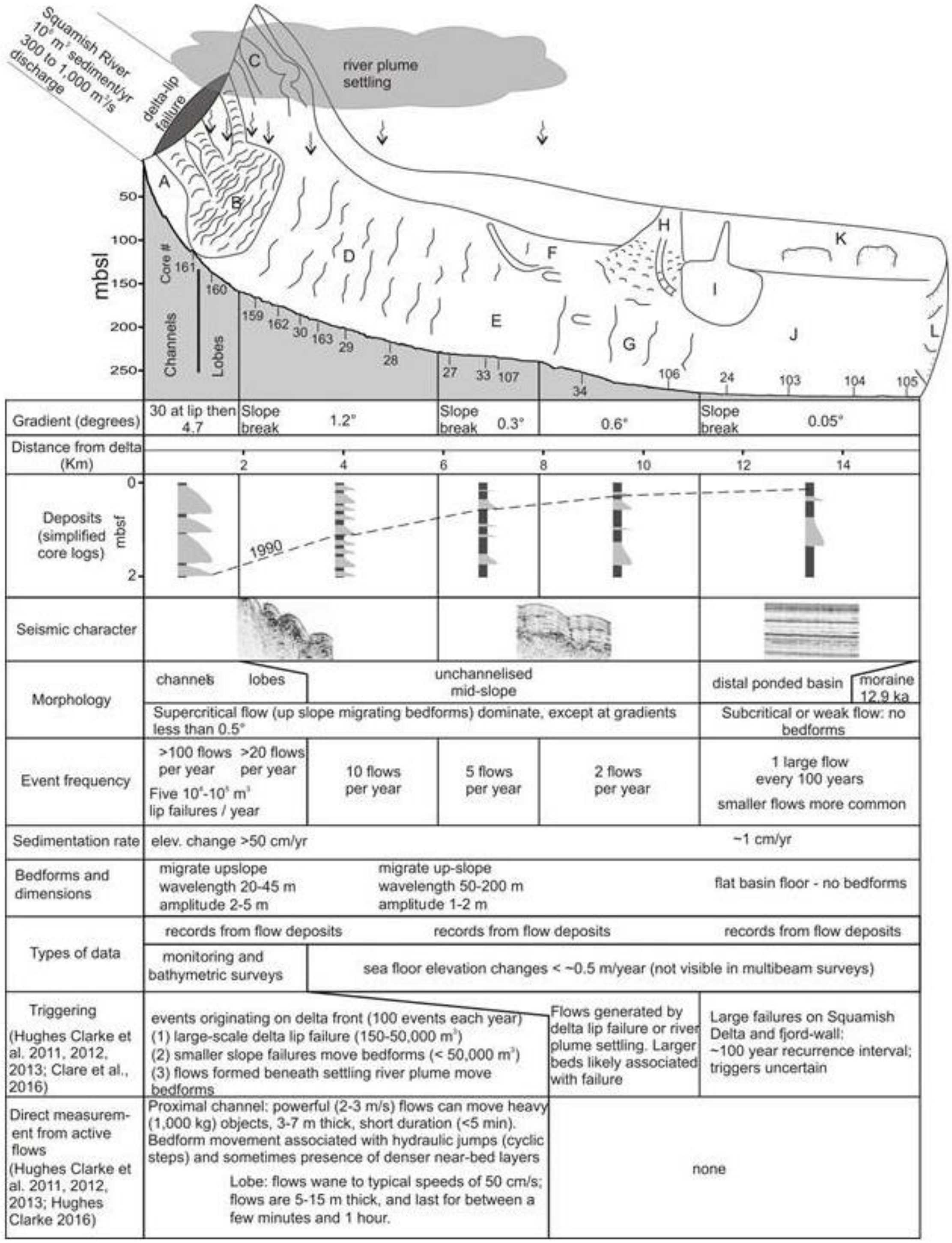

Figure S5-5 Key features of the Howe Sound fjord system showing longitudinal profile with average slope gradient and core positions. Simplified graphic logs which represent changes in depositional characteristics on different basin zones with a dashed line showing change in deposition based on 20 year post-mining interval. **A**. Active channels with cyclic steps; **B**. Lobe deposits with active sinuous bedform migration; **C**. Relict channels; **D**. Mid-slope with continuous bedforms; **E**. Flat mid-slope section with featureless seafloor; **F**. Irregular seabed scours; **G**. Lower mid-slope with continuous bedforms; **H**. Britannia Fan with channel and active bedforms; **I**. Debris flow deposit; **J**. Flat distal ponded basin with featureless seafloor; **K**. Fjord wall slide scars; **L**. Porteau Cove Sill (from Stacey et al. 2018).

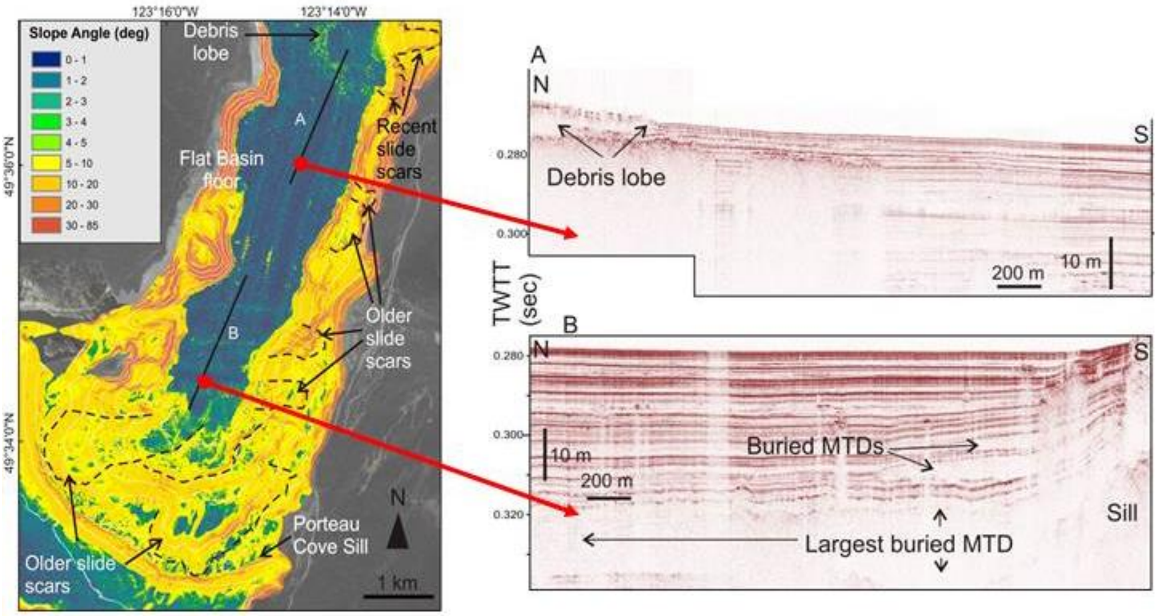

Figure S5-6 Map of seafloor gradients at the Porteau cove Sill showing several slide scars on the steep fjord wall and north side of the sill. Lines A and B show location of Huntec sub-bottom profiles of the distal ponded basin. **A**. The surface of the debris lobe comprises large blocks draped by recent sedimentation; this deposit is dated to approximately 1963. **B**. The ponded basin comprises sub-parallel, high-amplitude and laterally continuous reflectors extending to great depth interrupted by thick, chaotic mass transport deposits (MTDs), the largest of which fills the area of the distal basin.

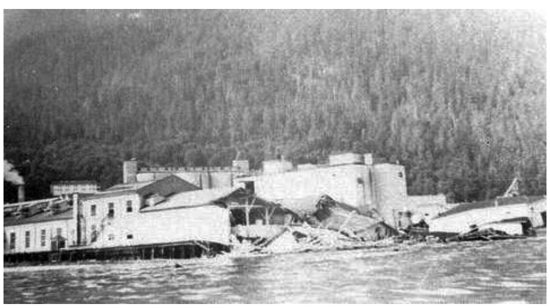

Figure S5-7 Damage at the Woodfibre mill attributed to tsunami generated by submarine mass movement (source: Squamish Museum archives).

Submergence of dock piles and their subsequent reappearance ~30 m seaward (Terzaghi 1956) indicates the approximate magnitude of displacement and may indicate a complex failure mode. Sidescan sonar surveying by Prior et al. (1981) identified extensive evidence of submarine landslides along this coarse-grained fan delta – arcuate scarps, chutes along the upper fan, and hummocky topography farther downslope – suggesting the occurrence of previous failures.

The Woodfibre town site and mill closed in, respectively, 1973 and 2003. Interest in the site for liquefied natural gas processing could again expose infrastructure at the site to hazards.

Britannia Beach

South of Squamish, the events in the vicinity Britannia Creek (**Figure S5-8** B) and Furry Creek (**Figure S5-8** C) indicate the disaster potential of resource development and residential development of Coast Mountain watersheds where facilities are built close to steep unstable slopes and on fans at the mouths of steep creeks (Evans 2000). Britannia Creek is 8.5 km long with a drainage area of 28.5 km^2 and creek gradients between 3° to 11°. In the late 19th century ore bodies were discovered in volcaniclastic rocks of the lower Cretaceous Gambier Group (Journeay et al. 2000).

In 1905, the Britannia Mining and Smelting Company Ltd. began its mining operations in the upper portion of the watershed. From 1905 to 1974, the Britannia Mine produced in excess of

454 million tonnes of copper, in addition to lead, zinc, gold and silver. Acid rock drainage (ARD) from the mine operations was a persistent problem over the lifespan of mining operations which led to significant contamination of Howe Sound in the vicinity of the submarine portion of the Britannia Beach fan. Today, ARD is effectively treated by addition of lime and marine habitats have recovered (Clague and Turner 2003). The mine is presently the site of the BC Mining Museum.

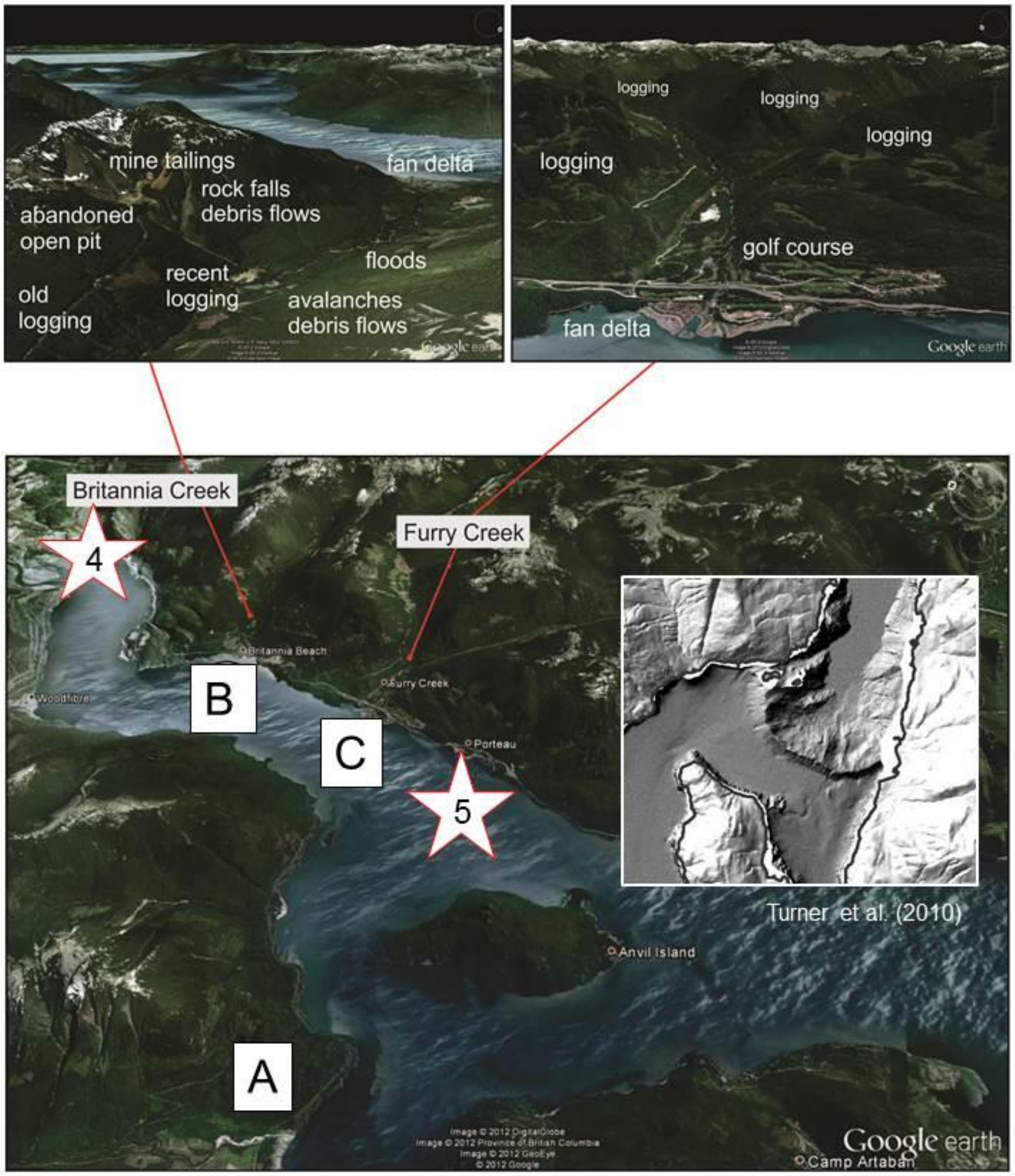

Figure S5-8 STOP 5 and STOP 6: Squamish River delta (star 5), Porteau Bluffs (star 6); and location of Woodfibre pulp mill (A), Britannia Beach (B) and Furry Creek (C) fan deltas and, showing land use activities and geohazards. Inset shows bathymetric expression of submerged end moraine occupying Howe Sound during ice retreat, around 12 ka (image modified from: Turner et al. 2010).

The original mining camp, Jane Camp, was established at an elevation of 1,000 m on a bench on the south side of the Britannia Creek valley within a cirque-like bowl on the northern side on the Britannia Mountain (**Figure S5-1** a).

In the early days of the mine, some employees were housed on the Britannia Creek fan on Howe Sound (**Figure S5-9** a), while workers were housed in camps scattered throughout the upland basin. An aerial tramline was used to connect the upper watershed with the beach community. During initial mine exploration and development activities most of the timber was clear-cut from the Britannia Creek watershed. Logs and debris from unstable embankments frequently clogged the channel at narrow passages.

Figure S5-9 Britannia Beach: a) prior to 1921 flood; b) after the 1921 flood (photos from Turner et al. 2010, courtesy of BC Ministry of Environment).

Just after midnight on March 22 1915, a landslide of rock, mud, and snow quickly overwhelmed Jane Camp. The landslide overran closely spaced mine buildings, including the mine office, cook house, dining room, store, rock crusher, candle house and tramway terminus, together with six houses and a large bunkhouse. The camp was buried with up to 15 m of debris. With 56 fatalities, the Jane Camp rock slide is the second most destructive landslide in Canadian history after the Frank Slide of 1903 (Evans 2000).

After the rock slide disaster of 1915, the mining company developed another upper watershed town site below Jane Camp in the 1920's. Although this town site only lasted a few years, a large debris avalanche swept over the site in 1990 knocking out the abandoned basement walls of what would have been several miners' cottages.

A new town site, Britannia Beach, was also established on the fan at the mouth of Britannia Creek. On 28 October 1921 a debris torrent struck the community. A wall of water, reported to be 20 m high, swept through the village and more than 50 of the 110 houses in the community were destroyed either directly by the flood or by being swept into Howe Sound (**Figure S5-9** b).

Two swaths of destruction were cut by the floodwaters as it swept through the community leaving an island of dislodged but not destroyed houses. The narrower, northern swath followed the immediate pre-flood stream course and the wider southern swath swept directly through a densely settled part of the settlement adjacent to the department store. Thirty-five families, a total of 100 people, were made homeless by the disaster and 37 were killed. The debris torrent occurred after 6 days of heavy rain culminating in a cloudburst that yielded 146 mm in the 24-hour period immediately prior to the flood. Conditions were made worse because a warm wind melted the snow in the mountains.

It was initially believed that the collapse of a natural dam of timber and soil debris had created a landslide dam. Later it was established that a 2.5 m wooden culvert became plugged with debris, ponding 60,000 m^3 of water before it failed. The coroner's inquest found the mining company criminally negligent (Blais-Stevens and Septer 2008).

In 1957, a submarine landslide occurred on the edge of the Britannia Creek fan and removed a portion of the newly constructed rail embankment. The slide left the rails hanging over a 150 m wide chasm (Couture and VanDine 2004).

In 1990, an old wooden dam in the upper portion of the watershed was purposely breached for safety reasons. Unfortunately, the resulting flood swept a large volume of logs and boulders down the channel and into Howe Sound. A natural event occurred a year later in August 1991 when an unusually high summer rainfall struck the southwestern British Columbia. The resulting water flood carried large volumes of sand, gravel, cobble and boulder debris over much of the fan. Highway 99 was over topped by debris and an elevated rail embankment acted as a dyke so the fan was flooded with up to a metre of water. Sand and silt settled out over the fan covering the residential yards, gardens and services areas and the highway (Evans 2000).

Today, the mountainside on the west side of the Jane Camp bench, opposite the source of the 1915 rock slide, is traversed by a series of large scarps and open cracks suggesting displacements of over 10 m. These displacements are likely in part due to subsidence caused by underground mining operations in the 1950s. Given the steepness of the slopes below the disturbed area, another major rock slide is a possibility. The disturbed area is presently being monitored by permanent survey prisms observed from a fixed instrument base at Jane Camp (Blais-Stevens and Septer 2008).

Furry Creek

Furry Creek, named after fur trapper Oliver Furry, is incised into a relict fan delta that has been mined for aggregate for over 30 years (**Figure S5-8** C). Deposits farther upstream provide a steady source of debris to the channel of the creek.

During intense rainstorms, such as those of the winter of 1982, pulses of blocky-bouldery debris threatened the low highway bridge crossing Furry Creek. The original bridge has since been replaced with a new structure with more clearance, and considerable development has occurred on the fan delta. Significant highway upgrades were completed for the 2010 Winter Olympics (Blais-Stevens and Septer 2008).

Today, a small community of multiplex homes and golf course can be found at Furry Creek.

STOP 6 Porteau Bluffs: mass movements and flood mitigation measures (30 minutes)

Introduction

Between Porteau Bluffs and Lions Bay, Highway 99 crosses a number of creeks with debris flow control structures and cuts through steep fractured bedrock slopes that require stabilization and creeks requiring debris flow defences (Hungr et al. 1987; **Figure S6-1**).

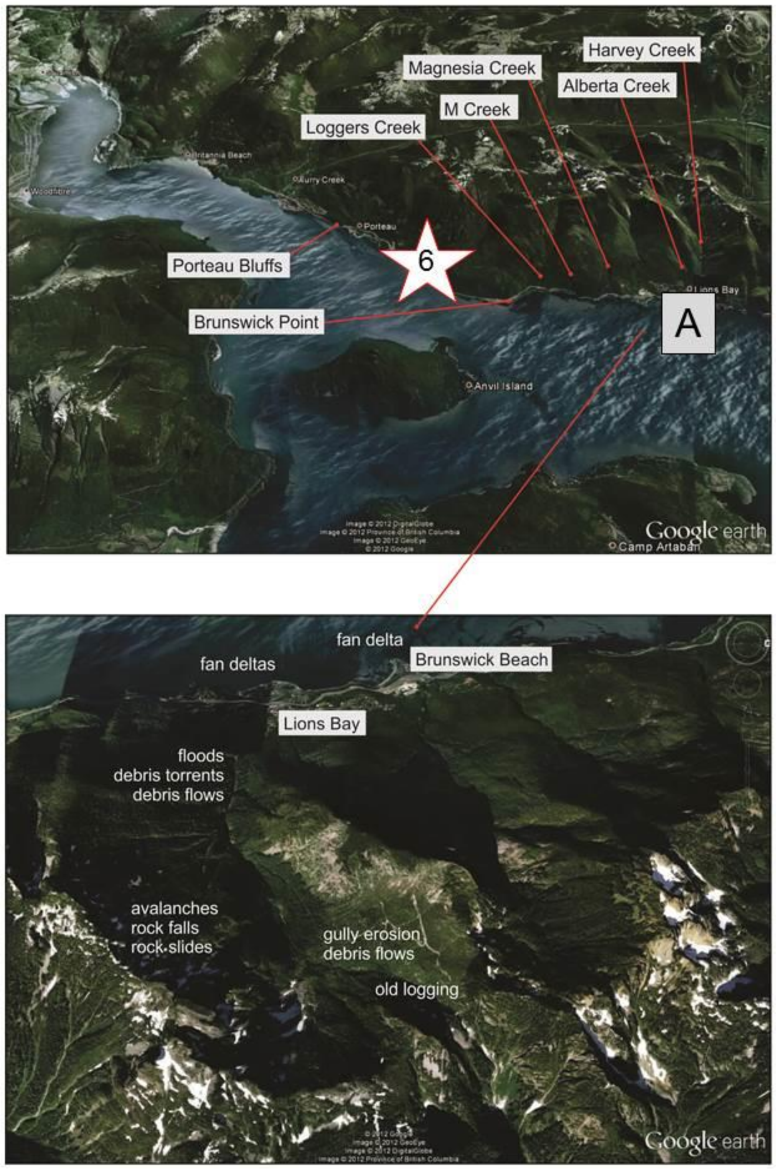

Figure S6-1 STOP 6: Porteau Bluffs (star 6), creeks experiencing debris flows and sites of major rockfalls onto Highway 99 and CN Rail from Brunswick Beach to Lions Bay (A).

Mitigation Measures

Extensive rock slope stabilization work has been undertaken along Howe Sound. For approximately 5 km between Porteau Bluffs south to Brunswick Point, Highway 99 passes through one of the most dangerous rockfall and rock slide zones in southwestern British Columbia. Many of the sites mentioned below are not readily accessible and will be discussed at STOP 6.

As you drive Highway 99, you will notice that many rock cuts have wire-mesh netting draped over their faces to prevent rock from falling onto the highway and railway. Other rock faces have been covered in shotcrete and extensively bolted as stabilization measures, in addition to being drilled to ensure adequate slope drainage.

Problems associated with channelized debris flows (‘debris torrents”) along Howe Sound are discussed at this stop (for additional information, see Hungr et al. 1984). Transportation infrastructure and public safety are at risk on small high-gradient fans near the present shoreline. Streams flowing across these fans are subject to sporadic debris flows that originate in adjacent steep watersheds.

These flows result from the failure and/or mobilization of relatively small volumes of Quaternary sediments, which are mainly of glacial and colluvial origin. They occur during periods of heavy rain, often accompanied by snowmelt, and may be associated with localized, high intensity precipitation cells. Once mobilized, the flows typically move down steep stream channels, often entraining additional sediment and plant detritus in the process. They decelerate in the lower reaches of streams, often coming to rest on fans along the shore of Howe Sound; some, however, reach the sea (Clague and Turner 2003).

Porteau Bluffs

At Porteau Cove, both the highway and railway pass below a long high rock cut in quartz diorite (*see* **Figure S7-2**). Excavation for the railway and highway in the mid-1950s resulted in vertical rock cuts over 100 m high (VanDine 2002). Blasting during construction opened several widely spaced (1 m to 5 m) incipient sheet joints in the weakly foliated rock mass. These “day-lighted” sub-parallel fractures dip southwest at approximately 50°, and are roughly perpendicular to the foliation and parallel to the sheet joints (**Figure S6-2**).

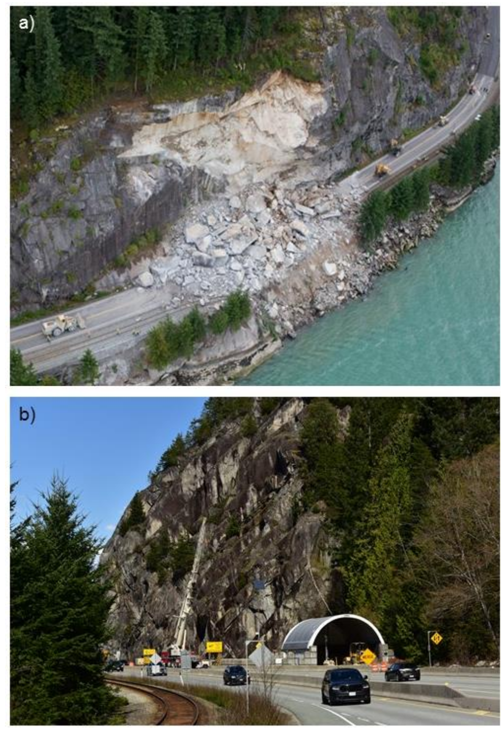

Figure S6-2 STOP 6: Porteau Cove Provincial Park, adjacent to Highway 99: a) Major rock slide blocked the highway and rail track in 2008, prompting significant upgrades in the corridor prior to the 2010 Winter Olympic Games (photo credit: CTV News, 2008). b) Quartz diorite bedrock is strongly fractured at approximately 20 cm to 50 cm spacing; an orientation parallel to the slope of the rock cut. The exposed surface has been stabilized with rock bolts and holes have been drilled to enhance drainage (white drainage pipes observed in the rock face). Chain-link mesh has also been installed to capture falling rock fragments to reduce the risk to rail traffic, passing vehicles and cyclists.

Repeated freeze-thaw cycles during winter months trigger rock slides at Porteau Bluffs, with sliding occurring on pre-existing planar surfaces. The wide spacing of the joints adds to the severity of the slides, because large rock blocks are involved.

On March 7 and November 26, 1964, several thousand cubic metres of rock slid from the Porteau Cove cut onto the highway. On February 9, 1969 a single rock block landed on a car travelling south along the highway killing three people. On February 17 and March 4, 1969, other falls were triggered by repeated freezing and thawing, and on July 25, 1970, a rock block as "big as a house" closed the highway.

On September 3, 1991, falling rock struck a northbound car and killed its driver (Clague and Turner 2003). In 1991, the BC Ministry of Transportation cleared vegetation and thoroughly scaled the cliff. Some 3,000 m of galvanized steel resin grouted threadbar anchors were installed, some up to 10 m in length. Permanent displacement prisms were attached for long-term monitoring (Hungr and Skermer 1998).

Rock bolts and dowels have been installed at numerous locations to pin potentially dangerous slabs and blocks of rock to the slope. Rock bolts, up to 10 m long, were installed in the rock slopes at Porteau Cove in 1991. Drainage holes have been drilled to reduce water pressures in some rock slopes, and several cuts have been treated with shotcrete. Frequent scaling of some rock cuts is carried out as part of a routine, on-going, rock slope maintenance program (Clague and Turner 2003).

Brunswick Point

In the Brunswick Point area, bedrock consists of intensely fractured northwest-trending meta-sedimentary and volcanic rocks (*see* **Figure S7-2**). At Brunswick Point (**Figure S6-1**), where the rock is closely jointed volcanic or meta-argillite, rockfalls are relatively small but frequent. This area has experienced repeated rockfalls ranging from individual small blocks to large wedge failures. The large failures are generally preceded by the breakout of smaller rock fragments along pre-existing fracture zones. On February 13, 1969, a rockfall of 6,000 m^3 closed the highway.

In 1972, one of the most problematic cuts through in the Brunswick Point area was stabilized by the application of a blanket of wire mesh and shotcrete 5 to 10 cm thick. However, effective scaling of this and other meta-argillite cuts has proven to be extremely difficult. A rockfall of 1,500 m^3 on August 25, 1976 closed the highway for two days and also caused a train derailment.

On January 16, 1982, while heavy snowfalls stopped traffic, a single large block fell from one of the cliffs, hit a stopped car, killing one person and badly injuring another. The rock block fell from a point 40 m above the road level and above the highway cut, and was the first from this particular segment of rock slope since deglaciation. As a result of the 1982 rockfall, the driver of the car sued the BC Ministry of Transportation for damages in 1985. After two appeals, the Supreme Court of Canada awarded the driver of the car $1 million in 1991 on the grounds that the BC Ministry of Transport failed to meet the standard of care by not conducting a climbing inspection (Couture and VanDine 2004).

Loggers Creek

At Loggers Creek, Highway 99 crosses extremely steep slopes consisting of fractured meta-volcanic rocks (**Figure S6-1**, *see* **Figure S7-2**). The largest rockfall recorded in the Gambier Group (10,000 m^3) occurred on October 20, 1990 when a natural slope above the highway failed near the creek. The rockfall blocked Highway 99 and the CN Rail track, severing the land route between Squamish and Vancouver. The highway was closed for 12 days, during which time vehicle movement between Squamish and Vancouver was only possible by a ferry between Horseshoe Bay and Darrell Bay (north of the rockfall).

Clean-up, repairs and preventative scaling cost approximately $11.4 million (2018 dollars). A secondary, smaller rockfall occurred during the scaling operations and injured two workers. Following the rockfall, the BC Government designed and constructed an emergency port facility for large car ferries at the north end of Howe Sound (Hungr and Skermer 1998).

M Creek

M Creek has a high gradient of 26° and flows from an elevation of about 1,300 m to a small fan on Howe Sound (**Figure S6-1**). During the night of October 27/28, 1981, a small debris/rock avalanche of surficial debris and fractured bedrock failed along a steep tributary along the margin of an old logging clear-cut at 1,150 m elevation. The debris temporarily blocked the main rain-swollen bedrock channel then descended to a logging road crossing where it burst a log jam and flowed down into the gorge, growing to a volume of approximately 15,000 m^3.

Having gained a velocity of several tens of metres per second, the boulder-rich front had sufficient momentum to knock out the central piers of the wooden trestle bridge over Highway 99, creating an 18 m deep chasm. An unoccupied residential building on the fan was carried into Howe Sound. Several vehicles approaching the bridge in plunged into the chasm and disappeared in the debris flowing towards Howe Sound. The accident claimed nine lives (Eisbacher 1983). In 1982 and 1983 a new reinforced concrete clear span bridge was constructed to replace the wooden trestle bridge (Hungr and Skermer 1998).

Magnesia Creek

Magnesia Creek has a drainage area of 4.7 km^2 and creek length of 4.7 km (**Figure S6-1**). The 200 year flood discharge is estimated at 75.7 m^3 s^{-1}. The watershed experienced a flood in 1960 and a debris flow in 1981. Multiple residences, access roads, Highway 99 and CN rail tracks are at risk from future debris flows. Mitigation measures include a debris basin and barrier completed in 1985. This was designed to accommodate a 44, 500 m^3 debris flow with a discharge volume of 400 m^3 s^{-1}. The basin has a storage capacity of 51,500 m^3 and spillway can cope with a discharge of 800 m^3 s^{-1} (VanDine 2002).

Alberta Creek

Alberta Creek is a relatively small stream draining 1.2 km^2 of steep mountain slopes with a relatively consistent channel gradient of 16º to 24º above a fan (**Figure S6-1**). The channel is deeply incised into steep unstable banks on the fan. The watershed is underlain by sheared and fractured meta-volcanics of the Gambier Group (*see* **Figure S7-2**). Aerial photographs show that the lower part of the creek was swept by a debris flow in the early 1930s, although Lions Bay, Highway 99 and CN Rail did not exist at that time.

By 1980, an established community existed on the fan on both sides of Alberta Creek. Fifteen houses were built within 30 m of the creek. One house was only 3 m from the creek and 0.5 m above it. In addition to the wooden trestle bridge on Highway 99, the creek was crossed by a concrete CN Rail bridge and five subdivision road culverts.

On February 11, 1983, an estimated 20,000 m^3 debris flow descended the creek. The highway bridge, all the subdivision culverts and fills and three houses were completely destroyed. The railway bridge and another house were damaged. Two teenage residents lost their lives. The event was likely started by a shallow slide of steep bedrock-derived colluvium undercut by the creek at elevation 700 m (an unlogged area).

The initial failure probably contained less than 100 m^3 of soil and rock fragments. Most of the debris was derived by mobilization of channel infilling and undercutting of unstable banks over the length of channel between the initial slide and the fan. About 10 to 20% of the debris was logs and woody debris. The debris flow occurred in six surges spaced over a half-hour interval. The largest surge may have been as much as 4 m deep at its peak, with a maximum discharge up to 350 m^3 s^{-1} (Couture and VanDine 2004).

Because of the steep slopes and dense population, Alberta Creek offered no suitable site for a debris basin, so an 800 m long flume or “shooting channel” was constructed to deliver water flood and debris flow discharges to Howe Sound. Two main considerations in the design were to prevent spill-over at bends by providing a uniform gently curving channel and to prevent depositional plugging by ensuring secure confinement of the flow at a range of discharge rates. The lined channel was also used to stabilize steep eroding banks that threatened a number of houses upstream of the fan (Hungr and Skermer 1998).

Figure S6-3 a) Debris torrent damage at Lions Bay from the 1981 event (source: Turner et al. 2010); b) debris basin at Charles Creek (source: O. Hungr).

Lions Bay

The Village of Lions Bay is built on the coalescing fans of Harvey and Alberta creeks (**Figure S6-1**). Development began in 1957 during construction of Highway 99, and today most of the community is located on the glaciofluvial fan and on mountain slopes, and 70 houses are situated on the coalesced Holocene fans of Harvey and Alberta creeks.

The Harvey Creek fan is a glaciofluvial delta containing cross-bedded sand and gravel deposits many tens of metres thick, of which the upper 10 to 20 m are coarse debris flow and flood deposits. Harvey Creek has a drainage area of 7 km^2, extending from the sea level to the highest point of the watershed at 1,646 m elevation. The main branch of the creek rises from the apex of the alluvial fan at 13º to 14º, and drains a large cirque basin at elevation 900 m. Four tributary branches drain steep headwall slopes, some of which were clear-cut logged in the 1960s (**Figure S6-1**). Basin geology is mainly quartz diorite (*see* **Figure S7-2**).

Heavy flooding in Harvey Creek occurred in 1969, 1972, 1973 and 1981 (**Figure S6-3 a**). During the storm of September 18 1969, when several other creeks along Howe Sound had debris flows, Harvey Creek was flowing at bank-full stage and carrying a substantial load of trees and boulders derived from unconsolidated deposits in the upper watershed. Clear-cut logging may have intensified runoff that mobilized the main pulse of debris. A peak discharge for the debris flood, or torrent, was estimated at >100 m^3 s^{-1}. This flood damaged several homes on the fan. Past debris flows from the Harvey Creek watershed are indicated by coarse bouldery deposits on the surface of the fan, the steepness of both the fan and the channel upstream, and by the availability of debris sources on the slopes and in the channels.

Measures taken to protect people and property in Lions Bay from future debris flows include the construction of debris catch basins, relocation of highway bridges, and lining of stream channels (**Figure S6-3 b**). Because the creek has potential for producing major debris flow events, a large debris basin with a retention capacity of 70,000 m^3 and barrier was constructed on the upper portion of the fan in 1985. The basin and barrier were designed similar to those for Charles Creek. Downstream of the basin, the creek was provided with a smoothly curving boulder-lined channel to control floods and debris flow discharges if the barrier was overtopped (VanDine 2002). The total cost of this and ancillary work has been estimated at up to $35 million (2018 dollars).

STOP 7 Cypress Mountain view point: bedrock and geological structures (30 minutes)

Introduction

STOP 7 (**Figure S7-1** a) is an opportunity to appreciate the physiographic setting of Vancouver and the Fraser River delta (*see* **STOP 8**). The Lower Mainland region as viewed from the Cypress Mountain view point comprises: 1) thrusted, folded, and faulted Tertiary and older sedimentary rocks; 2) glacially derived Pleistocene deposits; 3) glaciomarine turbidite sequences from the latest deglaciation; and 4) a modern Fraser River delta sequence which includes all components of delta sedimentation processes (e.g. turbidity currents, channel, levee, levee-overspill, debris flows, river bedload, hemipelagic deposition, tidal reworking).

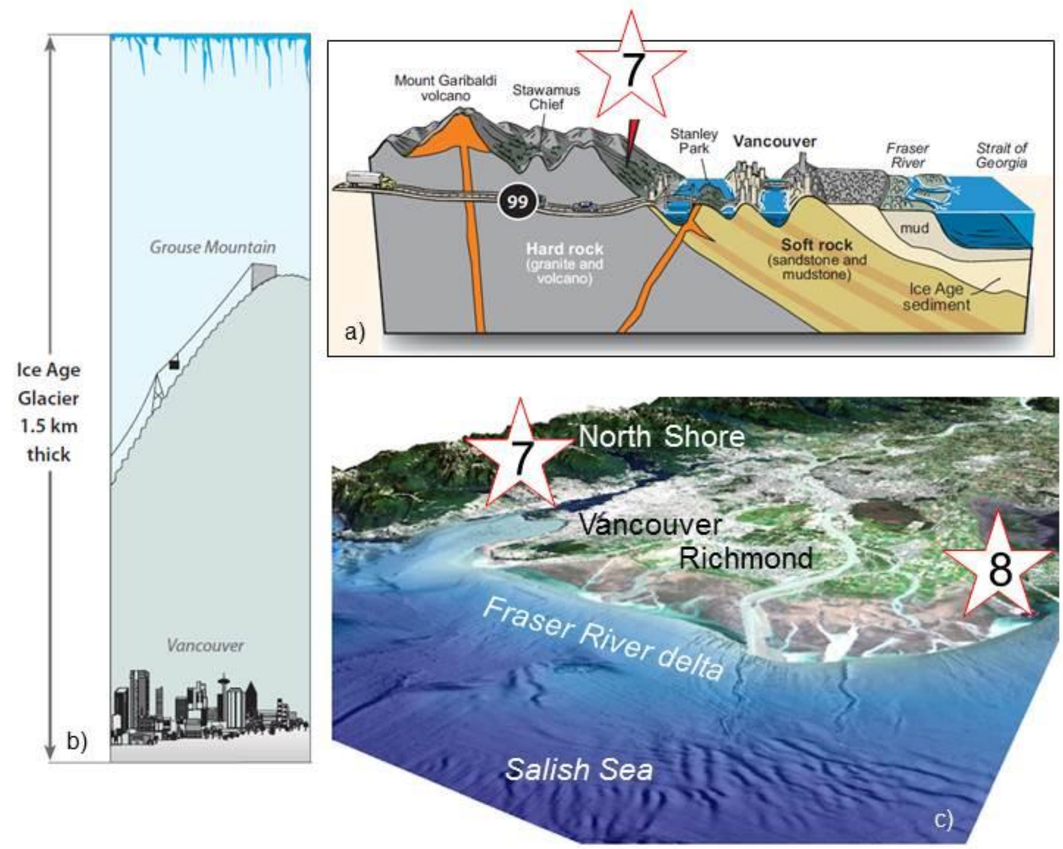

Figure S7-1 a) STOP 7 Cypress Mountain, North Shore, showing bedrock geology (adapted from: Turner et al. 2010); b) Schematic cross section showing ice thickness over Vancouver at the last glacial maximum (adapted from: Turner et al. 2010); and c) STOP 8 Tsawwassen and Fraser River delta, Salish Sea basin (source of image: David Mosher).

Geological Setting

From Squamish (**STOP 5**) to the Cypress Mountain view point (**STOP 7**) you will observe Jurassic to middle Cretaceous quartz diorite, granodiorite, and diorite of the Coast Plutonic Complex (**Figure S7-2** mKg, mKd, mKgsq, JKg, JKd) intruding Mesozoic island arc assemblages of the Wrangellia terrane (**Figure S7-2** JB), and sedimentary and volcanic rocks of the overlapping Gambier Assemblage (**Figure S7-2** JKG, JKGA; JKG, JKGA). Remnants of these older sedimentary-volcanic assemblages are preserved as metamorphic sheets and roof pendants between the intrusive complexes, and juxtaposed along major northwest-trending faults of the southern Coast Belt Thrust System (**Figure S7-2**N). Metamorphic foliation in these rocks trend northwest and parallels the topographic grain of the Coast Mountains. Younger fracture sets, shear zones, and mafic dikes are parallel to, but also discordant with older penetrative fabrics (Journeay et al. 2000).

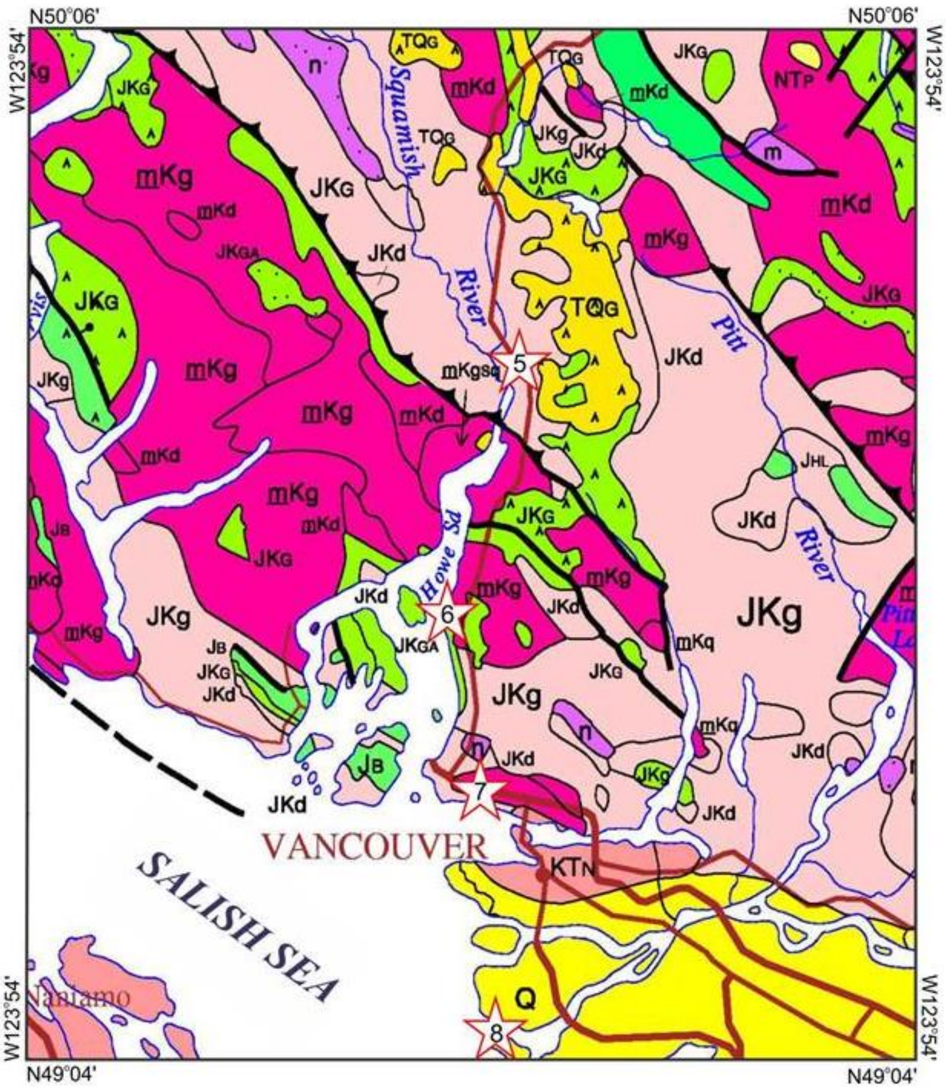

Figure S7-2 Tectonic assemblage map with field stops indicated. Q, Qc: Quaternary; TQG: Tertiary and Quaternary, Garibaldi, volcanic rocks; KTN: Upper Cretaceous-Oligocene, Nanaimo, volcanic rocks; mKg, mKd, mKgsq: Mid-Cretaceous, plutonic rocks; JKg, JKd: Late Jurassic-Early Cretaceous, plutonic rocks; JKG, JKGA: Upper Jurassic-Lower Cretaceous, Gambier, volcanic rocks; JB: Lower and Middle Jurassic, Bonanza volcanic rocks; N: Lower and Middle Jurassic, metamorphic rocks, orthogneiss (modified from: Journeay et al. 2000).

Along the southwestern flank of the Coast Mountains, late Cretaceous to Eocene fluvial sediments (**Figure S7-2** KTN) onlap the deeply eroded Coast Plutonic Complex. Several volcanic complexes were active north of Squamish during the last 2 Ma along the Garibaldi Volcanic Belt: part of a Pliocene-Recent volcanic province that extends from British Columbia southward into the Washington and Oregon states in the USA.

During the late Pliocene to Pleistocene, the volcanic edifices of Mount Garibaldi, Mount Cayley and Mount Meager were superimposed onto the rapidly uplifting southern Coast Mountains (rate, *ca*. 0.75 km/Ma). The eruptive centres trend north-northwest and were likely controlled by pre-Pleistocene fracture zones that dissect the landscape. The most recent eruptions along this northern segment of the volcanic chain occurred approximately 2.3 and 2 ka in the Mount Meager area (Souther 1977). Recent activity consists of rock avalanches, debris flows and landslides (Evans 1987).

Neotectonic activity and seismicity of the southern Coast Mountains are linked to northeastward underplating of oceanic crust (Juan de Fuca Plate) along the Cascadia subduction zone. Most historic seismicity has been localized along the subduction zone and Benioff zones (Parrish 1983; *see* **Figure S1-2**). The largest onshore earthquake in recent history (M 7.3) had its epicentre on central Vancouver Island (see **STOP 4**) and occurred on June 23, 1946 (Rogers 1980; *see* **Figure S4-1** a). Shaking related to this seismic event caused a number of slope failures and extensive ground subsidence in southwestern British Columbia (Mathews 1979).

Over 1 km of ice covered the Vancouver area during the last glaciation, and deposits (**Figure S7-2** Q, Qc) related to advance and retreat of the southwestern sector of the Cordilleran Ice Sheet blanket bedrock below 200 m elevation (**Figure S7-1** b).

STOP 8 Fraser River Delta: geohazards and marine infrastructure (30 minutes)

Introduction

At **STOP 8**, near Tsawwassen, a deep granitic basin beneath the lower Fraser River valley is infilled by nearly 4 km of Mesozoic and Cenozoic sandstones (**Figure S8-1**). This clastic infill tapers towards the North Shore and Coast Mountains (**Figure S7-1** a). The structural depression lies near the west margin of the North America Plate and forms what is now the Salish Sea.

Overlying these basement rocks and underlying modern deltaic sediments are approximately 1 km of Quaternary deposits resulting from various stages of multiple Pleistocene glaciations. Modern sediments are limited to the Fraser River delta and low-lying areas around the margins of the Salish Sea, where they are currently being deposited and eroded (**Figure S8-1**).

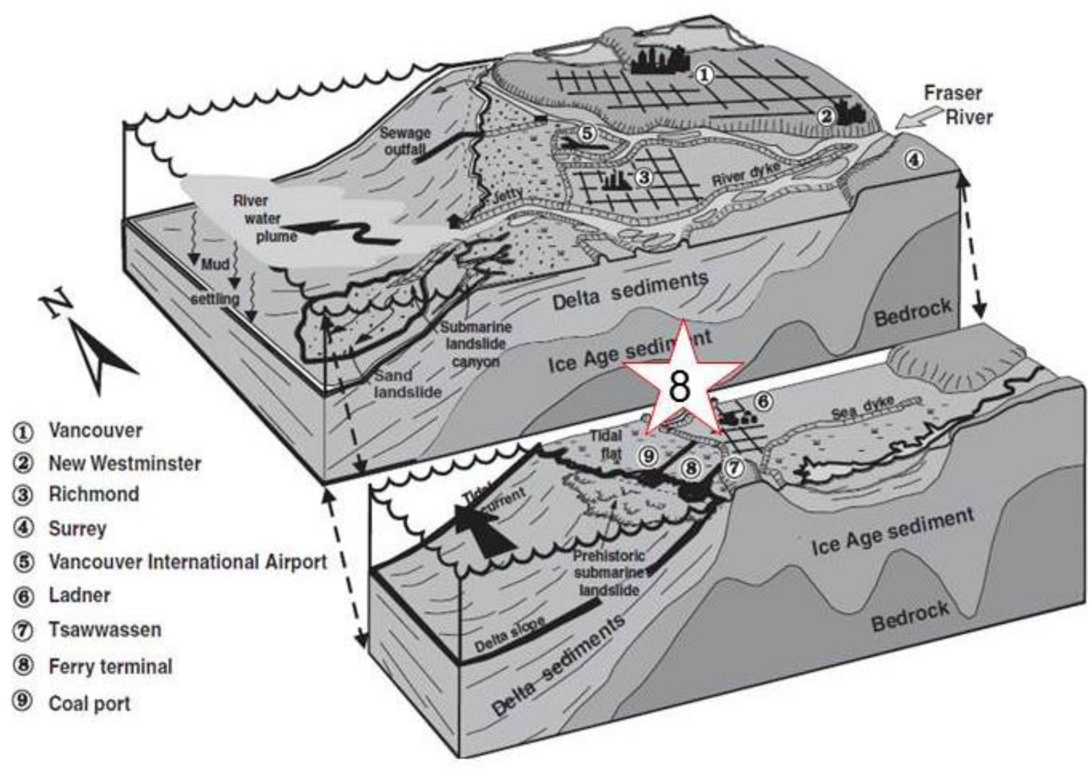

Figure S8-1 Schematic of Fraser River delta morphology, structure, and stratigraphy (from Mosher et al. 2004 and modified from Turner et al. 1996).

Fraser River flood hazards

Fraser River drains an area of 233,000 km^2 and is the longest river in British Columbia. The river basin extends into the Rocky Mountains on the east and the Coast Mountains on the west, but most of the watershed drains the Interior Plateau. Because of the large size of the drainage basin, the major flood threat along the lower Fraser River is from snowmelt. Large floods typically result from a combination of four factors: 1) a heavy snowpack; 2) melt delayed by a cold spring and cool conditions during early summer; 3) a rapid and large rise in temperature that is sustained for many days; and 4) rainfall during the period of heavy snowmelt (Clague and Turner 2003).

The mean annual flow of Fraser River at Hope, which is situated below 93% of the drainage basin, is 2720 m^3 s^{-1}. The mean monthly discharge at this site ranges from 846 m^3 s^{-1} (March) to 7030 m^3 s^{-1} (June). The highest daily discharge from 1912–1990 was 15,200 m^3 s^{-1} (measured on May 31, 1948). This flow was exceeded by an even larger discharge in 1894, estimated to have been about 17,000 m^3 s^{-1}. Both produced major floods (Clague and Turner 2003).

Fraser River emerges from the Fraser Canyon near Hope, crosses the Fraser Lowland, and flows into the Salish Sea just south of Vancouver (**Figure S7-1** c). Below Hope, the Fraser River floodplain has an area of about 75 000 hectares. Of this, about 55 000 hectares are protected by 247 km of dykes and 23 pump stations built between 1968 and 1995 at a cost of almost $450 million (2018 Canadian dollars).

The largest recorded flood of Fraser River occurred in 1894 following a winter of heavy snowfall and a cool spring. The flood peaked on June 9 and held that level for several days before falling (Clague and Turner 2003). The peak flow overtopped and breached dykes from Agassiz to Richmond, and large areas of the floodplain were inundated. Flood damage occurred in rural areas and in low-lying communities (e.g., Port Haney, Chilliwack Landing, Matsqui Prairie, Nicomen Island, and Harrison Reserve). Siltation and debris prevented crops from being planted in the Chilliwack, Sumas and Matsqui areas.

The most recent major flood occurred in early June 1948 and is one of Canada's worst flood disasters. A late spring, followed by very wet conditions and a rapid onset of warm temperatures, triggered rapid melting of a heavy snowpack in late May. The river level rose and overtopped dykes in the Fraser Lowland beginning on May 26. Flood waters peaked on June 10 at Mission, within 30 cm of the 1894 flood level. By that time, the river had breached over a dozen dykes and flooded 20,000 ha of land (Clague and Turner 2003). Much of Agassiz and Rosedale, and parts of Mission were inundated. Vancouver was cut-off from the rest of Canada, except by air. Ten people died, 200 families were left homeless, and 16,000 people were evacuated because of the flooding. Three thousand buildings were destroyed and eighty-two bridges were washed out. The total cost of the disaster is estimated to be $210 million (2018 Canadian dollars) (Clague and Turner 2003).

Fraser River tributaries flood most commonly during periods of heavy rainfall in fall or winter (Clague and Turner 2003). Flooding at the Fraser River delta may be caused by storm surges or high tides at times of high river levels.

Flood hazard mitigation measures

The dyking system was the product of the joint federal-provincial Fraser River Flood Control Program (fraserbasin.bc.ca). Chilliwack, Harrison Hot Springs, Agassiz, and parts of New Westminster and Mission are some of the many communities protected by the dykes. The Fraser River delta is ringed by river and sea dykes, providing protection to Richmond, Steveston, and Ladner (Clague and Turner 2003). Today, this dyke system protects over $50 billion worth of development and infrastructure in the lower mainland.

Dyke design is based on a water elevation equivalent to the 1894 flood. At Hope, this discharge has an estimate recurrence interval of 1 in 160 years. The dykes are generally trapezoidal in shape, composed of compacted sand and gravel, and are 3.5 m wide at the top. They have been built with a freeboard of 0.6 m over the 1894 equivalent water elevation. Sea dykes on the Fraser delta have been built up to a 1 in 200 year water level, as estimated from tidal records, with 0.7 m freeboard (Clague and Turner 2003).

Impacts of Future Fraser River floods

The potential impact and cost of a severe Fraser River flood in the Fraser Lowland have increased substantially since 1948. Settlement and commercial and industrial development have increased considerably on the floodplain in recent years as the regional population and economy have grown, especially in the 21st Century. Highways and railways have assumed a greater importance to the economy of western Canada during this period. With climate change and extreme weather conditions anticipated, both the development and transportation routes will be vulnerable to future floods large enough to overwhelm the dyking network and other flood control measures (Clague and Turner 2003).

Fraser River Delta

The Fraser River delta lies in the zone of most frequent crustal earthquakes in Canada and is categorized as the zone with the highest seismic risk as a consequence. The higher risk is also a result of the major societal infrastructure on the delta, including Canada's second busiest international airport that transports >23 million passengers per year, Canada's busiest ferry terminal carrying more than 3 million passengers per year, and Canada's busiest shipping port handling over $200 billion in goods in 2017. The delta supports a major highway infrastructure including six bridges and a tunnel. The tunnel was opened in 1959 prior to any earthquake building codes and hosts 80,000 vehicles per day. The delta also supports a major electrical transmission corridor supplying power to Vancouver Island (**Figure S8-2**).

Figure S8-2 Infrastructure elements at risk on the Fraser River delta and area of interest for the GSC (red polygon) (source of image: Gwyn Lintern).

Geomorphic history of delta formation

Fraser River began to build its delta into the Salish Sea about 10 ka, after the last glaciation (Clague et al. 1983). Under the burden of glacial ice, the land had been isostatically depressed, causing relative sea level at 14 ka (before present) to be over 90 m higher than it is today. With the removal of the weight of the glaciers, the land rebounded, causing relative sea level to fall. It had fallen to more than 12 m below its present position by 8 ka (Mathews et al. 1970). By about 5 ka, global eustatic sea level rise had brought sea level back to within a few metres of its present position, and sea level has continued to rise a few centimetres per hundred years since that time (**Figure S8-2**).

At about 5 ka, Fraser River began to discharge west into the Salish Sea (Clague et al. 1998). During the last 5 ka, the Fraser River delta has prograded westward into the deeper water. Considerable channel meandering and anastomosing of channels are known to have occurred, even in historical times, although channel locations have been fixed by dykes and jetties over the last century.

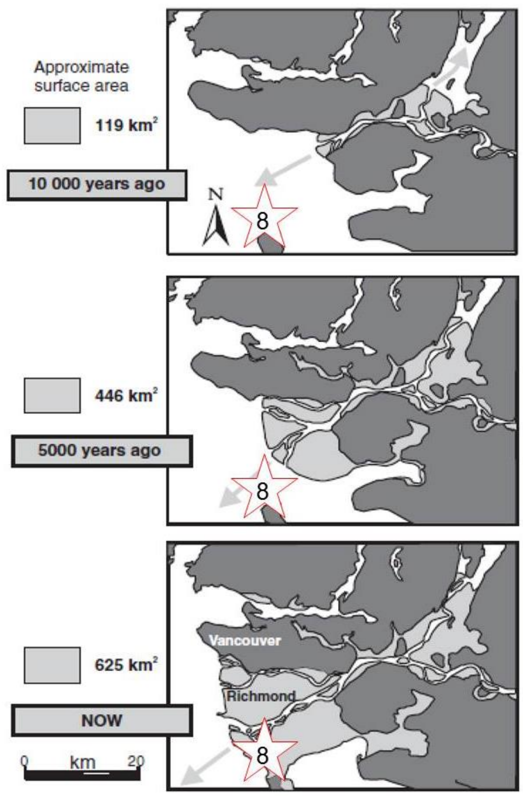

Figure S8-3 Growth of the Fraser River delta over the last 10 ka (modified from Clague et al.1991).

Progradation of the delta into the Salish Sea created a 40 km long coastal zone (**Figure S8-3**). Tidal flats extend about 9 km from the delta dykes to the subtidal slope. The delta has an area in excess of 1000 km^2; the onshore portion is about 450 km^2, the intertidal region is 215 km^2, and the foreslope is about 350 km^2. A further 3500 km^2 within the Salish Sea are affected by sedimentation of material derived from Fraser River. The slope break, marking the modern transition from the intertidal flats to the foreslope, lies at about the 10 m depth contour. The western delta slope is inclined 1° to 23° (average about 2°–3°) towards the marine basin of the Salish Sea and terminates at about 300 m water depth, 5 km to 10 km seaward of the edge of the tidal flats.

Geomorphology of the Fraser River delta

There are five significant surficial morphological elements of the Fraser River delta (**Figure S8-4** a). Extensive deltaic plains are underlain almost continuously by channel-fill deposits of sand (Monahan et al. 1993). Active river channels are constrained in their locations by dykes and jetties.

The 350 km^2 foreslope ranges in water depth from 10 m to 250 m, with slopes up to 23°, but averaging 2 to 3°. Erosive channels, gullies, and sea valleys transect the foreslope and are maintained by sediment mass-flow processes. An extensive prodelta occupies much of the southern Salish Sea.

Seismic Hazard

Great earthquakes (M >8) are characterized by their long duration of strong shaking along large rupture surfaces (Rogers 1994). The extensive region of affected by shaking means that many communities are potentially at risk; whereas the duration of shaking adversely impacts infrastructure and liquefaction potential of saturated deltaic sediments (Rogers et al. 1998).

In Canada's National Building Code, *seismic hazard* is defined as the level of horizontal ground shaking (acceleration or velocity) with a 10% probability of being exceeded over a 50 year period (Rogers 1994). Ground surface response of thick, soft deltaic deposits to seismic shaking differs from that of bedrock. For the greater Vancouver region, amplification of seismic waves in deep alluvial sediments on the Fraser River delta will be enhanced by high-rise structures. Low S-wave velocities (< 200 m/s) indicate thick sequences of postglacial Holocene sediment that are prone to amplification (**Figure S8-4** b).

Slope failure by landslides and soil liquefaction also contribute to the seismic hazard. You have already seen examples of slope failure in response to the 1946 Vancouver Island earthquake on **DAY 1** at **STOP 4**. The steep, fractured bedrock slopes of the Sea-to-Sky transportation corridor are also prone to earthquake-generated landslides.

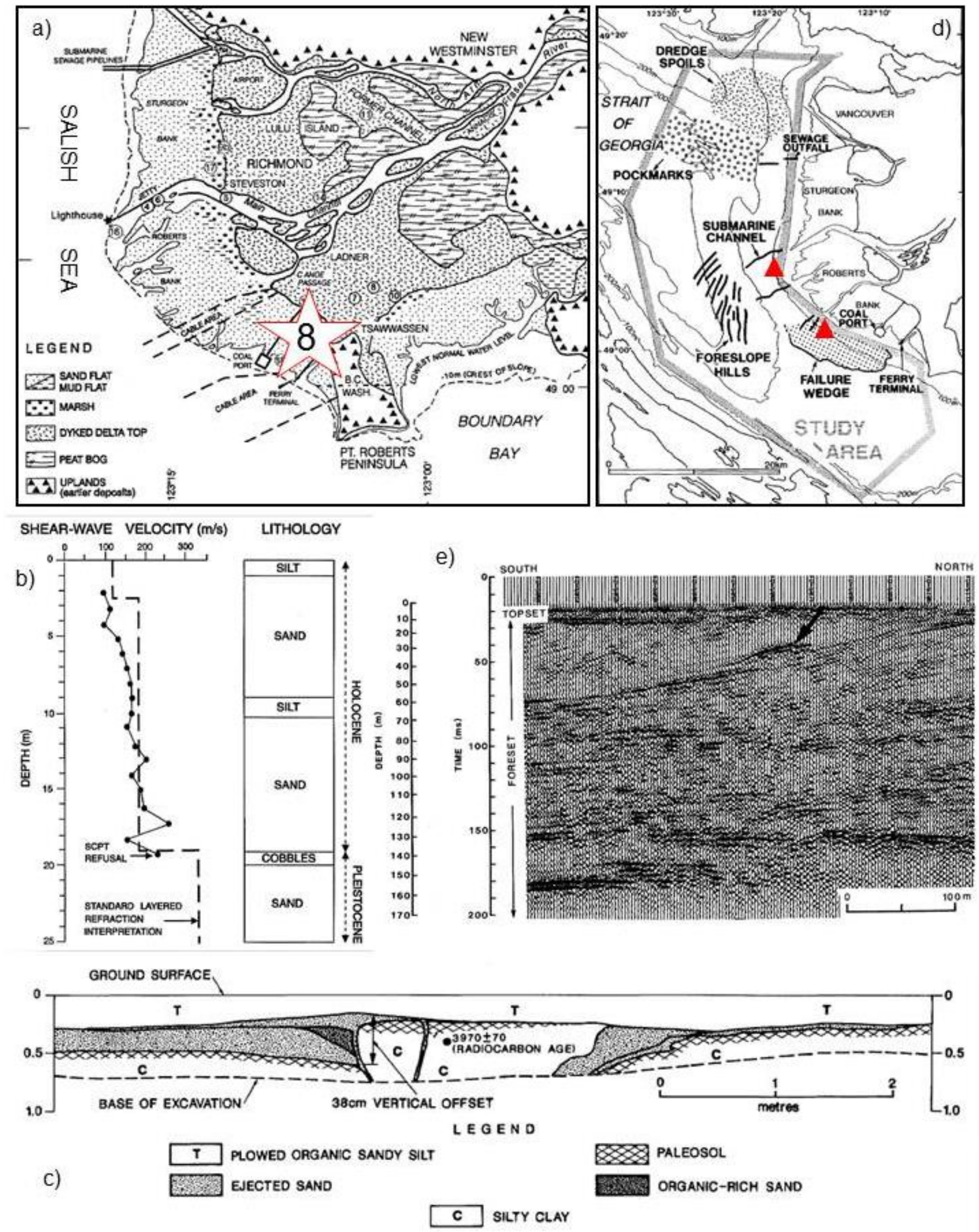

Figure S8-4 a) Geomorphology of Fraser River delta (modified from Luternauer et al. 1994); b) borehole stratigraphy, seismic cone penetrometer and surface refraction indicate firm glacial deposits at depths of 20 m below surface (modified from Luternauer et al. 1994); c) sand dykes and sand vents exposed in deltaic sediments (modified from Clague et al. 1992); d) seismic resolution profile showing buried failure deposit (arrow) off Roberts Bank (modified from Luternauer et al. 1994); e) surficial features of the delta slope and Salish Sea, red triangles indicate location of migrating dune ridges (modified from Luternauer et al. 1994).

Liquefaction deposits (e.g., sand dykes and sills) found in parts of the Fraser River delta provide evidence of strong shaking from large pre-historic earthquakes in the region (<3 ka, Clague et al. 1982; **Figure S8-4** c).

Ground-motion amplification

It has long been known that thick 'soft soil' sites, such as the deltaic sediments of the Fraser River delta, are prone to ground-motion amplification in certain frequency ranges as a result of earthquake shaking (Reiter, 1990). Although the earthquake type (source and magnitude) and the travel path (direction and attenuation) are fundamentally important, site geology also exerts a major influence. It is possible that site resonance effects may result from large shear-wave velocity contrasts within the unconsolidated overburden, such as between the Holocene–Pleistocene deposits (Hunter et al., 1998). Analysis of recent earthquakes have shown that for thick soil sites, horizontal ground motion amplification in the range of 0.5 to 4 Hz can be 3 to 5 times that of bedrock, with even larger amplification over limited frequency ranges where Quaternary sediments are thinning (<50 m) towards the northern edge of the delta or elsewhere within the delta where bedrock and/or Pleistocene deposits come close to the surface (**Figure S8-5**).

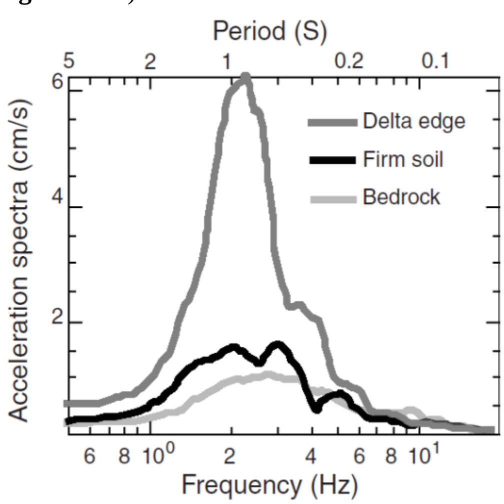

Figure S8-5 Frequency spectra of ground response from the M 5.3 Duvall earthquake in May 1996, comparing responses in bedrock, firm ground (till), and the northern edge of the Fraser River delta. The delta site shows amplification almost six times that of bedrock at a frequency of 2–3 Hz (Rogers et al. 1998; Mosher et al. 2004).

Liquefaction

If a cohesionless soil is sufficiently loose and the static shear stress is greater than the large-strain undrained shear strength, flow liquefaction is possible. Flow liquefaction can be initiated with either dynamic or static loading and may result in rapid flow slides (Monahan 1999).

When a cohesionless soil is exposed to rapid undrained cyclic loading (i.e., seismic shaking), excess pore pressures can develop, resulting in liquefaction that can lead to ground oscillations, lateral spreading and flow sliding (Watts et al. 1992). The channel-fill sediment facies, which underlies much of the surface of the modern delta, comprises the most liquefiable sediments (Christian et al. 1998).

A number of features have been identified from the geological record that are interpreted to represent liquefaction and slope-failure events, including sand boils, dykes, slumps and slides. Good summaries of these features are provided in Hamilton and Luternauer (1983), Hamilton and Wigen (1987), Pullan et al. (1998), Clague et al. (1998), Hart et al. (1992), Hart (1993) and Mosher and Hamilton (1998). Modern delta sediment thicknesses range from 19 m to 305 m and are extremely variable spatially because of the undulating bedrock and Pleistocene topography (**Figure S8-6**).

Submarine mass movements and their consequences

Delta slope failures are a consequence of seismic ground shaking and liquefaction, storm surges in the Salish Sea, or flood events from Fraser River. A number of surface features on the Fraser River delta slope are attributed to submarine mass-movements. Ancient mass-movement deposits and slides have been identified in seismic profiles of the delta slope west of **STOP 7** in the Foreslope Hills (**Figure S8-4** d; **Figure S8-7** a) and off Roberts Bank (**Figure S8-4** e; **Figure S8-7** b).

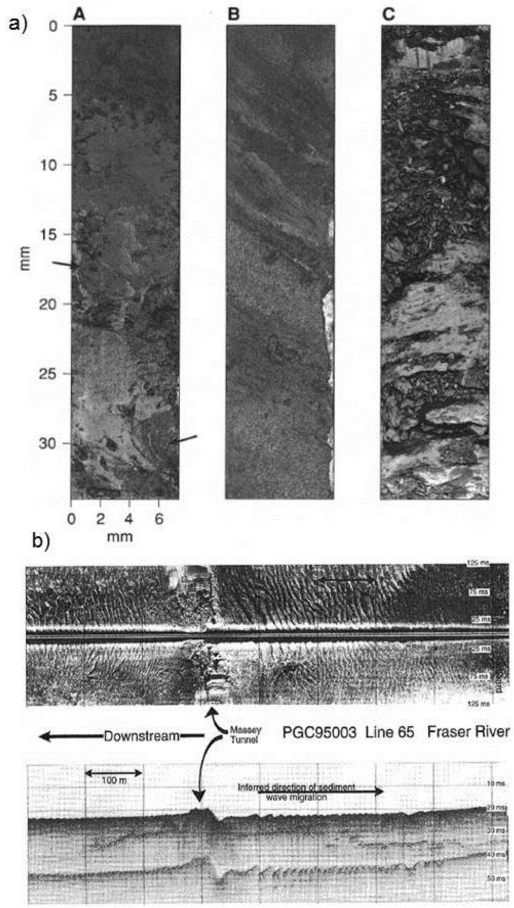

Figure S8-6 a) Deformation features in cores of Pleistocene sediments from borehole FD94-3. A) Convolute bedding (arrows), 124 m depth. B) High-angle stratification, 216 m depth. C) Sheared surfaces within dense clayey silt, 155 m depth. The deformation in A and B is syndepositional to early postdepositional; that in C is postdepositional (source: Clague et al.1998). b) Sidescan sonar (top) and seismic profile (bottom) across the Massey Tunnel of Fraser River (modified from: Luternauer et al. 1998).

Offshore sediment failures

Flow liquefaction is common at Sandheads, at the outer edge of the delta plain (**Figure S8-3** a). As the channel of Fraser River is now constrained to this location, all sediment load of the river that is not otherwise removed by dredging is funneled through this point. Sediment accumulates and fails downslope regularly (**Figure S8-7**). These failures are believed to be initiated by pore pressure response to surface waves, rapid sedimentation and tidal drawdown. Interstitial gas may also establish preconditioning factors (Chillarige et al. 1997).

In early investigations of the offshore region of the Fraser River delta, sediment failures were recognized off of Roberts Bank and the Foreslope Hills were considered to be the result of a massive sediment failure (Luternauer and Finn 1983). Mosher and Thomson (2002), however, showed that the Foreslope Hills are sediment waves formed by estuarine circulation, and driven by fresh water of Fraser River outflow and saline water due to tidal fluxes. The Roberts Bank Failure Complex was interpreted by Mosher and Hamilton (1998) as an amalgamation of failures that resulted from river mouth failures at a time when the river was free to avulse.

Deposition of fluvial sediment in distributary channels contributes to retrogressive failures at their heads. In 1985, 3 x 10^6 m^3 of fluvio-deltaic sediment failed, creating a scarp within 100 m of a lighthouse on Sturgeon Bank (**Figure S8-4** d). Downslope movement is promoted by interstitial gas and high sedimentation rates generating high pore pressures in fine-grained deltaic deposits (Luternauer et al. 1994),

Dunes off Roberts Bank (**Figure S8-4** d; **Figure S8-7** a) migrate slowly northwest in the direction of flood tidal current, and on occasion bury electrical transmission cables. The source of sand in the dunes is assumed to be erosion of seafloor sediments. This is leading to shoreline retreat and over-steepening of Roberts Bank adjacent to port facilities (Luternauer et al. 1994).

Stacey (2013) undertook work to determine the magnitude and frequency of large flows being deposited on the levees of the main submarine canyon at Sandheads (**Figure S8-8**). Over the past decades he was able to determine that some large flow deposits accompanied river flooding seasons. Landslide deposits tend to occur in sets of 2-4 with a return interval of 10 to 15 years during the past 40 years (based on ^{210}Pb dating).

Smaller event beds occur on average every four to five years.

Following on the work from the 1990s (e.g., Luternauer et al. 1998), it was recognized that the Fraser delta had most of the forcing factors that could contribute to submarine landslides or turbidity currents: over-steepened by deposition, strong currents undercutting the base of the slope, gassy sediment causing excess pore pressure during large tides, storm surges and earthquakes.

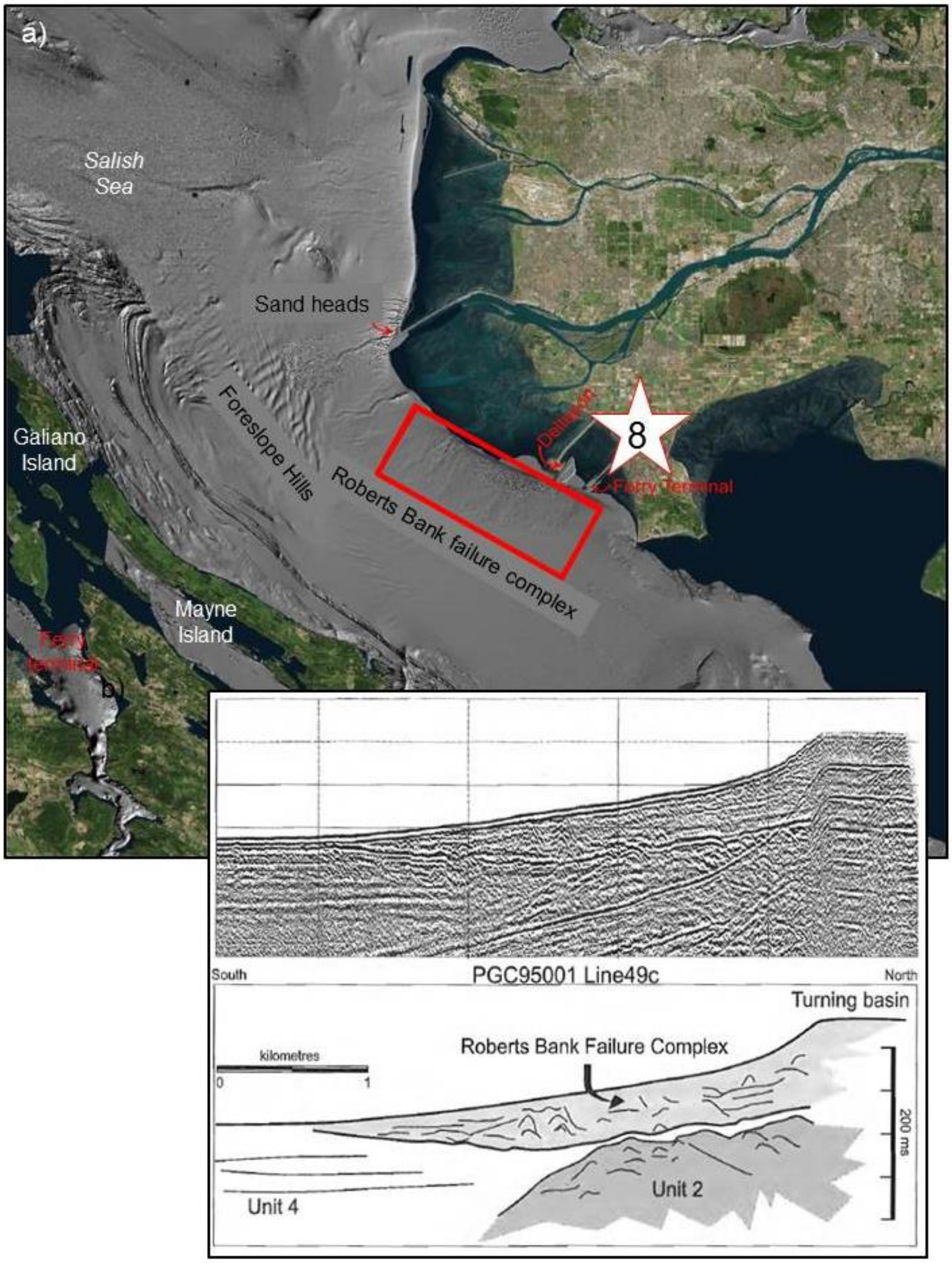

Figure S8-7 a) Location of offshore sediment failures discussed at STOP 8; b) seismic profile across the Roberts Bank failure complex (Luternauer et al. 1994).

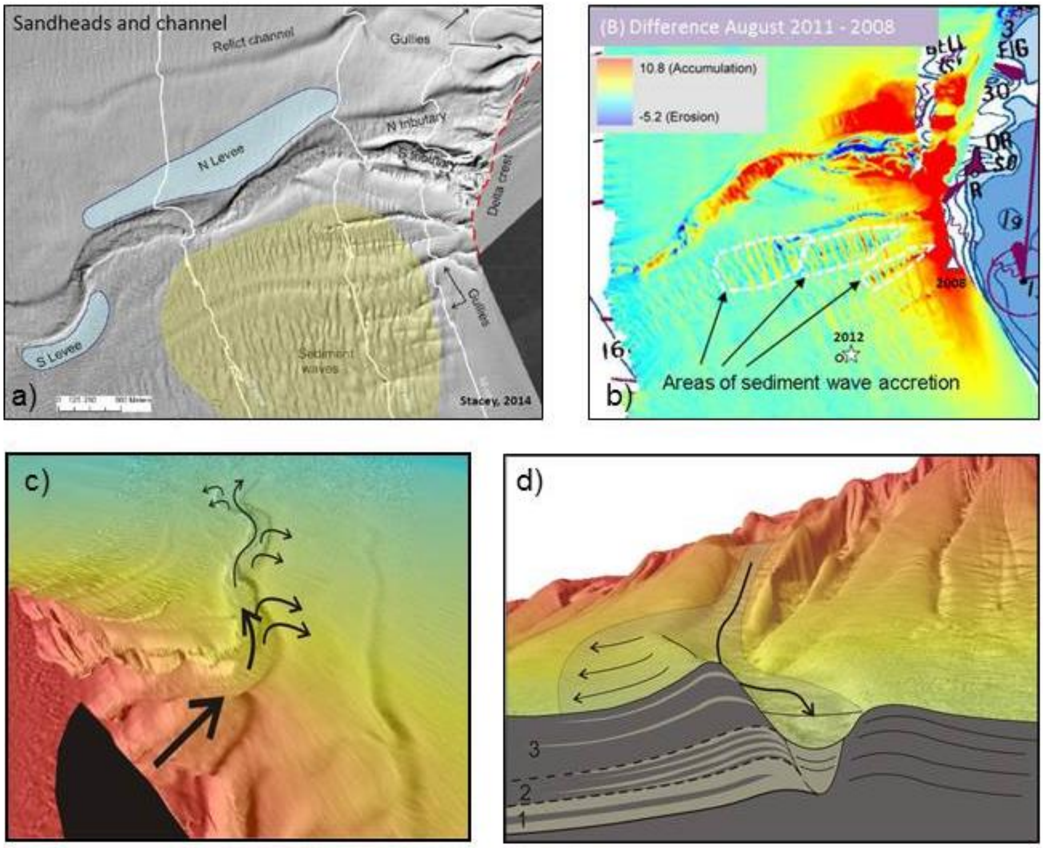

Figure S8-8 Sediment wave accretion at the head of the Sandheads channel result in turbidity currents that flow through the channel. Overspill deposits occur at bends in the channel creating well developed levee deposits: a) morphology of Sandheads channel; b) areas of erosion and accumulation of sediment; c) oblique view looking west; d) oblique view looking east (Stacey 2013).

The GSC (Lintern and Hill 2011) has taken advantage of the nearby Ocean Networks Canada Cabled Observatory by running a branch cable up onto the delta to measure the above parameters at all of their different time-scales.

Initially, the delta dynamics laboratory (DDL) platforms were buried and tumbled downslope, proving the existence of turbidity currents in the wave field south of the delta main canyon. A new platform includes an ejectable anchor for massive central ballast, and legs which penetrate the sediment (**Figure S8-9**).

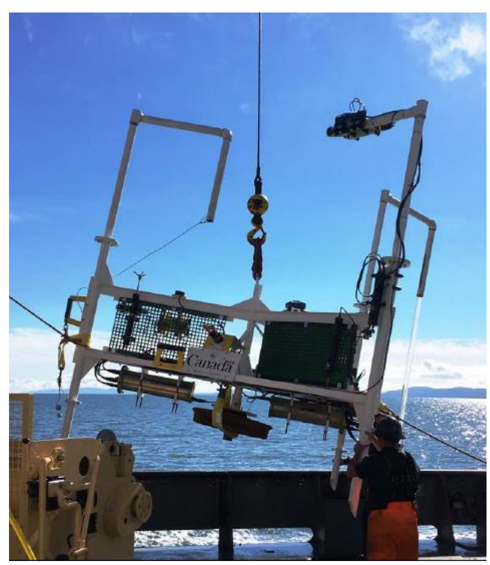

Figure S8-9 Deployment of avalanche resistant delta dynamic laboratory (DDL), April 2017 (photo: Gwyn Lintern).

Multiple powerful turbidity currents have been measured and analysed. Researchers are now able to predict under what conditions the turbidity currents are expected. During spring tides, when the settling river plume at the end of the ebb combines with sediment re-suspended from the seabed during following strong flood tides, near-bed concentrations become hyperpycnal and turbidity currents occur (Lintern et al. 2016; **Figure S8-10**).

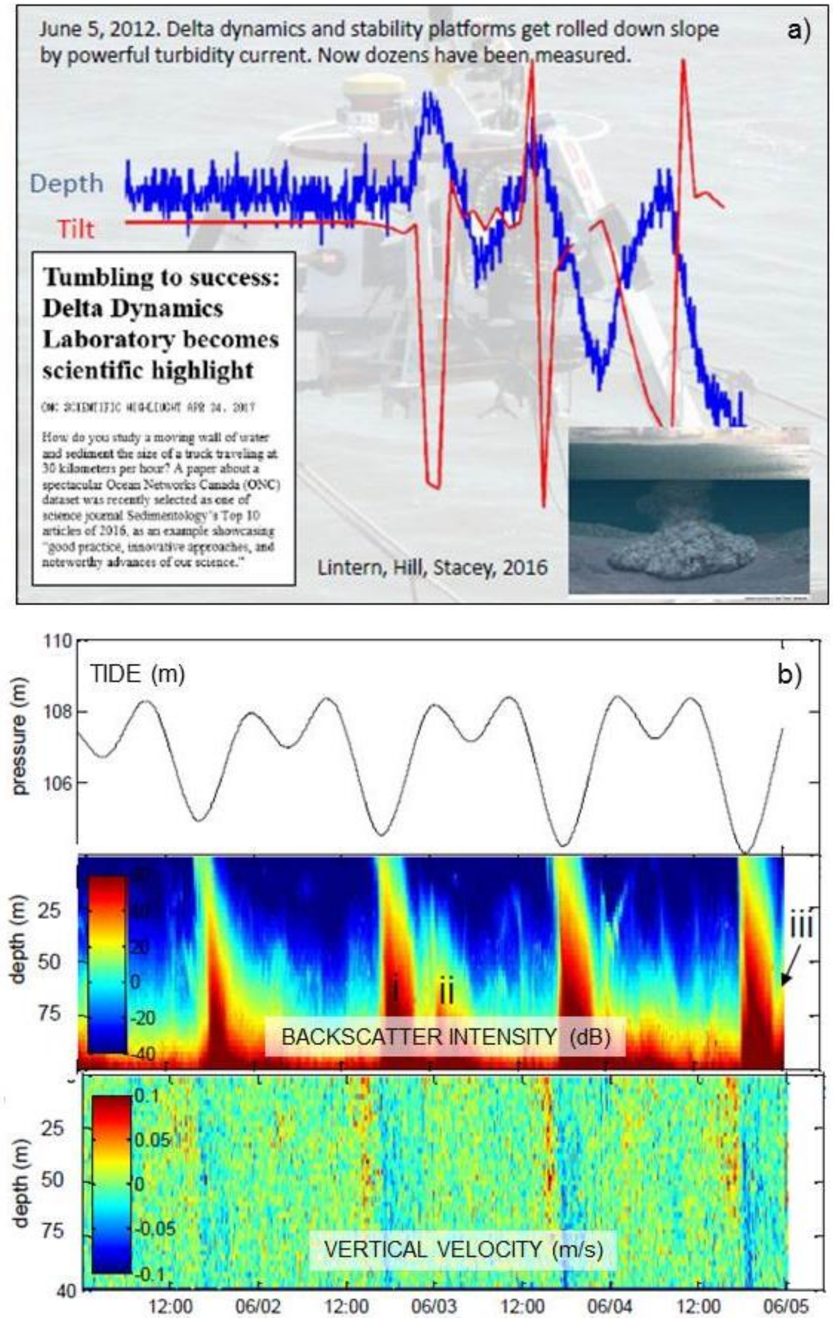

Figure S8-10 Plume deposition and re-suspension: a) monitoring turbidity flows with the delta dynamic laboratory (DDL); b) at iii, when sediment deposition from the ebb tide plume combines with sediment resuspension from the strong flood tide, densities become hyperpycnal and turbidity currents occur (Lintern et al. 2016).

Tsunamis

Port facilities, the western dyke system and low-lying communities are at risk from tsunamis generated by large, rapid submarine mass movements (Luternauer et al. 1994).

However, there is no evidence of tsunamis in the southern Salish Sea (contrast with **STOP 5**). Nonetheless, due to the potential of a delta front collapse, the result has been modeled in order to assess the risk to the southern mainland and Vancouver Island. Bornhold et al. (2001) modeled a tsunami that would result if the Roberts Bank Failure Complex occurred as a single instantaneous event (**Figure S8-11** a). Their results show that a large slide could generate tsunami waves up to 18 m high on the east shores of Galiano Island and Mayne Island (**Figure S8-7** a; **Figure S8-11** b). Fortunately, the tidal flats of the delta foreshore would deflect and reduce wave energy, such that waves at the shoreline in the lower Mainland would likely not exceed heights of 2 m.

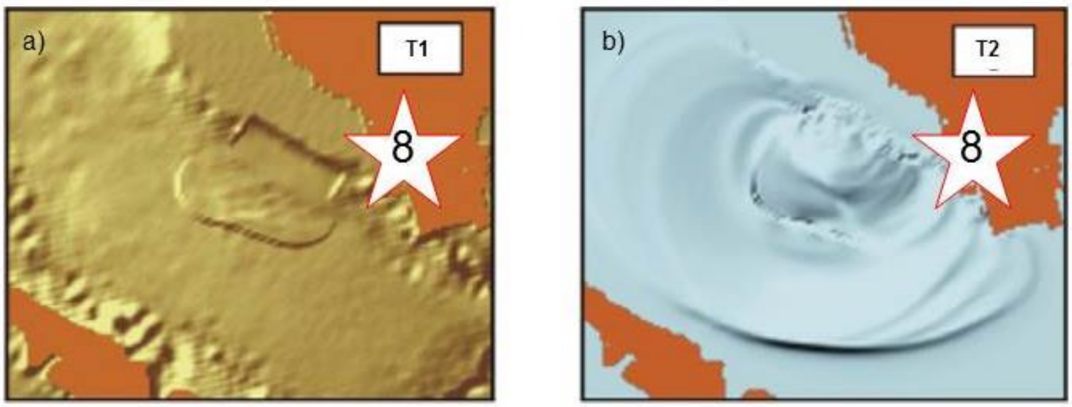

Figure S8-11 Roberts Bank slope failure modeled as a single event with consequent tsunami waves generated by displacement of delta front sediments. T1 - slump event; b) T2 – displacement tsunami (Bornhold et al. 2001).

Coastal protection measures

Over the past 150 years, urbanization and industrial development have adversely impacted the sedimentology and biodiversity of the Fraser River delta. Agricultural lands and sensitive ecosystems have been lost to housing and commercial development. Pollutants and contaminants are discharged from a number of sources (e.g., lumber operations, waste storage sites and sewage treatment plants). Dredging for river navigation and construction material is leading to net erosion of sensitive coastal ecosystems (e.g., eel grass habitat) (Mosher et al. 2004).

Critical infrastructure at risk of damage or destruction include submarine transmission cables supplying electricity and communications to Vancouver Island; sewage outfall pipelines from greater Vancouver; the Robert's Bank coal port; BC Ferries facilities at Tsawwassen; and the Vancouver International Airport.

Causeways to the ferry terminal and coal port facilities were designed mitigate the impacts of erosion of eel grass habitat. Dykes and jetties inhibit the migration of channels and storage of sand in channel deposits on the delta plain. A consequence of this flood control measure is that sand transported by the river is carried to the delta front where its accumulation leads to slope failure (Luternauer et al. 1994).

References

Bednarski, J.M. 2015. Surficial geology and Pleistocene stratigraphy from Deep Bay to Nanoose Harbour, Vancouver Island, British Columbia; Geological Survey of Canada, Open File 7681, 30 pages (1 sheet), https://doi.org/10.4095/295609

Bednarski, J.M. and Rogers, G.C. 2012. LiDAR and digital aerial photography of Saanich Peninsula, selected Gulf Islands, and coastal regions from Mill Bay to Ladysmith, southern Vancouver Island, British Columbia;. Geological Survey of Canada, Open File 7229, 7 pages, https://doi.org/10.4095/291819

Blais-Stevens, A., Bornhold, B.D., Kemp, A.E.S., Dean, J.M. and Vaan, A.A. 2001.Overview of Late Quaternary stratigraphy in Saanich Inlet, British Columbia: results of Ocean Drilling Program Leg 169S; Marine Geology; Vol. 174 (1-4); pp. 3-26

Blais-Stevens, A., Geertsema, M., Schwab, J., Bornhold, B. and Mosher, D. 2006. A brief overview of landslide-generated tsunamis affecting North America; 1st Specialty Conference on Disaster Mitigation, Calgary, Alberta; 11 pages

Blais-Stevens, A. 2008. Surficial geology and landslide inventory of the upper Sea-to-Sky Corridor, British Columbia; Geological Survey of Canada; Open File 5324; 1:50:000 scale map

Blais-Stevens, A. and Hungr, O. 2008. Landslide hazards and their mitigation along the Sea-to-Sky Corridor; Proceedings of the 4th Canadian Conference on Geohazards: from causes to management; Presse de l'Université Laval, Quebec; pp. 495-502

Blais-Stevens, A. and Septer, D. 2008. Historical accounts of landslides and flooding events along the Sea-to-Sky Corridor, British Columbia, from 1855-2007; Geological Survey of Canada; Open File 5741; 119 p.

Blais-Stevens, A. and Kung, R. 2009. Landslide susceptibility maps of the Sea-to-Sky Corridor, British Columbia; Geological Survey of Canada Open File 6169; 1:50:000 scale map

Blais-Stevens, A., Rogers, G.C. and Clague, J.J. 2011. A revised earthquake chronology for the last 4,000 years inferred from varve-bounded debris-flow deposits beneath an inlet near Victoria, British Columbia; Bulletin of the Seismological Society of America; Vol. 101 (1); pp. 1-12

Bobrowsky, P.T. and Clague, J. J. 1990. Holocene sediments from Saanich Inlet, British Columbia and their neotectonic implications; Geological Survey of Canada; Current Research, Part E; Paper 90-1E; pp. 251-256

Bornhold, B.D., Firth, J.V. et al. 1998 Initial Report; Ocean Drilling Program Leg 169S; Proceedings Volume; doi:10.2973/odp.proc.ir.169S.1998

Bornhold, B.D., Thomson, R.E., Rabinovich, A.B., Kulikov, E.A. and Fine, I.V. 2001. Risk of landslide-generated tsunamis for the coast of British Columbia and Alaska. An Earth Odyssey; 54th Canadian Geotechnical Conference Proceedings; 16 -19 September 2001, Calgary, Alberta; pp. 1450-1454

Chillarige, A.V., Robertson, P.K., Morgenstern, N.R. and Christian, H.A. Evaluation of the in situ state of Fraser River sand. Canadian Geotechnical Journal; Vol. 34; pp. 510-519

Christian, H.A., Mosher, D.C., Barrie, J.V., Hunter, J.A., Luternauer, J.L., 1998. Seabed instability on the Fraser River delta; In Clague, J.J., Luternauer, J.L., Mosher, D.C. (Eds.); Geology and Natural Hazards of the Fraser River Delta, British Columbia; Geological Survey of Canada Bulletin 525; pp. 217-230

Church, I., Cartwright, D., Kuus, P., Hamilton, T., Pratomo, D. and Eisan, B. 2012. The Squamish ProDelta: Monitoring Active Landslides and Turbidity Currents; Canadian Hydrographic Conference Proceedings; 15p.

Clague, J.J. 1981. Late Quaternary geology and geochronology of British Columbia; Part 2: Summary and discussion of radiocarbon-dated Quaternary history; Geological Survey of Canada; Paper 80-35; 41 p.

Clague, J. J. 1996. Paleoseismology and seismic hazards, southwestern British Columbia; Geological Survey of Canada; Bulletin 494; 88p.

Clague, J.J., Armstrong, J.E. and Mathews, W.H., 1980. Advance of the Late Wisconsin Cordilleran Ice Sheet in southern British Columbia since 22,000 yr B.P.; Quaternary Research; Vol 13; pp. 322-326

Clague, J.J., Harper, J.R., Hebda, R.J., and Howes, D.E. 1982. Late Quaternary sea levels and crustal movements, coastal British Columbia; Canadian Journal of Earth Sciences; Vol. 19; pp. 597-618

Clague, J.J. and Souther, J.G. 1982. The Dusty Creek landslide on Mount Cayley; Canadian Journal of Earth Science; Vol. 19; pp. 524-539

Clague, J.J., Luternauer, J.L., and Hebda, R.J. 1983. Sedimentary environments and postglacial history of the Fraser Delta and lower Fraser Valley, British Columbia; Canadian Journal of Earth Sciences; Vol. 20; pp. 1314-1326

Clague, J.J., Luternauer, J.L., Pullan, S.E., Hunter, J.A. 1991. Postglacial deltaic sediments, southern Fraser River delta, British Columbia; Canadian Journal of Earth Sciences; Vol. 28; pp. 1386-1393

Clague, J.J., Naesgaard, E., and Sy, A. 1992. Liquefaction features on the Fraser Delta: evidence for prehistoric earthquakes? ; Canadian Journal of Earth Sciences; Vol 29; pp.1734–1745.

Clague, J.J. and Bobrowsky, P.T. 1994. Evidence for a large earthquake and tsunami 100-400 years ago on western Vancouver Island, British Columbia; Quaternary Research; Vol. 41; pp. 176-184

Clague, J.J., Luternauer, J.L. and Mosher, D.C. (Eds.) 1998. Geology and Natural Hazards of the Fraser River Delta, British Columbia; Geological Survey of Canada Bulletin 525, 270 pp.

Clague, J.J. and Turner, R.W. 2003. Critical earth science issues along transportation corridors in southwestern British Columbia; In Geological Field Trips in Southern British Columbia; Geological Association of Canada – Cordilleran Section; GAC-MAC-SEG Joint Annual Meeting, Vancouver, B.C.; pp. 187-240

Couture, R. and VanDine, D. 2004. Field Trip Guidebook – Some Geological Hazards of North Vancouver and along the Sea-to-Sky Highway, British Columbia; Geological Survey of Canada; Open File 4642; 84 p.

Cui, Y., Miller, D., Schiarizza, P. and Diakow, L.J. 2017. British Columbia digital geology; British Columbia Ministry of Energy, Mines and Petroleum Resources; British Columbia Geological Survey; Open File 2017-8; 9 p.

E-Fauna BC 2018. Electronic Atlas of the Wildlife of British Columbia. URL ibis.geog.ubc.ca

Eisbacher, G.H. 1983. Slope stability and mountain torrents, Fraser Lowlands and southern Coast Mountains, British Columbia; Field trip Guidebook Trip 15; Geological Association of Canada / Mineralogical Association of Canada / Canadian Geophysical Union Joint Annual Meeting, Victoria, B.C.; 46 p.

Evans, S.G. 1987. A rock avalanche from the peak of Mount Meager, British Columbia; Geological Survey of Canada Current Research; Part A; Paper 87-1A; pp. 929-934

Evans, S.G. 2000. The 1915 and 1921 disasters at Britannia Mine complex, Howe Sound, British Columbia; geotechnical implications for intensive resource development in steep mountain watersheds in the Coast Mountains; In Proceedings of Geological Association of Canada Symposium; Calgary, AB.

Evans, S.G. and Savigny, W. 1994. Landslides in the Vancouver-Fraser Valley-Whistler region; In J. Monger (Ed.); Geology and Geological Hazards of the Vancouver Region; Geological Survey of Canada; Bulletin 481; pp. 251-286

Friele, P.A. and Clague, J.J. 2002. Re-advance of glaciers in the British Columbia Coast Mountains at the end of the last glaciation; Quaternary International; Vol. 87; pp. 45-58.

Fyles, J.G. 1963. Surficial geology of Horne Lake and Parksville map areas, Vancouver Island, British Columbia; Geological Survey of Canada, Memoir 318; 142 p.

Halstead, E.C. 1968 The Cowichan Ice tongue, Vancouver Island; Canadian Journal of Earth Sciences; Vol. 5 (6); pp. 1409-1415

Hamilton, T.S. and Luternauer, J.L., 1983. Evidence of seafloor instability in the south-central Strait of Georgia: a preliminary compilation; in Current Research, Part A; Geological Survey of Canada; Paper 83-1A; p. 417–421

Hamilton, T.S., Wigen, S.O., 1987. The Foreslope Hills of the Fraser Delta: Implications for tsunamis in Georgia Strait; International. Journal Tsunamis Soc.; Vol. 5; pp. 15-33

Hart, B.S., Prior, D.B., Barrie, J.V., Currie, R.G., Luternauer, J.L., 1992. A river mouth submarine channel and failure complex, Fraser Delta, Canada; Sedimentary Geology; Vol. 81; pp.73-87

Hart, B.S., 1993. Large-scale in situ rotational failure on a low-angle delta slope: The Foreslope Hills, Fraser Delta, British Columbia, Canada. Geophysical Marine Letters; Vol. 13; pp. 219-226

Hickin, E.J. 1989. Contemporary Squamish River sediment flux to Howe Sound, British Columbia; Canadian Journal Earth Sciences; Vol. 26; pp. 1953-1963

Hughes Clarke, J.E., Brucker, S. and Muggah, J. 2012. The Squamish ProDelta: Monitoring Active Landslides and Turbidity Currents; Canadian Hydrographic Conference Proceedings, 15 p.

Hicock, S.R. and Armstrong, J.E. 1983 Vashon Drift: definition of the formation in the Georgia Depression, southwestern British Columbia; Canadian Journal of Earth Sciences; Vol. 22; pp. 748-757

Hizzett, J. L., Hughes Clarke, J. E., Sumner, E. J., Cartigny, M. J. B, Talling, P. J. and Clare, M. A. 2017. Which triggers produce the most erosive, frequent and longest runout turbidity currents on deltas? Geophysical Research Letters; Vol. 45; pp. 855-863

Hungr, O., Morgan, G.C., and Kellerhals, R. 1984. Quantitative analysis of debris torrent hazards for design of remedial measures; Canadian Geotechnical Journal; Vol. 21; pp. 663-677

Hungr, O., Morgan, G.C., VanDine, D.F. and Lister, D.R. 1987. Debris flow defences in British Columbia; Reviews in Engineering Geology, Geological Society of America; Vol. 7; pp. 201-223

Hungr, O. and Skermer, N.A. 1998. Debris torrents and rock slides, How Sound to Whistler Corridor. Technical Tour Guidebook; Trip 6; In J. Clague (Ed.); Technical Tour Guide Books; 8th IAEG Congress; Vancouver, B.C.

Hunter, J.A., Douma, M., Burns, R.A., Good, R.L., Pullan, S.E., Harris, J.B. Luternauer, J.L. and Best, M.E. 1998. Testing and application of near-surface geophysical techniques for earthquake hazards studies, Fraser River delta, British Columbia; In Geology and Natural Hazards of the Fraser River Delta, British Columbia, (Eds.) J.J. Clague, J.L. Luternauer, and D.C. Mosher; Geological Survey of Canada, Bulletin 525; pp.123-146

Huntley, D.H., Bobrowsky, P.T. and Clague, J.J. 2001. Ocean Drilling Program Leg 169S: surficial geology, stratigraphy and geomorphology of the Saanich Inlet area, southeastern Vancouver Island, British Columbia; Marine Geology; Vol. 174 (1-4), pp. 27-41

Hyndman, R.D. 1995. Giant earthquakes of the Pacific Northwest; Scientific American; Vol. 273; pp. 68-75

IPCC 2013. Climate Change 2013: physical science basis. Contribution of Working Group I to the Fifth Assessment Report of the Intergovernmental Panel on Climate Change; http://www.ipcc.ch

Journeay, M.J., Williams, S.P., and Wheeler, J.O. 2000. Tectonic assemblage map, Vancouver, British Columbia-USA; Geological Survey of Canada Open File 2948a; scale 1:1,000,000

Lintern, D.G. and Hill, P. 2010. An Underwater laboratory at the Fraser River delta; EOS; Vol. 91 (38); pp. 333–344.

Lintern, D.G., Hill, P.R. and Stacey, C. 2016. Powerful unconfined turbidity current captured by cabled observatory on the Fraser River delta slope, British Columbia, Canada; Sedimentology; Vol. 63 (5); pp. 1041-1064; doi:10.1111/sed.12262

Ludwin, R.S., Dennis, R., Carver, D., McMillan, A.D., Losey, R., Clague, J.J., Jonientz-Trisler, C., Bowechop, J., Wray, J. and James, K. 2005. Dating the 1700 Cascadia Earthquake: Great Coastal Earthquakes in Native Stories; Seismological Research Letters; Vol. 76; pp. 140-148

Luternauer, J.L. and Finn, W.D.L. 1983. Stability of the Fraser River Delta front; Canadian Geotechnical Journal; Vol. 20; pp. 603-616

Luternauer, J., Barrie, V., Christian, H., Clague, J., Evoy, R., Hart, B., Hu nter, J., Killeen, P., Kostaschuck, Mathewes, R., Monahan, P., Moslow, T., Mwenifumbo, C., Olynyk, H., Patterson, R., Pullan, P., Roberts, M., Robertson, P., Tarbottom, M and Woeller, D. 1994. Fraser River delta: geology, geohazards and human impact; In J. Monger (Ed.); Geology and Geological Hazards of the Vancouver Region; Geological Survey of Canada; Bulletin 481; pp. 197-220

Luternauer, J.L., Mosher, D.C., Clague, J.J., Atkins, R.J., 1998. Sedimentary environments of the Fraser delta. In Clague, J.J., Luternauer, J.L., Mosher, D.C. (Eds.), Geology and Natural Hazards of the Fraser River Delta, British Columbia. Geological Survey of Canada; Bulletin 525; pp. 27-39.

Massey, N.W.D., MacIntye, D.G., Desjardins, P.J. and Cooney, R.T. 2005. Digital Geology Map of British Columbia; British Columbia Ministry of Energy, Mines and Petroleum Resources; British Columbia Geological Survey; Geofile 2005-1; 1:250,000 scale map

Mathews, W.H., 1958. Geology of Mount Garibaldi map-area, southwestern British Columbia, Canada; Bulletin of the Geological Society of America; Vol. 96; pp. 161-198

Mathews, W.H., Fyles, J.G. and Nasmith, H.W. 1970. Postglacial crustal movements in southwestern British Columbia and adjacent Washington State; Canadian Journal of Earth Sciences; Vol. 7, pp. 690-702

Mathews, W.H. 1979. Landslides of central Vancouver Island and the 1946 earthquake; Seismological Society of America Bulletin 69; pp. 445-450

Monahan, P.A., 1999. The application of core penetration test data to facies analysis of the Fraser River Delta, British Columbia; Ph.D. Thesis; School of Earth and Ocean Sciences, University of Victoria, Victoria, British Columbia; 392 p.

Monahan, P.A., Luternauer, J.L. and Barrie, J.V. 1993. A delta plain sheet sand in the Fraser River Delta, British Columbia, Canada; Quaternary International; Vol.20; pp. 27–38

Mosher, D.C., Christian, D.C., Hunter, J.A. and Luternauer, J.L. 2004. Onshore and Offshore Geohazards of the Fraser River Delta; In Fraser River Delta: Issues of an Urban Estuary; B.J. Groulx, D.C. Mosher, J.L. Luternauer, and D.B. Bilderback (Eds.); Geological Survey of Canada; Bulletin 567; pp. 67-81

Mosher, D.C. and Hamilton, T.S. 1998. Morphology, structure and stratigraphy of the o¡shore Fraser delta and adjacent Strait of Georgia. In Clague, J.J., Luternauer, J.L., Mosher, D.C. (Eds.), Geology and Natural Hazards of the Fraser River Delta, British Columbia. Geological Survey of Canada, Bulletin 525, pp. 147-160.

Mosher, D. C. and Moran, K. 2001. Post-glacial evolution of Saanich Inlet, British Columbia: results of physical property and seismic reflection stratigraphic analysis; Marine Geology; Vol. 174 (1-4); pp. 59-77

Mosher, D.C., and Thomson, R.E. 2002. The Foreslope Hills: large-scale, fine-grained sediment waves in the Strait of Georgia, British Columbia; Marine Geology; Vol.192; pp. 275-295

Mosher, D.C., Monahan, P.A., Barrie, J.V. and Courtney, R.C. 2009. Submarine failures in the Strait of Georgia, British Columbia: landslides of the 1946 Vancouver Island Earthquake; Journal of Coastal Research; Vol. 27 (2); 19 p.

Moore, D.P. and Mathews, W.H. 1978. The Rubble Creek landslide, southwestern British Columbia; Canadian Journal of Earth Sciences; Vol. 15; pp.1039-1052

Parish, R., Thomson, S. and Coward, G. 1994. Tree book: learning to recognize trees of British Columbia. Canadian forest Service and British Columbia Ministry of Forests; Special Publication; 196 p.

Parrish, R.R. 1983. Cenozoic thermal evolution and tectonics of the Coast Range of British Columbia: 1. Fission track dating apparent uplift rates and pattern of uplift; Tectonics; pp. 601-633

Pojar, J. and Mackinnon, A. 1994. Plants of Coastal British Columbia, including Washington, Oregon and Alaska; British Columbia Ministry of Forests and Lone Pine Publishing; ISBN 1-55105-042-0

Prior, D.B. and Bornhold, B.D. 1984. Geomorphology of slope instability features of Squamish Harbour, Howe Sound, British Columbia; Geological Survey of Canada; Open File 1095

Prior, D.B. and Bornhold, B.D. 1986. Sediment transport on subaqueous fan delta slopes, Britannia Beach, British Columbia; Geo-Marine Letters; Vol. 1; pp. 85-90

Prior, D.B., Wiseman, W.J. and Gilbert, R. 1981. Submarine slope processes on a fan delta, Howe Sound, British Columbia; Geo-Marine Letters; Vol. 1 (2); pp. 85-90

Pullan, S.E., Hunter, J.A., Jol, H.M., Roberts, M.C., Burns, R.A. and Harris, J.B. 1998. Seismostratigraphic investigations of the southern Fraser River delta; In Geology and Natural Hazards of the Fraser River Delta, British Columbia; (Eds.) J.J. Clague, J.L. Luternauer and D.C. Mosher; Geological Survey of Canada; Bulletin 525; p. 91–122

Read, P.B. 1990. Mount Meager Complex, Garibaldi Belt, southwestern British Columbia; Geoscience Canada; Vol. 17; pp. 167-170

Reiter, L.1990. Earthquake Hazard Analysis: Issues and Insights; Columbia University Press, New York, New York, 254 p.

Rogers, G.C. 1980. A documentation of soil failure during the British Columbia earthquake of 23 June, 1946; Canadian Geotechnical Journal; Vol. 17; pp. 122-127

Rogers, G.C., 1994. Earthquakes in the Vancouver area. In J. Monger (Ed.); Geology and Geological Hazards of the Vancouver Region; Geological Survey of Canada; Bulletin 481; pp. 197-220

Rogers, G.C., Cassidy, J.F. and Weichert, D.H.1998. Variations in earthquake ground motion on the Fraser delta from strong-motion seismograph records; In Geology and Natural Hazards of the Fraser River Delta, British Columbia; (Ed.) J.J. Clague, J.L. Luternauer and D.C. Mosher; Geological Survey of Canada; Bulletin 525; pp. 195–210

Souther, J.G. 1977. Volcanism and tectonic environments in the Canadian Cordillera – a second look; Geological Association of Canada Special Paper 16; pp. 17-24

Stacey, C.D. 2013. Frequency and initiation mechanisms of submarine slides on the Fraser Delta front; MSc thesis; School of Earth and Ocean Science, University of Victoria; 149 p.

Stacey, C.D., Hill, P.R., Talling, P.J., Enkin, R.J., Hughes Clarke, J. and Lintern, D.G. 2018. How turbidity current frequency and character varies down a fjord-delta system: Combining direct monitoring, deposits and seismic data; Sedimentology; in review

Tanigawa, K., Sawai, Y., Bobrowsky, P., Huntley, D., Goff, J. and Shinozaki, T. 2017. Geological evidence for tsunamis prior to the 1700 Cascadia earthquake from Vancouver Island Canada; Geological Society of America; Proceedings and Abstracts; T181 Poster; Seattle, Washington

Terzaghi, K. 1956. Varieties of submarine slope failures; In Proceedings of the 8th Texas Conference on Soil mechanics and Foundation Engineering; Austin, Texas; pp. 1-41.

Thom, B. 2003. The Anthropology of Northwest Coast Oral Traditions; Arctic Anthropology; Vol. 40; pp. 1-28

Thompson, S.C., Clague, J.J., and Evans, S.G., 1997. Holocene activity of the Mount Currie scarp, Coast Mountains, British Columbia, and implications for its origins; Environmental Geoscience; Vol. III; pp. 329-348

Turner, R.J.W., Clague, J.J., and Groulx, B.J., 1996. Geoscape Vancouver; Geological Survey of Canada; Open File 3309; 1 sheet

Turner, R., Kelman, M., Ulmi, M., Turner, T. and Franklin, R. 2010. Sea to Sky GeoTour; Geological Survey of Canada; Special Publication; ISBN 978-1-100-14554

VanDine, D. 2002. Debris flow control structures; Guidebook, field trip Vancouver and Highway 99, British Columbia; Sediment-related Issues Committee; Third World Water Forum, Japan

Watts, B.D., Seyers, W.C., and Stewart, R.A. 1992. Liquefaction susceptibility of Greater Vancouver Area soils; In Symposium on Geotechnique and Natural Hazards; Vancouver Geotechnical and Canadian Geotechnical Societies, 6–9 May, pp. 145–157

Acknowledgements

Open File 8405 benefitted from the contribution of Cooper Stacey (GSC-Sidney), and was critically reviewed by Andrée Blais-Stevens (GSC-Ottawa). Artwork is by David Huntley. DAY 1 cover painting: *Denman Nocturne* (2000). DAY 2 cover painting: *Fjordscape* (2014). Back cover painting: *Pacific Geoscience Centre* (2012).

FIELD NOTES

FIELD NOTES